

# **Nitrification in wastewater treatment at its biological oxygen limit**

**Cristiana Carvalho Moraes**

A thesis submitted to Newcastle University for the partial fulfilment of the requirements of  
the degree of Doctor of Philosophy

November 2018



Environmental Engineering Research Group  
School of Civil Engineering and Geosciences



## Abstract

Using low dissolved oxygen (DO) concentrations in activated sludge could improve the energy and environmental sustainability of wastewater treatment plants (WWTPs). At present there is limited information about the influence of low DO on nitrifying bacteria: the mode of acclimatization of ammonia-oxidizing bacteria (AOB); the mechanistic basis for the biological adaptation of AOB under those conditions; and the impact of low DO on the emissions of the greenhouse gas (GHG). We operated four reactors in continuous mode at low (0.2 mg/L) and high (6.5 mg/L) DO. Improvements in ammonia ( $\text{NH}_3$ ) and nitrite ( $\text{NO}_2^-$ ) oxidation were observed in reactors at low DO after two months, though neither form of nitrogen was removed completely. Quantitative PCR of the  $\text{NH}_3$  monooxygenase (*amoA*) and  $\text{NO}_2^-$  oxidoreductase (*nxrB*) genes showed similar cell concentrations of AOB and nitrite-oxidizing bacteria (NOB) cells in all reactors, though AOB biomass declined in the initial phase at low DO. The AOB found at low DO reactors were phylogenetically associated with the *Nitrosomonas europaea*/*Nitrosococcus mobilis* lineage and appeared to be selected from the seed, representing a very small percentage of the original community. The effect of initial cell concentration on AOB adaptation was modelled using two species, linking adaptation time and the initial concentration of the species selected. High growth yields in the AOB adapted to low DO conditions suggested a mixotrophic metabolism. The production of nitrous oxide ( $\text{N}_2\text{O}$ ) was observed in batch experiments using activated sludge samples from both DO conditions. Higher production was observed in low DO experiments achieving 402 nmol/L.h against 11 nmol/L.h of  $\text{N}_2\text{O}$  in high DO. However, this production represented a very small percentage (1.5% and 0.03% in low and high DO respectively) of the total  $\text{NH}_3$  removed, suggesting the occurrence of simultaneous nitrification and denitrification. The impact of  $\text{N}_2\text{O}$  production was estimated by two methods and suggested that plants must save 0.16 kWh/m<sup>3</sup> of treated wastewater or 0.02 kWh/m<sup>3</sup> of treated wastewater per each mg of  $\text{NH}_3$  oxidized, to make climate sense. Fluorescence *in situ* hybridisation (FISH) and fluorescent-activated cell sorting (FACS) were combined to analyse AOB genomes in reactors operated at low and high DO. AOB cells fixed in ethanol revealed positive signal with high fluorescent signal intensity when using Cy5 and SYTO 9 and when cells were pre-treated with ultrasonication. AOB were enriched, forming up to 14% of the total sorted population, but it was still not sufficient to guarantee a good assembly and thus reconstruct genomes. Though the feasibility of FISH-FACS to separate targeted uncultivated populations was demonstrated, optimization of the protocol is still needed.



## Acknowledgments

First I would like to thank my supervisor, Professor Tom Curtis for giving me the opportunity to work in a major European project and for his help and support during my PhD, in particular his encouragement and enthusiasm were uplifting and appreciated. I would like to thank my second supervisor Ian Head for all the productive discussions. I am also grateful to Professor Robert Upstill-Goddard for allowing me to use his laboratory, for his professional guidance and insightful comments and for helping me with the writing of this thesis.

A huge thanks to Ben, Amy, Micol and Rebeca who all had a central role in my PhD project. Ben thanks for helping me to produce the best sequencing data I could have and all the additional/extra support. Amy, whose contribution was indispensable, mainly all your help in the practical work such as monitoring the reactors whenever I was away, preparing samples for flow cytometry analyses and helping to interpret those results. Rebeca, our discussions were super useful and added a valuable contribution for this thesis. Micol thanks for your suggestions and guidance and for spending an entire week in Newcastle only to help me with the reactor set up and troubleshooting. It would have been much more difficult without you all here.

I am grateful to all the people in the laboratories at Civil Engineering and Geosciences Building, Newcastle University. Many thanks go to David, Sarah and Donna for their advice and excellent technical assistance in the laboratory. David and Harry thanks for all your helped and for always creating a good mood and make people smile. Thank you to Florence and Fei for looking after my reactors during the Christmas season so I could visit my family. I want to thank Dana for all help with her model and Joana for helping me in the microlab when I started. Also, thanks to Russell Davenport whose advice and contribution was important when working with FISH and was also readily available for clearing doubts.

I would also like to thank the staff at the Flow Cytometry Core Facility in Newcastle University, in particular to Andrew and David for their assistance and valued discussions. I am grateful to Trevor Booth, at Newcastle Universities BioImaging suite, for his expertise and patience and helping me to get the best microscopy images possible.

This research project was funded by MERMAID, a Marie Skłodowska-Curie Initial Training Network, under grant 607492. I am thankful for their financial support and for providing me interesting and valuable workshops and seminars and the opportunity to attend numerous conferences. Thanks to all people involved in this project specially to Arnaud, who was very patient with all our issues and helped me to work with a particularly challenging

sequencing data, and to Alex and Vaibhav, who also supported me through that phase. Also, thanks to Lene for her laboratory assistance during the time I spent at Technical University of Denmark.

I would also like to mention the administration at Newcastle University and Professor David Graham for solving all technical/bureaucratic problems and arranging all my travels.

Finally, special thanks to my friends in Newcastle and mainly to the ‘Coffee Gang’ as those moments made me much happier and gave me heavenly energy to carry on. Most importantly, thanks to my family and my future husband, Filipe, for putting up with me and supporting me at all times.

## Abbreviations

AMO	Ammonia monooxygenase enzyme
<i>amoA, amoB, amoC</i>	Ammonia monooxygenase genes
Anammox	Anaerobic ammonia oxidation
ANOSIM	Analysis of similarities
ANOVA	Analysis of variance
AOA	Ammonia-oxidizing archaea
AOB	Ammonia-oxidizing bacteria
BLAST	Basic Local Alignment Search Tool
BOD	Biochemical oxygen demand
bp	Base pairs
BWA	Burrows-Wheeler Aligner
CANON	Completely autotrophic nitrogen removal over nitrite
CARD-FISH	Catalyzed reporter deposition fluorescence <i>in situ</i> hybridization
CGR	Centre for Genomic Research
CLSM	Confocal laser scanning microscope
COD	Chemical oxygen demand
Comammox	Complete ammonia oxidiser
CSTR	Continuous Stirred Tank Reactor
Cy3	Tetramethyl isothicyanate
Cy5	Indocarbocyanine
cyt	Cytochrome
DEMON	<i>Deammonification process</i>
DNA	Deoxyribonucleic Acid
DNRA	Dissimilatory nitrite reduction to ammonia
dNTP	Deoxynucleoside triphosphate
DO	Dissolve oxygen
DTU	Technical University of Denmark
EDTA	Ethylenediamine tetraacetic acid
FA	Free ammonia

FACS	Fluorescence-activated cell sorting
FISH	Fluorescence <i>in situ</i> hybridization
FOV	Fields of View
FSC	<i>Forward scatter</i>
GHG	Greenhouse gas
HAO	Hydroxylamine oxidoreductase enzyme
HMM	Hidden Markov model
HPLC	High-performance liquid chromatography
HRP	Horseradish-peroxidase
HRT	Hydraulic retention time
HTS	<i>High-throughput sequencing</i>
HZO	Hydrazine-oxidizing enzyme
MAR-FISH	Microautoradiography combined with Fluorescence <i>in situ</i> hybridization
MDA	<i>Multiple displacement amplification</i>
MLSS	Mixed liquor suspended solids
<i>nirK</i>	Nitrite reductase gene
NOB	Nitrite-oxidizing bacteria
<i>nosRZDFYL</i>	Nitrous oxide reductase genes
NXR	Nitrite oxidoreductase enzyme
<i>nxrA, nxrB</i>	Nitrite oxidoreductase genes
ORFs	Open reading frames
OTU	Operational taxonomic unit
PCA	Principal component analysis
PCR	Polymerase chain reaction
PBS	Phosphate buffer saline
PFA	Paraformaldehyde
PTFE	Polytetrafluoroethylene
qPCR	Quantitative real-time PCR
QIIME	Quantitative Insights Into Microbial Ecology
RACS	Raman-activated cell sorting
RDP	Ribosomal database project
RNA	Ribonucleic Acid
rRNA	Ribosomal RNA

RRT	Resource Ratio Theory
SHARON	Single reactor system for high rate ammonia
SRT	Sludge retention time
SSC	Side scatter
TCA	Tricarboxylic acid cycle
TKN	Total Kjeldahl Nitrogen
TSS	Total suspended solids
UHP	Ultra-high purity
VSS	Volatile suspended solids
WWTP	Wastewater treatment plant

## Nomenclature

$F_d$	Fraction of active biomass
$K_d$	Endogenous decay
$k_{DO}$	Half saturation constant for oxygen
$k_{NH_3}$	Half saturation constant for ammonia
$N$	AOB concentration
$rN_2O$	$N_2O$ production rate
$rTKN$	TKN consumption rate
$X_{AOB}$	AOB biomass
$Y_{AOB}$	AOB Growth yield
$Y_{N_2O}$	$N_2O$ fraction
$\mu_{max}$	Maximum specific growth rate
$\Delta G^\theta'$	Gibbs free energy

## Table of Contents

<b>Abstract.....</b>	i
<b>Acknowledgments .....</b>	iii
<b>Abbreviations .....</b>	v
<b>List of Figures.....</b>	xi
<b>List of Tables .....</b>	xvi
<b>Chapter 1. Introduction.....</b>	1
1.1 Literature review .....	1
1.1.1 <i>WWTP and energy management</i> .....	1
1.1.2 <i>Nitrogen removal</i> .....	3
1.1.3 <i>Nitrification process</i> .....	4
1.1.4 <i>Factors controlling nitrifying activity</i> .....	11
1.1.5 <i>Culture independent techniques</i> .....	14
1.2 Scope and goals of the study .....	17
<b>Chapter 2. Experimental plan.....</b>	18
2.1 Adaptation of nitrifying bacteria at low DO conditions .....	18
2.2 Impact of N <sub>2</sub> O emissions in activated sludge operated at low DO concentrations .....	18
2.3 A flow cytometry–fluorescence in situ hybridization method to sort AOB under low dissolved oxygen .....	19
<b>Chapter 3. Adaptation of nitrifying bacteria at low dissolved oxygen conditions .....</b>	20
3.1 Introduction .....	20
3.2 Materials and Methods .....	22
3.2.1 <i>Continuous reactor</i> .....	22
3.2.2 <i>Monitoring and sample preparation</i> .....	23
3.2.3 <i>DNA extraction</i> .....	24
3.2.4 <i>Preparing standards for quantitative PCR</i> .....	24
3.2.5 <i>Quantitative PCR of nitrifiers</i> .....	25
3.2.6 <i>Calculation of AOB biomass, fraction and yield</i> .....	26
3.2.7 <i>Modelling AOB dynamics at low DO</i> .....	26
3.2.8 <i>Amplicon sequencing</i> .....	27
3.2.9 <i>Statistical analysis</i> .....	30
3.3 Results and Discussion.....	30
3.3.1 <i>Effect of DO concentration on nitrification performance</i> .....	30
3.3.2 <i>Nitrifying community adapted under low DO</i> .....	32

3.3.3 Possible metabolic pathways of AOB.....	43
3.4 Conclusions.....	44
<b>Chapter 4. Impact of nitrous oxide emissions in activated sludge operated at low dissolved oxygen concentrations .....</b>	<b>46</b>
4.1 Introduction.....	46
4.2 Materials and methods .....	47
4.2.1 Setup and operation of continuously stirred bioreactors.....	47
4.2.2 Batch experiments .....	48
4.2.3 Calculation of $N_2O$ production rate .....	49
4.2.4 Statistical analysis.....	50
4.3 Results and Discussion .....	50
4.3.1 $N_2O$ production at different oxygenation levels .....	50
4.3.2 Contribution of DO to $N_2O$ emissions from WWTP .....	53
4.4 Conclusion .....	56
<b>Chapter 5. Detection and isolation of ammonia-oxidizing bacteria grown under low dissolved oxygen by fluorescence in situ hybridization - flow cytometry cell sorting protocol .....</b>	<b>57</b>
5.1 Introduction.....	57
5.2 Materials and Methods.....	59
5.2.1 Fixation test.....	59
5.2.2 FISH hybridization and DNA staining .....	59
5.2.3 Sonication.....	61
5.2.4 Flow cytometry and Sorting .....	61
5.2.5 DNA extraction and amplification .....	62
5.2.6 Amplification of amoA gene by PCR.....	62
5.2.7 DNA library preparation, sequencing and post-processing .....	63
5.2.8 Extract reads associated with AOB.....	63
5.3 Results and Discussion .....	64
5.3.1 Hybridization efficiency and detection of AOB by flow cytometry .....	64
5.3.2 Effect of sonication on AOB .....	67
5.3.3 Sorting of AOB and whole genome amplification .....	68
5.3.4 Sequencing verification of AOB sorted genomes .....	70
5.3.6 Metagenomics assembly.....	73
5.4 Conclusion .....	78
<b>Chapter 6. General conclusions.....</b>	<b>79</b>

<b>Chapter 7. Future work.....</b>	81
<b>Chapter 8. Appendix.....</b>	83
8.1 FA concentration .....	83
8.2 Description of the risk based model (Ofițeru and Curtis, 2009) .....	83
8.3 Calculation of N <sub>2</sub> O production.....	84
8.4 Estimation of the N <sub>2</sub> O impact in real WWTP conditions .....	85
8.5 Flow cytometry dot plots for activated sludge samples .....	86
8.6 Enrichment of AOB from activated sludge full-scale treatment plant.....	88
8.7 Extraction of AOB genomes .....	90
<b>References .....</b>	92

## List of Figures

<b>Figure 1.1</b> UK GHGs emissions estimated in 2016 DBEIS (2017): total GHGs (light blue line) and CO <sub>2</sub> (dark blue line).....	2
<b>Figure 1.2</b> Schematic illustration of the microbial process reactions in the nitrogen cycle. Abbreviations: Anammox, anaerobic ammonium oxidation; DNRA, dissimilatory NO <sub>2</sub> <sup>-</sup> reduction to NH <sub>3</sub> ; Adapted from Daims <i>et al.</i> (2016). .....	4
<b>Figure 1.3</b> NH <sub>3</sub> catabolism of AOB and the proteins involved. The roman numbers refer to the enzyme complex III (ubiquinol-cytochrome <i>c</i> reductase) and complex IV (cytochrome <i>c</i> oxidase) in the respiratory chain. Adapted from Sayavedra-Soto and Arp (2011). .....	6
<b>Figure 3.1</b> Design of the four laboratory bioreactors set-up.....	23
<b>Figure 3.2</b> Nitrification performance in laboratory-scale chemostat reactors operated at low and high DO conditions. TKN removal (black circles), NO <sub>2</sub> <sup>-</sup> concentration (dark grey triangles) and NO <sub>3</sub> <sup>-</sup> concentration (light grey squares) in reactors with low aeration (a) and high aeration (b).....	31
<b>Figure 3.3</b> Average pH measured in the reactors at low and high aeration.....	32
<b>Figure 3.4</b> AOB cell abundances (grey diamond) obtained from qPCR in the reactors under low (a) and high (b) DO concentrations and their respective TKN consumption (black square) over 143 days.....	34
<b>Figure 3.5</b> Exponential regression curve of the AOB cell abundance under low DO. The slope of the line represents the specific growth rate of the adapted AOB following an exponential growth ( $r^2 = 0.9$ ). .....	35
<b>Figure 3.6</b> Model for two species (AOB1 – red; and AOB2 – blue; total AOB – green) with the experimental parameters: 130 mg/L of NH <sub>3</sub> in the inlet (purple) and 0.2 mg/L of DO. Initial concentrations of the two species were modelled with arbitrary values in which the concentrations of AOB2 varied: 1 (a), 0.001 (b), 0.01 (c), 0.1 (d), 10 (e) and f (100).....	36
<b>Figure 3.7</b> Relative abundance of the AOB close related sequences from 16S rRNA sequencing in the reactors at low and high DO over 66 days. Each bar represents the sample collected at a certain time and condition and all the different clusters are represented by colours: cluster 6 (red) and cluster 7 (blue). Each sample was run in duplicate: replicate 1 (black) and 2 (grey). The grey bars represent the sequences with no species assignments. ....	38
<b>Figure 3.8</b> Observed OTUs average at times 0, 3, 17, 30, 44 and 66 days in low and high DO. ....	38

<b>Figure 3.9</b> PCA analysis based on the Bray Curtis similarity of the OTUs derived from Illumina sequencing <i>amoA</i> gene. Clusters are separated by oxygen treatment and reactors: low DO (blue – R1_L and R2_L) and high DO (red – R3_H and R4_H). ....	39
<b>Figure 3.10</b> Relative abundance of the 100 most abundant AOB close related sequences from <i>amoA</i> gene sequencing in the reactors at low and high DO over 66 days. Each bar represents the sample collected at a certain time and condition and all the different clusters are represented by colours: cluster 0 (red), cluster 2 (gold), cluster 6 (blue) and cluster 7 (purple). Each sample was run in duplicate: replicate 1 (black) and 2 (grey). The grey bars represent the sequences with no species assignments. ....	40
<b>Figure 3.11</b> <i>Nitrospira</i> (black) and <i>Nitrobacter</i> (grey) cell abundances (cells/mL) obtained from qPCR in the reactors under low DO (diamond) and high (square) conditions over 127 days. ....	42
<b>Figure 3.12</b> COD (grey) and alkalinity (black) concentration measured in the low aeration (squares) and high aeration (circles). ....	43
<b>Figure 4.1</b> Schematic diagram of the experimental system: four laboratory-scale bioreactor operated at low (R1_L and R2_L) and high (R3_H and R4-H) DO (a); Batch experiments (b); GC analysis for N <sub>2</sub> O analysis (c). ....	49
<b>Figure 4.2</b> N <sub>2</sub> O emissions for each batch experiment operated at different times and different oxygen concentrations (a): low DO (black diamond) and high DO (grey square). These analyses enabled to calculate the N <sub>2</sub> O production rate by linear regression (b). ....	52
<b>Figure 4.3</b> Variation of electricity equivalent estimated from a constant NH <sub>3</sub> fraction at different NH <sub>3</sub> influent assuming an effluent of 2 mg NH <sub>3</sub> /L. ....	55
<b>Figure 5.1</b> AOB and all bacteria labelled with Cy3 (red) and FITC (green), respectively after a hybridization time of 2h. Cells were fixed in paraformaldehyde (a), glycerol (b) and ethanol (c). Bar, 4.5 mm. ....	65
<b>Figure 5.2</b> Flow cytometry outputs of bacteria cells from activated sludge samples fixed with glycerol (a), paraformaldehyde (b) and ethanol (c). Cells fixed in glycerol were hybridized with: Cy3 and SYTO 9 (I), Cy3 and FITC (II), Cy5 and SYTO 9 (III) and Cy5 and FITC (IV); AOB cell clusters were selected using scattergrams of Cy3/Cy5 versus FITC/SYTO 9 (big square) and sorted using the respective subsets plotted by SSC versus Cy3/Cy5 (small square). Cells fixed in ethanol were tested at different times: 24 months (I), 6 months (II), 2 months (III). The different colours indicate the different populations: glycerol fixation – regions with a red dark outline indicate the target population with the respective percentage relative to the sub-population with red light; ethanol and paraformaldehyde fixation – regions	

with a red outline indicate the target population with the respective percentage relative to total DNA with blue colour. ....	66
<b>Figure 5.3</b> Flow cytometry outputs of the sonication test applied to samples from activated sludge. (a) Scattergrams of the different pre-treatments showing SYTO 9 versus Cy5: bath sonication for 2 (I), 4 (II), 6 (III), and 8 (IV) min and ultrasonication for 2x30 s at 24 W (V), 2x15 s at 74 W (VI) and 2x30 s at 74 W (VII). The different colours indicate the different populations: regions with a red outline indicate the target population with the respective percentage relative to total DNA with blue colour. (b) Histograms of SYTO 9 (I) and Cy5 (II) for all different pre-treatments.....	68
<b>Figure 5.4</b> Flow cytometry scattergrams based on SYTO 9 versus Cy5 parameters of the AOB sorting of four bioreactor samples: (a) R1_L, (b) R2_L, (c) R3_H and (d) R4_H. Each plot contains $2 \times 10^6$ events and the AOB region of the plot indicates the events gated for sorting. The different colours indicate the different populations: region with a red outline indicate the sorted target population with the respective percentage relative to total DNA with blue colour. ....	69
<b>Figure 5.5</b> Agarose gel electrophoresis (1.5% agarose) of PCR amplicons of <i>amoA</i> gene in the MDA extracts. Lane 1 and 6 represent ladder (50 - 2,000 bp DNA molecular weight ladder) and lane 2, 3, 4 and 5 represent reactor R1_L, R2_L, R3_H and R4_H, respectively.	70
<b>Figure 5.6</b> Taxonomic distribution based on 16S gene sequences of the sorted samples: a – R1_L; b – R2_L; c – R3_H; d – R4_H. The data were visualized using Krona (Ondov <i>et al.</i> , 2011). The percentages correlate each phylogeny within the total assigned sequences. ....	71
<b>Figure 5.7</b> Binning of scaffolds into population genomes from the metagenomes laboratory-scale reactors by differential coverage: (a) R1_L and R2_L; (b) R3_H and R4_H. Each circle represents a scaffold (only $\geq 5$ kbp are shown), scaled by the square root of their length and coloured by phylum level assignment of essential genes. The potential genome bins are represented by grouping similarly coloured circles.....	74
<b>Figure 5.8</b> PCA of the subset bins: (a) genome bins 1 (I), 2 (II) and 3 (III) in the low DO samples; (b) genome bins 1 (I), 2 (II) in the high DO samples. The scaffolds are scaled by length and coloured by GC content. ....	75
<b>Figure 5.9</b> Phylogenetic tree generated from alignment of <i>amoCAB</i> sequences obtained by BLAST and the <i>amoCAB</i> genes sequences retrieved in the extracted AOB genomes. The tree is based on the maximum likelihood phylogenetic method and shows the relationship between the low (RL_1 and RL_2 - blue) and high (RH_3 and RH_4 - red) DO reactors. The bootstrap consensus tree was inferred from 1,000 replicates. ....	77

<b>Figure 8.1</b> Flow cytometry outputs of bacteria cells from activated sludge samples fixed with glycerol (a), paraformaldehyde (b) and ethanol (c). Cells fixed in glycerol were hybridized with: Cy3 and SYTO 9 (I), Cy3 and FITC (II), Cy5 and SYTO 9 (III) and Cy5 and FITC (IV); AOB cell clusters were initially selected using scattergrams of SSC/FSC or Cy5/SYTO 9. Cells fixed in ethanol were tested at different times: 24 months (I), 6 months (II), 2 months (III). The different colours indicate the different populations: regions with a blue outline indicate the total population with the respective percentage relative to the total number of events with black.....	86
<b>Figure 8.2</b> Flow cytometry outputs of the sonication test applied to samples from activated sludge. Scattergrams of the different pre-treatments showing SYTO 9 versus Cy5: bath sonication for 2 (I), 4 (II), 6 (III), and 8 (IV) min and ultrasonication for 2x30 s at 24 W (V), 2x15 s at 74 W (VI) and 2x30 s at 74 W (VII). The different colours indicate the different populations: regions with a blue outline indicate the total population with the respective percentage relative to the total number of events with black.....	87
<b>Figure 8.3</b> Flow cytometry outputs of the concentration test applied to samples from activated sludge. Scattergrams of the different concentrations of Cy5 showing SYTO 9 versus Cy5: 2.5 (I), 5 (II), 10 (III), and 20 (IV) $\mu\text{g}/\mu\text{L}$ . The different colours indicate the different populations: regions with a red outline indicate the target population with the respective percentage relative to total DNA with blue colour.....	87
<b>Figure 8.4</b> Flow cytometry outputs of the multi probe test applied to samples from activated sludge. Cells were hybridized with all probes (a): Cy3/Cy5 (I), Cy5/SYTO 9 (II) and Cy3/SYTO 9 (III); hybridized with only Cy5 (b); hybridized with only Cy3 (c): all Cy3 (I), Nsm156 (II) and Nsv443 (III). The different colours indicate the different populations: regions with a red outline indicate the target population with the respective percentage relative to total DNA with blue colour.....	88
<b>Figure 8.5</b> Flow cytometry scattergrams based on SYTO 9 versus Cy5 parameters of the AOB sorted in samples collected from full-scale activated sludge plant. Each plot contains $2 \times 10^6$ events and the AOB region of the plot indicates the events gated for sorting. The different colours indicate the different populations: region with a green outline indicate the sorted target population with the respective percentage relative to total DNA with blue colour.....	88
<b>Figure 8.6</b> Taxonomic distribution based on 16S gene sequences of the sorted samples collected from activated sludge treatment plant. The data were visualized using Krona (Ondov <i>et al.</i> , 2011). The percentages correlate each phylogeny within the total assigned sequences.	89
<b>Figure 8.7</b> PCA of the subset genome bins 1 (a), 2 (b) and 3 (c) in the low DO samples. The scaffolds are scaled by length and coloured by GC content. ....	90

**Figure 8.8** PCA of the subset genome bins 1 (a) and 2 (b) in the high DO samples. The scaffolds are scaled by length and coloured by GC content.....91

## List of Tables

<b>Table 3.1</b> Description of the primers used for the qPCR and sequencing analysis.....	25
<b>Table 3.2</b> Kinetic parameters for the AOB species .....	27
<b>Table 4.1</b> Characteristics of the laboratory-scale reactors operated at different DO concentrations .....	48
<b>Table 4.2</b> Nitrogen removal (TKN) and production ( $\text{NO}_2^-$ , $\text{NO}_3^-$ , $\text{N}_2\text{O}$ ) rate and percentage of $\text{N}_2\text{O}$ emission in activated sludge laboratory-scale reactors operated at low and high DO.....	52
<b>Table 5.1</b> Oligonucleotide probes and primers used in this study.....	60
<b>Table 8.1</b> Summary of nitrogen compounds concentrations and mass balance.....	85
<b>Table 8.2</b> Estimation of $\text{N}_2\text{O}$ impact in electricity equivalent at different HRTs. ....	85
<b>Table 8.3</b> Estimation of $\text{N}_2\text{O}$ impact in electricity equivalent assuming a TKN effluent of 2 mg/L .....	86

## Chapter 1. Introduction

### 1.1 Literature review

#### 1.1.1 WWTP and energy management

WWTPs play an important role in the water reuse and recycling. These plants are designed to reduce the concentration of pollutants present in wastewaters including: organic compounds, toxic organics, nitrogen and phosphorus and, in certain circumstances, pathogens. This allows engineers to return water to the environment without prejudicing public health and environmental quality. WWTP technology has evolved to meet both the growing demand of water resources, increasing urban populations and more stringent environmental conditions (US Environmental Protection Agency, 1993). The traditional plant technologies remove nutrients and organic matter content by the use of aerated biological processes, which typically operate in suspended growth (activated sludge), attached growth (trickling filters and biological contactors), combined suspended and attached growth or lagoons (Tchobanoglous *et al.*, 2003).

One biological wastewater treatment technology, activated sludge, is probably responsible for treating most municipal sewage and many industrial wastewaters. Initially, a conventional sewage treatment removes coarse solids and other large materials by screening and grit removal following a primary sedimentation to remove floating and settleable materials. In the activated sludge process the organic matter remaining after primary sedimentation is converted to carbon dioxide ( $\text{CO}_2$ ), water and biomass by a heterogeneous microbial culture of bacteria, protozoa, rotifers, and fungi. This biomass is responsible for the degradation of nitrogenous compounds present in the wastewater by autotrophic microorganisms that use inorganic compounds as their electron donor and  $\text{CO}_2$  as their carbon source (Tchobanoglous *et al.*, 2003). The activated sludge treatment process comprises an aerated tank with diffused aeration or mechanical aeration, followed by a secondary clarifier (Evans and Furlong, 2003). An adequate oxygen concentration must be maintained in the aeration tank to ensure the oxygen transfer from the gas phase to the liquid phase and thus to maintain the presence of active and waste degrading microorganisms (Tchobanoglous *et al.*, 2003). The supply of oxygen is an energy intensive process (Tchobanoglous *et al.*, 2003; McCarty *et al.*, 2011). Typically, 3% of the overall electrical energy usage of many developing countries is for

wastewater treatment (Curtis, 2010). In the UK, the water industry uses around 0.6 kWh/m<sup>3</sup> in wastewater treatment, about 50% of this is used for aeration (Curtis, 2010; McCarty *et al.*, 2011). The current and foreseeable increases in electricity prices have increased and will increase the expense of these treatment systems. The sustainable design and management of WWTP requires that we minimize the energy use (Curtis, 2010; McCarty *et al.*, 2011). To understand how we can minimise energy demands without the process failure, it is necessary to understand both the minimum oxygen requirements of nitrification in WWTPs and the true physiology of the process.

Saving energy in WWT processes by improving energy efficiency can also provide environmental benefits (US Environmental Protection Agency, 1993). The largest GHG emissions in UK is CO<sub>2</sub> accounting 82% in 2015 (DBEIS, 2017). Although the GHGs emissions have decreased in recent years (Figure 1.1), the water industry is still a significant user of energy and represents around 1% of the UK's CO<sub>2</sub> emissions (Ofwat, 2010). This value may increase due to population growth and the energy demands of meeting increases in water quality standards (Curtis, 2010; Byrns *et al.*, 2012). The challenge is to reduce both energy consumption and GHGs emissions without compromising the effluent quality in order to mitigate climate change. Activated sludge plants are still used has the main process for nutrient removal, mainly because of the large number of plants implementing this technology and the lack of better alternatives (Curtis, 2010). Therefore, we must adapt this WWT system to increase its economic and environmental sustainability.

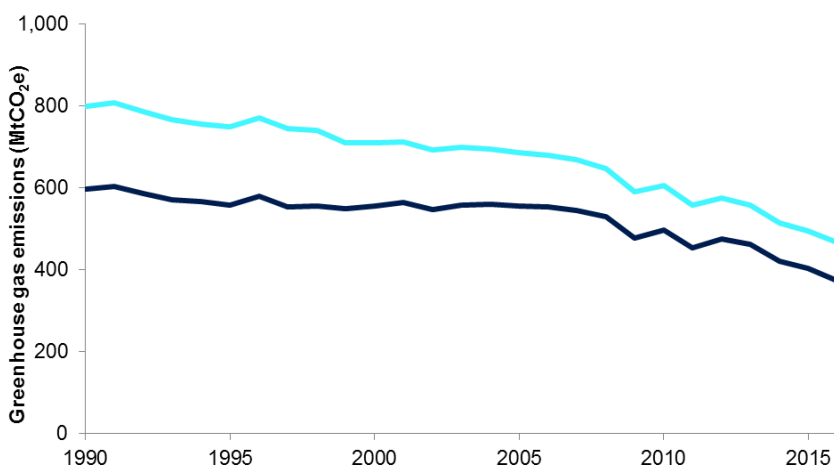


**Figure 1.1** UK GHGs emissions estimated in 2016 DBEIS (2017): total GHGs (light blue line) and CO<sub>2</sub> (dark blue line).

## 1.1.2 Nitrogen removal

One of the major components of proteins and nucleic acids in the biomass, nitrogen is considered an essential element for life. It can assume different oxidation states range from -3 to +5, serving as an electron donor or acceptor in a variety of mediated transformations (i.e. fixation, ammonification, nitrification and denitrification). Nitrogen exists in many forms in the Earth and can be present in wastewater sewage as ammonium ( $\text{NH}_4^+$ ), ammonia ( $\text{NH}_3$ ), nitrite ion ( $\text{NO}_2^-$ ), nitrate ion ( $\text{NO}_3^-$ ), nitrogen gas ( $\text{N}_2$ ) and organic nitrogen (protein, amino acids and amino sugars) (US Environmental Protection Agency, 1993).

Domestic sewage contains typically 25 – 45 mg/L of nitrogen compounds typically derived from anthropogenic sources (Barnes and Bliss, 1983; Tchobanoglous *et al.*, 2003). The presence of nitrogen in surface waters is a major concern, since it can have adverse ecological and human health effects. The accumulation of nitrogen in the surface water causes eutrophication which increases the concentration of algae and decreases the concentration of DO with predictable and deleterious effects on the respiration of fish, benthic aquatic animals, and benthic algae. Also,  $\text{NH}_3$  is toxic to aquatic organisms, such as fish, and high levels of  $\text{NO}_3^-$  and  $\text{NO}_2^-$  in drinking waters can cause infant methemoglobinemia and carcinogenesis (US Environmental Protection Agency, 1993). Removal of the nitrogen compounds from wastewaters needs to be very effective, with major reductions being achieved routinely (Rittmann and McCarty, 2001).

Nitrogen elimination from wastewater comprises several processes which alternates between oxic and anoxic conditions: assimilation, ammonification, nitrification, denitrification and fixation (Figure 1.2) (Barnes and Bliss, 1983; Tchobanoglous *et al.*, 2003; Daims *et al.*, 2016). Assimilation uses inorganic nitrogen to form new biomass and ammonification comprises the mineralization of organic nitrogen into  $\text{NH}_3$ . Nitrification is a crucial process in the nitrogen removal based on the oxidation of  $\text{NH}_3$  to  $\text{NO}_2^-$  by AOB and then  $\text{NO}_2^-$  to  $\text{NO}_3^-$  by NOB (Tchobanoglous *et al.*, 2003; Prosser, 2005). Denitrification is the reduction of  $\text{NO}_2^-$  or  $\text{NO}_3^-$  to gaseous nitrogen compounds (Tchobanoglous *et al.*, 2003).  $\text{N}_2$  is the main end product while the nitric oxide (NO) and  $\text{N}_2\text{O}$  occur, at low concentrations, as intermediates (Schmidt *et al.*, 2003). Denitrification is carried out by chemoorganotrophic, lithoautotrophic, and phototrophic bacteria and some heterotrophic fungi (Shoun and Tanimoto, 1991; Zumft, 1997). However, autotrophic bacteria are also able to denitrify under oxygen-reduced or anoxic conditions, which means that they can shift to  $\text{NO}_2^-$  or  $\text{NO}_3^-$  respiration when oxygen concentration is limited (Bock *et al.*, 1995).

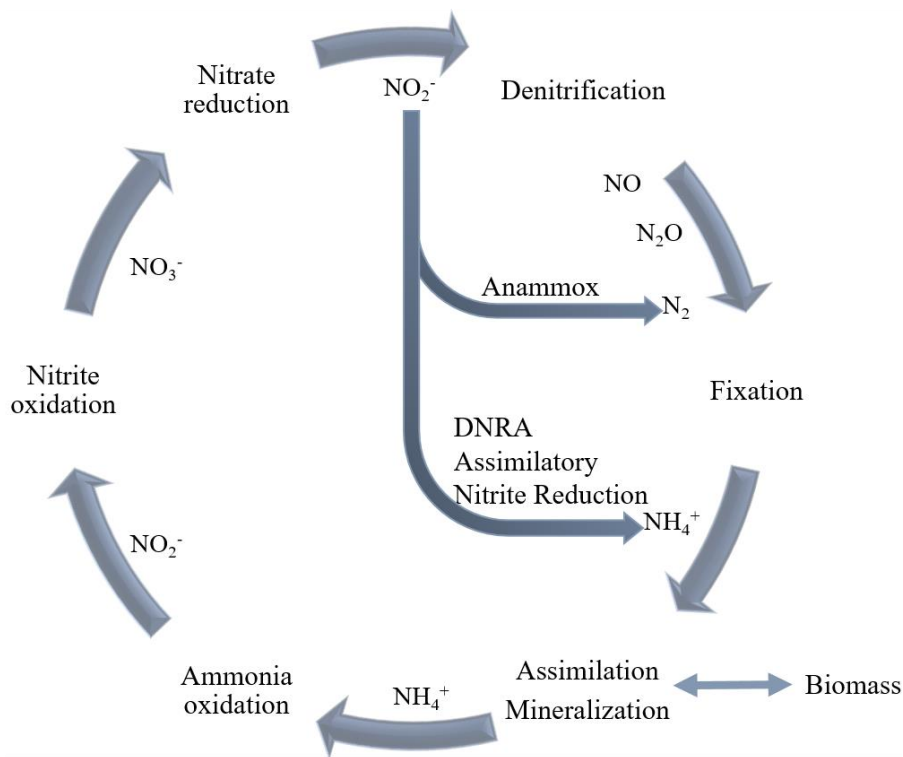


**Figure 1.2** Schematic illustration of the microbial process reactions in the nitrogen cycle. Abbreviations: Anammox, anaerobic ammonium oxidation; DNRA, dissimilatory  $\text{NO}_2^-$  reduction to  $\text{NH}_3$ ; Adapted from Daims *et al.* (2016).

### 1.1.3 Nitrification process

#### 1.1.3.1 Stoichiometry and energetics of nitrification

Nitrification involves two sequential oxidation steps:

(1.1)



(1.2)



Based on the stoichiometric equations above, the theoretical oxygen demand required for complete oxidation of  $\text{NH}_3$  is 4.57 g  $\text{O}_2/\text{g N}$  oxidized, with 3.43 g  $\text{O}_2/\text{g N}$  for the first step in nitrification ( $\text{NH}_3$  oxidation) and 1.14 g  $\text{O}_2/\text{g N}$  for the second step in nitrification ( $\text{NO}_2^-$  oxidation) (Tchobanoglous *et al.*, 2003). Looking at the equations, 2 mol of acidity are produced per each mol of  $\text{NH}_4^+$  (Tarre and Green, 2004). Consequently, approximately 7.14 g of alkalinity as  $\text{CaCO}_3$  for each g of  $\text{NH}_4^+-\text{N}$  converted is required for alkalinity to buffer the system (Tchobanoglous *et al.*, 2003).

The energy released per mole of nitrogen is higher in the first step of nitrifiers than in the second step ( $\Delta G^\circ = -275 \text{ kJ/mol}$  for  $\text{NH}_3$  oxidation to  $\text{NO}_2^-$  and  $\Delta G^\circ = -74 \text{ kJ/mol}$  for  $\text{NO}_2^-$  oxidation to  $\text{NO}_3^-$ ). The yield (the biomass produced per mass of  $\text{NH}_4^+$  or  $\text{NO}_2^-$  oxidized) of nitrifying organisms depends on the efficiency with which the organisms convert the energy released into cells (US Environmental Protection Agency, 1993; Daims *et al.*, 2016). Due to their chemolithotrophic nature, nitrifiers have a low growth yield. In particular, as autotrophs, nitrifying bacteria obtain their carbon from the fixation of inorganic  $\text{CO}_2$  through the Calvin-Bassham-Benson cycle: this requires energy. As little energy is obtained through the oxidation of inorganic chemical compounds, the specific growth rates and growth yields of these bacteria are low in comparison to heterotrophic bacteria which consume organic compounds and do not need to fix  $\text{CO}_2$  (Prosser, 1989). Also nitrogen, as electron donor, releases less electrons and generates less energy for the formation of new biomass than organic electron donors do (Rittmann and McCarty, 2001).

The kinetics and metabolic activities involved in nitrification process depend also on several reaction intermediates and enzymes. Specific oxygen uptake and nitrifier biomass yield coefficients are very important parameters in the design and operation of efficient nitrifying WWTPs (Tchobanoglous *et al.*, 2003).

### **1.1.3.2 Nitrifying bacteria in activated sludge**

#### **1.1.3.2.1 AOB**

AOB are generally aerobic chemolithoautotrophs that use  $\text{NH}_3$  for energy and reduce  $\text{CO}_2$  to obtain carbon (Sayavedra-Soto and Arp, 2011). The catabolic process of  $\text{NH}_3$  oxidation to  $\text{NO}_2^-$  requires four different specialized proteins (Figure 1.3). The oxidation of  $\text{NH}_3$  is firstly catalysed to hydroxylamine ( $\text{NH}_2\text{OH}$ ) by an intermediate ammonia monooxygenase (AMO), followed by the oxidation of  $\text{NH}_2\text{OH}$  to  $\text{NO}_2^-$  by hydroxylamine oxidoreductase (HAO) (Hollocher *et al.*, 1981; Prosser, 2005). AMO is a membrane-bound heteromultimeric enzyme consisted of three polypeptides, while HAO is a periplasmic homotrimer containing multiple *c*-type hemes (Hooper *et al.*, 1997; Arp *et al.*, 2002). Two tetraheme *c* cytochromes, cyt  $c_{554}$  and cyt  $c_{m552}$ , are involved in the electron flux between the HAO and ubiquinone pool (Dispirito *et al.*, 1986; Whittaker *et al.*, 2000). The genes encoding these key enzymes are: *amoCAB* operon encodes the genes for AMO (McTavish *et al.*, 1993; Bergmann and Hooper, 1994; Sayavedra-Soto *et al.*, 1998) and the *hao-orf2-cycAB* operon encodes the genes for HAO and the two cytochromes (Bergmann *et al.*, 1994, 2005;

Sayavedra-Soto *et al.*, 1994). Identical copy number of the four genes are present in AOB genomes (Sayavedra-Soto and Arp, 2011).

Besides the genes for NH<sub>3</sub> catabolism, the genome profile for some AOB revealed genes involved in iron uptake, heavy metal tolerance, multidrug resistance and urease activity (Chain *et al.*, 2003; Koper *et al.*, 2004; Klotz *et al.*, 2006; Stein *et al.*, 2007). Although the autotrophic metabolism predominates, complete metabolic pathways for the utilisation of some organic carbon compounds, such as pyruvate, fructose, and glutamate, are present in the genomes but the transporters for those compounds are absent (Chain *et al.*, 2003; Stein *et al.*, 2007). Moreover, all known AOB genomes harbor the genes to express both copper-containing dissimilatory NO<sub>2</sub><sup>-</sup> reductase (*nirK*) and several NO reductases, but genes encoding N<sub>2</sub>O reductase are absent (Casciotti and Ward, 2001; Beaumont *et al.*, 2004, 2005; Upadhyay *et al.*, 2006; Garbeva *et al.*, 2007).

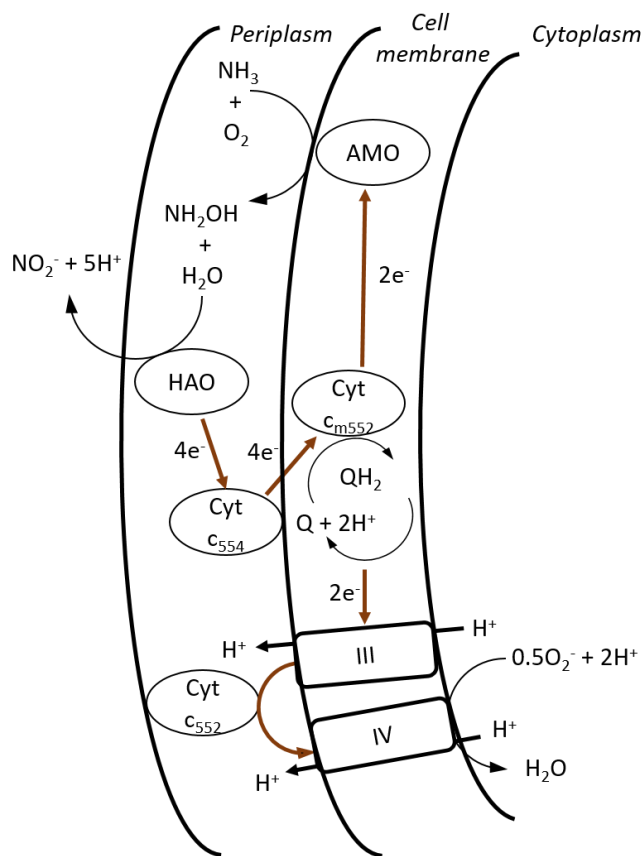


**Figure 1.3** NH<sub>3</sub> catabolism of AOB and the proteins involved. The roman numbers refer to the enzyme complex III (ubiquinol-cytochrome *c* reductase) and complex IV (cytochrome *c* oxidase) in the respiratory chain. Adapted from Sayavedra-Soto and Arp (2011).

Considerable effort has been expended on ecological and physiological characterization of nitrifiers. Taxonomically, AOB belong to two groups: Betaproteobacteria

and Gamaproteobacteria. The family *Nitrosomonadaceae* is the most studied of the Betaproteobacteria, including the genera *Nitrosomonas*, *Nitrosospira*, *Nitrosovibrio* and *Nitrosolobus* genera (Head *et al.*, 1993; Teske *et al.*, 1994; Utåker *et al.*, 1995; Purkhold *et al.*, 2000; Koops *et al.*, 2006). Generally, *Nitrosomonas* genus is divided into several lineages: *Nitrosomonas europaea*/*Nitrosococcus mobilis*, *Nitrosomonas communis*, *Nitrosomonas oligotropha*, *Nitrosomonas marina*, *Nitrosomonas crytolerans* and *Nitrosomonas* sp. Nm143 (Koops *et al.*, 2006). On the other hand, members of the *Nitrosococcus* genus are purple sulfur bacteria (*Chromatiaceae* family) which are affiliated with the class Gammaproteobacteria (Klotz *et al.*, 2006). Currently, the complete genome sequences of five AOB have been published: *Nitrosomonas europaea* ATCC 19718, isolated from wastewater (Chain *et al.*, 2003); *Nitrosomonas eutropha* C-91, isolated from sewage (Stein *et al.*, 2007), *Nitrosospira multiformis* ATCC 25196, isolated from soil (Norton *et al.*, 2008), *Nitrosococcus oceanii* ATCC 19707 (equal to C-107), isolated from marine source (Klotz *et al.*, 2006), and *Nitrosomonas ureae* Strain Nm10, isolated from soils (Kozlowski *et al.*, 2016). The AOB genomes are smaller than many other members of Proteobacteria at approximately 3 Mb (Arp *et al.*, 2007).

AOB have been identified in different natural and engineered environments including WWTPs (Kowalchuk and Stephen, 2001). The adaptation and competition under low/high NH<sub>3</sub> or oxygen concentrations is different within the AOB bacteria and the ecosystem (Geets *et al.*, 2006). Different species have differing affinities for NH<sub>3</sub> (Geets *et al.*, 2006). *N. oligotropha* and *Nitrosospira* clusters are able to outcompete *N. europaea* cluster at very low NH<sub>3</sub> concentrations (Bollmann *et al.*, 2002). Whereas *N. europaea* and *Nitrosococcus* cluster can tolerate high NH<sub>3</sub> concentrations (Sayavedra-Soto and Arp, 2011). Furthermore, the sublineage *N. oligotropha*-like AOB were exclusively dominant in limited DO conditions and *N. europaea* and *N. oligotropha* lineages were the prevalent AOB in systems where DO concentration was high (de Bie *et al.*, 2001; Gieseke *et al.*, 2001; Bellucci *et al.*, 2011; Fitzgerald *et al.*, 2015). However, the adaptation of members of the *N. europaea* and *N. oligotropha* linages has been reported under low oxygen concentrations, where *N. oligotropha* lineage was dominant under non-limiting oxygen (Park and Noguera, 2004, 2007).

Different metabolisms have been associated with anoxic conditions (Arp *et al.*, 2007). In the absence of oxygen, NH<sub>3</sub> is oxidized to NH<sub>2</sub>OH and NO, replacing molecular oxygen by nitrogen dioxide or nitrogen tetroxide (Schmidt and Bock, 1997, 1998). Under anoxic conditions, AOB species are able to denitrify (Abeliovich and Vonshak, 1992; Bock *et al.*, 1995). It is believed that *N. europaea* and *N. eutropha* can grow mixotrophically under oxygen limiting or anaerobic conditions in the presence of pyruvate, lactate, acetate, serine,

succinate and fructose (Beyer *et al.*, 2009; Schmidt, 2009; Bellucci *et al.*, 2011). The biological mechanism for the adaptation to low DO for nitrification are not fully understood, particularly the presence or absence of characteristic genes and regulation of gene expression in AOB.

### 1.1.3.2.2 NOB

The second step of nitrification,  $\text{NO}_2^-$  oxidation to  $\text{NO}_3^-$ , is carried out by NOB. This reaction is catalysed by the  $\text{NO}_2^-$  oxidoreductase (NXR) enzyme complex, which is a heterodimer consisting of one  $\alpha$  subunit (large subunit) and one  $\beta$  subunit (small subunit), encoded by the *nxrA* and *nxrB* genes, respectively (Starkenburg *et al.*, 2011). The NXR transports two electrons per oxidized  $\text{NO}_2^-$  into the electron transport chain (Daims *et al.*, 2016). The molecular organization of the NXR varies among different NOB lineages (Starkenburg *et al.*, 2011).

All known NOB are Gram-negative eubacteria with the ability to use  $\text{NO}_2^-$  as a sole source of energy and  $\text{CO}_2$  as the main source of carbon (Abeliovich, 2006). NOB are more diverse than AOB and seven genera have been classified with the phenotype of  $\text{NO}_2^-$  oxidation: *Nitrobacter* (Woese *et al.*, 1984), *Nitrotoga* (Alawi *et al.*, 2007), *Nitrococcus* (Watson and Waterbury, 1971), *Nitrospira* (Watson *et al.*, 1986; Ehrlich *et al.*, 1995), *Nitrospina* (Watson and Waterbury, 1971; Lücker *et al.*, 2013; Speck *et al.*, 2014), *Nitrolancea* (Sorokin *et al.*, 2012), and ‘*Candidatus Nitro-maritima*’ (Ngugi *et al.*, 2016), belonging to four different phyla Proteobacteria (Alphaproteobacteria, Deltaproteobacteria, Betaproteobacteria), Chloroflexi, Nitrospinae and Nitrospirae. The NOB are not uniformly distributed in the environment (Daims *et al.*, 2016). *Nitrobacter* contains four described species isolated from soil, freshwater in sewage and marine environments. *Nitrospira* often dominates soils and wastewater treatment (Daims, Nielsen, *et al.*, 2001; Starkenburg *et al.*, 2011). Whilst, the phylum Nitrospinae predominates in the marine habitats (Daims *et al.*, 2016).

The lithotrophic growth of NOB is slow. Some strains are able to grow mixotrophically utilizing pyruvate but not acetate, butyrate, and propionate (Bock, 1976; Watson *et al.*, 1986; Starkenburg *et al.*, 2008). Under anaerobic conditions, NXR enables heterotrophic growth with  $\text{NO}_3^-$  as electron acceptor and formate as electron donor (Koch *et al.*, 2015). Some researchers have suggested that the organotrophic growth rates of *Nitrobacter* strains are much slower than lithoautotrophic growth rates (Delwiche and Finstein, 1965) in opposite to the higher growth of *Nitrospira marina* under mixotrophic conditions (Watson *et al.*, 1986).

Nevertheless, Starkenburg *et al.* (2008) found higher growth yield and rate for *Nitrobacter hamburgensis* in the presence of D-lactate and  $\text{NO}_2^-$ , served as the sole carbon source and as energy source respectively.

The competition of *Nitrobacter* and *Nitrospira* in activated sludge of WWTPs for  $\text{NO}_2^-$  is based on different strategies. While *Nitrobacter* is thought to be an r-strategist growing fast and having a low substrate affinity, *Nitrospira* grows slowly and has higher affinity for  $\text{NO}_2^-$  and oxygen (a K- strategist) (Schramm *et al.*, 1999; Kim and Kim, 2006; Dytczak *et al.*, 2008). This suggests that *Nitrospira* will have a competitive advantage at low substrate concentration (Schramm *et al.*, 1999).

Recently several researchers have shown members of the genus *Nitrospira* that catalyse complete nitrification (comammox) (Daims *et al.*, 2015; van Kessel *et al.*, 2015). These *Nitrospira* bacteria possess the full genetic complement to oxidize  $\text{NH}_3$  to  $\text{NO}_3^-$  and utilize the same enzymes AMO and HAO for  $\text{NH}_3$  oxidation, though their forms are distinct from the homologs in AOB.

### **1.1.3.2.3 Ammonia-oxidizing archaea (AOA) and anaerobic ammonium oxidation (Anammox)**

There have been a number of exciting discoveries in the nitrogen cycle in the last few years.

The participation of AOA in the oxidation of  $\text{NH}_3$  to  $\text{NO}_2^-$  was discovered in marine surface waters and soil when amo-like genes were associated with archaeal scaffolds (Venter *et al.*, 2004; Treusch *et al.*, 2005). Könneke *et al.*, (2005) isolated the first nitrifying archaeon, *Nitrosopilus maritimus* strain SCMI, which is affiliated with the group I Crenarchaeota. Metagenomic and metabolic studies have been established to identify AOA in many environments, such as marine and estuarine sediments, oxic and suboxic water columns and activated sludge (Francis *et al.*, 2005; Park *et al.*, 2006).

AOA are generally chemolithoautotrophs, like AOB (Könneke *et al.*, 2005). But the genome sequences of the isolated archaeon organisms revealed deviations from the classical bacterial nitrifying and carbon fixation system (Walker *et al.*, 2010). The three major differences are reported: copper appears to be the primary metal used in electron transfer reactions (rather than iron); the absence of HAO homologue and cytochrome c proteins; the absence of genes coding for the ribulose bisphosphate carboxylase/oxygenase and other

enzymes of the Calvin-Bassham-Benson cycle pointed to the 3-hydroxypropionate/4-hydroxybutyrate pathway as a variant for CO<sub>2</sub> fixation.

The presence of AOA in activated sludge has been demonstrated in many studies (Park *et al.*, 2006; Zhang *et al.*, 2009; Sonthiphand and Limpiyakorn, 2011). Park *et al.* (2006) detected AOA in samples collected from WWTPs operating with aerated-anoxic processes (low DO conditions) and long retention times, but no AOA was observed in treatment plants operated at high DO. However, more recent studies have not detected AOA in reactors operated at low DO concentrations (Bellucci *et al.*, 2011; Liu and Wang, 2013; Fitzgerald *et al.*, 2015). Also, a preference of AOA for low NH<sub>3</sub> concentrations has been reported due to their high affinity for NH<sub>3</sub> (Martens-Habbena *et al.*, 2009; Sonthiphand and Limpiyakorn, 2011).

A novel metabolism was also discovered in the last past years: oxidation of NH<sub>3</sub> under anaerobic conditions (anammox) (Mulder *et al.*, 1995). The novel organisms were obtained from denitrifying bioreactors and were related to members of the order Planctomycetales. So far, there are five recognized genera of anammox bacteria: *Candidatus* ‘Brocadia’, ‘Kuenenia’, ‘Scalindula’, “Jettenia” and ‘Anammoxoglobus’ genera that have all been enriched from activated sludge and natural habitats like marine sediments and oxygen minimum zones (van Niftrik and Jetten, 2012).

In the metabolic pathway of NH<sub>3</sub> oxidation into N<sub>2</sub>, the electron acceptor is NO<sub>2</sub><sup>-</sup> (Strous *et al.*, 1998). The sequential anammox process consists of the conversion of NO<sub>2</sub><sup>-</sup> into NH<sub>2</sub>OH by NO<sub>2</sub><sup>-</sup> reducing enzyme (NR) followed by the reaction between NH<sub>2</sub>OH with the NH<sub>4</sub><sup>+</sup> to produce hydrazine (N<sub>2</sub>H<sub>4</sub>), which is mediated by hydrazine hydrolase (HH). In the final step, N<sub>2</sub>H<sub>4</sub> is converted into N<sub>2</sub> by a hydrazine-oxidizing enzyme (HZO) (Jetten *et al.*, 2001).

The anammox process is restricted by the slow growth rate and low cell yield (Strous *et al.*, 1998) of the bacteria. Moreover, it is inhibited by many factors including: high concentrations of NH<sub>3</sub>, NO<sub>2</sub><sup>-</sup>, organic matter (nontoxic organic matter and toxic organic matter), salts, heavy metals, phosphate and sulphide (Strous *et al.*, 1999; Jin *et al.*, 2012). Anammox bacteria have a high affinity for their substrates (K<sub>s</sub> of NH<sub>3</sub> and NO<sub>2</sub> is < 5 μM) and their metabolism is also reversibly inhibited by very low oxygen levels (Strous *et al.*, 1998).

The discovery of NH<sub>3</sub> oxidation under anaerobic conditions and the nitrogen removal via NO<sub>2</sub><sup>-</sup> instead of the traditional NO<sub>3</sub><sup>-</sup> has been proposed as an attractive alternative in engineered ecosystems (Schmidt *et al.*, 2003). In processes combining anammox bacteria with partial nitrification, the available NH<sub>3</sub> is partially oxidized to NO<sub>2</sub><sup>-</sup> by aerobic ammonia-

oxidizers, whilst the NOB are washed out (Blackburne *et al.*, 2008). In the final step, anammox bacteria convert  $\text{NO}_2^-$  into  $\text{N}_2$ . Application of these processes reduces the oxygen and organic carbon requirements for nitrification and denitrification respectively, achieves a lower sludge production and enhances the denitrification rate (Katsogiannis *et al.*, 2003; Peng and Zhu, 2006). Moreover, the denitrification via  $\text{NO}_2^-$  instead of  $\text{NO}_3^-$  can contribute to the reduction of  $\text{CO}_2$  emissions (Peng and Zhu, 2006). Systems include CANON (completely autotrophic removal of nitrogen over  $\text{NO}_2^-$ ), the DEMON (pH controlled deammonification), or SHARON (single reactor system for high rate  $\text{NH}_3$  removal over  $\text{NO}_2^-$ ) have been designed to couple the partial nitrification and anaerobic  $\text{NH}_3$  oxidation under oxygen limitation (Schmidt *et al.*, 2003).

#### **1.1.4 Factors controlling nitrifying activity**

##### **1.1.4.1 Effects of DO**

In activated sludge, DO is a very important control parameter with significant impact on the rates of nitrifier growth and nitrification efficiency. The oxygen demand required to oxidize a certain amount of biochemical oxygen demand (BOD) and produce biomass, and the oxygen transfer efficiency are influenced by the geometry of the reactor and operational parameters (operational DO, temperature, sludge property, organic loading and mixed liquor suspended solids (MLSS) concentration), limit the required aeration (Hanaki *et al.*, 1990; Tchobanoglous *et al.*, 2003). Stenstrom and Song (1991) applied a model to investigate the effects of oxygen transfer efficiency and heterotrophic competition in nitrification and the limiting DO concentration in activated sludge ranged from 0.5 to 2.5 mg/L. They demonstrated that the activated sludge floc size and density, organic shock loading and heterotrophic/nitrifier competition can increase significantly the limiting DO value. Exposure to high organic loading results in a greater substrate concentration and therefore higher organic removal and oxygen consumption rate by heterotrophs. The higher activity of heterotrophic biomass causes the assimilatory uptake of  $\text{NH}_3$  and inhibits  $\text{NH}_3$  oxidation (Hanaki *et al.*, 1990). Since, heterotrophic bacteria have faster growth and higher affinity for oxygen, the washout of nitrifying bacteria may occur when the DO is low, resulting in failure of the process. A DO concentration greater than 2 mg/L is typically specified to ensure high nitrogen efficiency (US Environmental Protection Agency, 1993; Tchobanoglous *et al.*, 2003).

Maintaining high DO levels will ensure good nitrification, but it will also lead to unnecessary power consumption and high operational costs (high energy consumption and larger plants) (Bellucci *et al.*, 2011). For instance, it is economically desirable to minimise the oxygen demand and maximise the nitrifying activity and therefore establish the minimum DO concentration applied in a treatment plant. The determination of this minimum oxygen level that can achieve the required effluent quality will allow better control of aeration (Phillips and Fan, 2005). It has been suggested that  $\text{NO}_2^-$  oxidation might be more sensitive to the low DO concentrations than  $\text{NH}_3$  oxidation, resulting in  $\text{NO}_2^-$  accumulation (Laanbroek and Gerards, 1993; Tchobanoglous *et al.*, 2003; Blackburne *et al.*, 2008). Some studies have reported complete nitrification with DO lower than 0.5 mg/l in chemostat lab-reactors, presumably due to the presence of adapted nitrifying bacteria (Park and Noguera, 2004; Bellucci *et al.*, 2011; Arnaldos *et al.*, 2013; Liu and Wang, 2013; Fitzgerald *et al.*, 2015). In a different strategy, intermittent aeration also proved successfully  $\text{NH}_3$  oxidation performing partial nitrification followed by denitrification via  $\text{NO}_2^-$  (Mota *et al.*, 2005; Gilbert *et al.*, 2014). The complete nitrification was achieved during aerated periods, but NOB was inhibited after 4h in the non-aerated periods (Mota *et al.*, 2005). Although this strategy saves energy and money by promoting simultaneous nitrification and denitrification using only an aerated-anoxic stage, the probability of failure is high compared to the conventional method (Ofițeru and Curtis, 2009).

A plausible negative impact of the low DO concentrations is the possibility of AOB using  $\text{NO}_2^-$  as an electron acceptor for the oxidation of  $\text{NH}_3$ , stimulating autotrophic denitrification and producing significant amounts of  $\text{N}_2\text{O}$  (Tallec *et al.*, 2006). This gas is considered as one of the critical GHGs. The appropriate control of DO levels can avoid the emission of  $\text{N}_2\text{O}$  during nitrification and denitrification processes (IPCC, 2007).

#### **1.1.4.2 Effects of solids retention time (SRT)**

The solids retention time (SRT) controls the concentration of microorganisms in a reactor and this determines the success of nitrification process. This parameter is directly related to the growth rate of active biomass, therefore, a longer SRT allows the retention of functional microorganisms with slow specific growth rate. The minimum operational SRT can be estimated by:

(1.3)

$$SRT_{min} = \frac{1}{\mu_{max} - K_d}$$

where  $\mu_{max}$  is the maximum specific growth rate and  $K_d$  is the endogenous decay coefficient (US Environmental Protection Agency, 1993; Tchobanoglous *et al.*, 2003). Heterotrophic bacteria have a  $\mu_{max}$  in a range of 4 to 13.2 day<sup>-1</sup>, contrasting to 0.62 to 0.92 day<sup>-1</sup> of nitrifying bacteria (Rittmann and McCarty, 2001). Because of the slow growth of nitrifiers, a sufficient SRT is essential to ensure complete nitrification and avoid washout. Depending on the temperature of the nitrifying system, SRT values may range from 10 to 20 days at 10°C to 4 to 7 days at 20°C.

Stenstrom and Poduska (1980) showed that the nitrifiers performance at different DO concentrations was dependent on the SRT. Under low DO conditions, nitrification can be achieved at higher SRT, but higher DO concentrations are needed when SRT is shorter. Maintaining a long SRT would affect the aeration tank volume, sludge production (due to sludge endogenous decay) and oxygen requirements. Thus, operational and energy costs would increase (Tchobanoglous *et al.*, 2003). To overcome this situation, Bellucci *et al.* (2011) proved reliable nitrification reducing the aeration (> 0.5 mg/L) and SRT (3 days).

#### **1.1.4.3 Effects of environmental factors**

Different factors have significant impact in the efficiency and performance of nitrification including pH, temperature, toxicity, metals and un-ionized NH<sub>3</sub> (Tchobanoglous *et al.*, 2003).

The growth rates of nitrifiers and saturation constants are greatly affected by temperature. Based on this factor, the SRT at which complete nitrification occurs progressively decreases with increasing temperature. The nitrification process occurs over a range of approximately 4-45°C.

In a conventional treatment plant, nitrifying bacteria consume alkalinity and a proper control of the pH is essential to maintain the process. Due to the pH sensitivity, the optimal condition of autotrophic bacteria growth have been found to be within pH range of 7.5 – 8 (Tchobanoglous *et al.*, 2003). Nitrification rates are thought decline when the pH is lower than 6.5 and higher than 9.4. As the pH increases the concentration of free ammonia (NH<sub>3</sub>) increases. On the other hand, the NO<sub>2</sub><sup>-</sup> oxidation will release hydrogen ions and decrease the pH and the equilibrium reaction will increase the nitrous acid (HNO<sub>2</sub>) concentration (Anthonisen *et al.*, 1976). These two forms of nitrogen are inhibitory to nitrifiers above

certain concentrations and conditions, such as the total nitrogen species concentration, temperature and pH. Thus, to achieve high nitrification rates, NH<sub>3</sub> and HNO<sub>2</sub> should be maintained as low as possible by keeping the pH between 7.5–8 (Tchobanoglous *et al.*, 2003).

Some organic and inorganic compounds have a negative effect on the performance of nitrifiers, including solvent organic chemicals, amines, proteins, tannins, phenolic compounds, alcohols, cyanates, ethers, carbamates, benzene and heavy metals (US Environmental Protection Agency, 1993). High salt concentrations in wastewater also affect the metabolic activity of nitrifying bacteria, reducing the microbial growth and NH<sub>3</sub> oxidation rate (Moussa *et al.*, 2006).

### **1.1.5 Culture independent techniques**

WWTPs have complex microbial communities in a chemically and physically well-defined natural environment (Amann *et al.*, 1998). Methods based on cultivation were traditionally applied to characterize microbes in wastewater, but most microorganisms are difficult to isolate or cultivate using these methods resulting in an underrepresentation of the true community diversity (Amann *et al.*, 1998; Ye *et al.*, 2012). The introduction of a suite of culture independent techniques has enhanced the study of complex microbial communities in WWTPs (Ye *et al.*, 2012). The complimentary nature of the different molecular techniques has increased our knowledge of the composition and dynamics of microbial communities in biological wastewater treatment reactors. Environmental genomic tools based on polymerase chain reaction (PCR) or probe hybridization techniques have made it possible to identify and quantify organisms. These techniques target a specific nucleic acid. Ribosomal RNA (rRNA) is the most widely used biomarker in molecular microbial ecology because it is ubiquitous and comprises conserved and variable regions (Woese, 1987).

FISH and quantitative real-time PCR (qPCR) are good examples of molecular techniques used to detect and quantify microorganisms that are important for environmental processes. FISH is a powerful method for visualizing and directly quantifying specific functional groups in a community setting. In essence FISH enables the researcher to target and hybridize regions of the rRNAs that are specific to a particular group or species (Amann, Krumholz, *et al.*, 1990). Thus, more than one organism can be accessed and characterized. FISH permits the direct counting of individual cells making it one of the best quantification methods (Coskuner *et al.*, 2005). The combination of FISH with confocal scanning laser microscopy (CSLM) has allowed the quantification of nitrifying bacteria in WWTPs and biofilms (Wagner *et al.*, 1995; Mobarry *et al.*, 1996; Daims, Nielsen, *et al.*, 2001; Daims, Ramsing, *et al.*, 2001; Gieseke *et*

*al.*, 2001), where AOB are typically observed as microcolonies (Coskuner *et al.*, 2005). However, the application of this method have some limitations: it is time consuming, it has low throughput, it requires high rRNA content to increase the signal from the target cells, and it is limited by problems of background fluorescence and resolution for accurate quantification (Kindaichi *et al.*, 2006).

Recently, faster quantification method – qPCR – has simplified the quantification of microorganisms (Klein, 2002). qPCR is based on continuous monitoring of the fluorescence intensity of target amplicons throughout the PCR reaction (Kindaichi *et al.*, 2006). Not only qPCR is a fast process, as it is also reliable, sensitive, precise and able to enumerate the relative abundance of microorganisms in complex environments, including the enumeration of rare species like nitrifying bacteria (Klein, 2002; Kindaichi *et al.*, 2006). However, bias in sample preparation, DNA extraction procedure, PCR (measures the gene copy number and not the cell number), quality of the standards and the choice of target gene influence the quality and accuracy of the quantification method (Klein, 2002; Baptista *et al.*, 2014). Two possible targets in qPCR, the phylogenetic 16 rRNA gene and the functional NH<sub>3</sub> monooxygenase (*amoA*) gene, were evaluated by qPCR (Dechesne *et al.*, 2016). This study highlighted problems in the estimation of abundance: overestimation associated with the 16S rRNA gene and underestimation when the *amoA*-based qPCR was used. In a different study, similar AOB abundance estimates between FISH and the *amoA* gene specific qPCR were obtained, although the 16S rRNA-based qPCR underestimated AOB numbers (Baptista *et al.*, 2014). Thus all quantification methods have advantages and disadvantages. The most appropriate quantification strategy will depend on the aims of the project in question. New approaches to the analysis of microbial communities have come from the development of next generation high-throughput sequencing technologies (Podar *et al.*, 2007). This relatively new research method has allowed the identification of bacteria, or closely related species, by the sequencing of their 16S rRNA gene. Although widely and successfully used the amplicon based methods have drawbacks (Ye *et al.*, 2012). Bias in the PCR reactions can restrict the sequencing data obtained: PCR limits the information to a particular gene; most measurements provide only relative abundance information; some lineages may be missed entirely due to primers mismatches and the restrict number of different primers that could target a wide range of bacteria (Ye *et al.*, 2012; Zhou *et al.*, 2015). Recently, metagenomic analysis sampled from an aquifer possilitou an expansion of the tree of life and described it as the candidate phyla raditation. This new branche represented 20 % of all bacteria that would be missed by using the 16S rRNA gene amplicon surveys (Brown *et al.*, 2015). Shotgun sequencing of genomic DNA from environmental samples offers a valuable

alternative to amplicon sequencing and can establish links between genetic composition of a specific organism and the metabolic activity encoded in their genes (Tringe *et al.*, 2005). This method consists of the direct sequencing of unamplified DNA and thus does not require prior knowledge of the organisms and enables the discovery of new species and genes and associations between them (Ye *et al.*, 2012). However, the complexity of microbial communities and the large number of species that are present at very low abundance (below 1%) in a community lead to insufficient sequencing depth or/and difficult in binning and assembly individual genomes (Venter *et al.*, 2004; Albertsen *et al.*, 2013).

To overcome these challenges, the recovery and separation of specific organisms from environmental samples has been proposed as a way to obtain complete genomes. Among these studies, the combination of FISH and FACS has revealed a promise method to separate single cells or populations from complex samples (Yilmaz *et al.*, 2010; Haroon *et al.*, 2013; Fujitani *et al.*, 2014, 2015). Flow cytometry is a critical technique in modern cell and developmental biology for the rapid sorting and counting of cells (Tracy *et al.*, 2010). This technique can rapidly detect and isolate population of cells with a desired biological characteristic based on the light scattering properties of cells and different multi-parametric analysis (Fuchs *et al.*, 2000; Foladori, Bruni, *et al.*, 2010). Compared with the conventional observation techniques, flow cytometry is faster, direct and can provide different types of information related to cell identification and regulation (Tracy *et al.*, 2010). Flow cytometry has been used for the recovery of AOB cells from autotrophic nitrifying granules (Fujitani *et al.*, 2015). The application of FISH-FACS is therefore a step forward for downstream molecular analysis and has advantages over other sorting methods (micromanipulation and microfluidic) including: higher throughput, greater specificity and speed (Haroon *et al.*, 2013).

Since the biological mechanisms of NH<sub>3</sub> oxidation are still not fully understand, the isolation of AOB for genome sequencing and characterization can expand our knowledge about these organisms and help to define the best conditions for the nitrification process. In this project, FISH-FACS was used to identify and sorting the AOB adapted at different DO conditions from activated sludge reactors and full-scale WTPPs.

## 1.2 Scope and goals of the study

The efficient treatment of a wastewater treatment plant (WWTP) requires high aeration levels mainly due to the intolerance of ammonia-oxidizing bacteria (AOB) to low dissolved oxygen (DO). The traditional processes are energy expensive and contribute to the greenhouse gas (GHG) emissions. Thus, there is an interest in developing nitrifying biomass that is adapted to low DO to reduce both the costs and the environmental impact of the WWTP process.

It is still unclear the influence of low DO on AOB community and the correlation between AOB lineages and DO. The conditions in WWTPs, in particular the DO, can select for different types of AOB with implications for their kinetic parameters and genome composition. Molecular microbial ecology can be used to describe the response of the AOB community to low DO and provide genomic and metabolic information for certain bacteria.

This study focuses on low energy nitrification and aims to provide a deeper insight into the structure and dynamic of the nitrifying bacteria selected under low DO conditions. The specific objectives are as follows:

- To monitor and compare the performance of activated sludge bioreactors operated at low and high DO concentrations.
- To quantify the nitrifying community (AOB and nitrite-oxidizing bacteria (NOB)) through out the operation and to correlate abundance with performance.
- To compare different sequencing strategies in order to assess the composition of the AOB selected under low and high DO.
- To evaluate the adaptation of AOB to low DO concentration and estimate the dynamics of that population by modelling two species with different DO kinetics under similar conditions but operated at low and high DO.
- To estimate the nitrous oxide ( $N_2O$ ) production from nitrifying activated sludge laboratory-scale reactors operated at different DO and investigate the environmental and economic impact of that production.
- To develop and optimize a combined molecular method (Fluorescence *in situ* hybridization (FISH) and fluorescent-activated cell sorting (FACS)) for the isolation of AOB colonies from activated sludge full-scale and laboratory-scale bioreactors.
- To elucidate the effect of DO on nitrifying bacteria by characterising the nitrifier genome selected under those conditions.

## Chapter 2. Experimental plan

The aforementioned objectives were implemented following the experimental plan:

### 2.1 Adaptation of nitrifying bacteria at low DO conditions

(Chapter 3)

Two pair of laboratory-scale reactors were set up and operated under low (2.0% v/v) and (21.0% v/v) oxygen conditions, respectively. Samples from each reactor were collected for chemical, physical, and microbial community analyses. Quantification, using qPCR targeting the bacterial *amoA* gene, was used to estimate the AOB population size and yields and subsequently model the growth of the AOB adapted to low DO nitrifying systems. Quantification of the NOB was also undertaken targeting the functional gene (*nxrB*). To investigate and compare the AOB community selected under different DO conditions, libraries of the 16S rRNA gene and the *amoA* gene were prepared from DNA extracted at different time points and sequenced by Ion Torrent and HiSeq Sequencing Technologies.

### 2.2 Impact of N<sub>2</sub>O emissions in activated sludge operated at low DO concentrations

(Chapter 4)

Emissions of N<sub>2</sub>O were further investigated. N<sub>2</sub>O production was accessed using sludge from continuous laboratory-scale reactors set up and operated at low (0.2 mg O<sub>2</sub>/L) and high (6.5 mg O<sub>2</sub>/L) DO (as described in 2.1). Batch experiments were conducted in glass flasks and air excluded in the sludge from low DO conditions. An equilibrium with the headspace was created and gas samples were taken over 48 h and measured using gas chromatography. Time dependent production of N<sub>2</sub>O was estimated from headspace N<sub>2</sub>O concentrations in mixed liquor batch experiments. The values obtained in these experiments were used to estimate the impact of N<sub>2</sub>O production in full-scale treatment plants at low DO by two methods: constant flux per unit volume of reactor and constant fraction of nitrogen load.

## **2.3 A flow cytometry–fluorescence in situ hybridization method to sort AOB under low dissolved oxygen**

(Chapter 5)

The separation of single cells of AOB using a modified FISH protocol combined with FACS was applied and optimized. The method was calibrated using samples of activated sludge collected from a nitrifying municipal wastewater. Different strategies were implemented to define the best gating: dyes, probe hybridization, gating parameters. Following the sorting cells, DNA was subsequently amplified and tested for AOB. Metagenomics analysis were finally performed to recover AOB genomes and understand their biological metabolism under low oxygen.

## Chapter 3. Adaptation of nitrifying bacteria at low dissolved oxygen conditions

### 3.1 Introduction

A conventional WWTP employing aerobic and anaerobic treatment is a significant consumer of energy. In developed economies approximately 3% of the total electricity consumed is used to treat wastewater, in which 50% is used for aeration in the activated sludge process, including nitrification (Curtis, 2010). The energy consumed not only increases the operation and maintenance costs, as it also has an impact in climate change. In order to improve the economic and environmental sustainability of wastewater treatment we need to develop efficient nutrient and organic removal by applying energy conservation processes (McCarty *et al.*, 2011).

The energy demands of many engineered nitrifying systems is primarily related to the aerobic metabolism of AOB (Prosser, 1986; Koops *et al.*, 2006). AOB are responsible for the first step of nitrification and can struggle to compete for oxygen with heterotrophs (Painter, 1986; US Environmental Protection Agency, 1993; Grady *et al.*, 1999). Thus, the consequence of decreasing the aeration might lead to incomplete nitrification and operators are typically advised to maintain a bulk DO concentrations over 2 mg/L to ensure reliable nitrification (US Environmental Protection Agency, 2013; Arnaldos and Pagilla, 2015).

In the last decade, the idea of selecting for AOB biomass that can oxidize NH<sub>3</sub> at low DO has gained traction. Indeed, complete nitrification has been achieved in a chemostat with DO concentrations of less than 0.5 mg/l and attributed to the presence of adapted nitrifying bacteria (Park and Noguera, 2004; Bellucci *et al.*, 2011; Arnaldos *et al.*, 2013; Liu and Wang, 2013; Fitzgerald *et al.*, 2015).

AOB, not AOA, are the main ammonia-oxidizers community in low DO reactors (Arnaldos *et al.*, 2013; Liu and Wang, 2013; Fitzgerald *et al.*, 2015). However, which of the AOB is a matter of debate. In the low DO studies, contradictory evidence on the adapted AOB lineages has been observed. In some reports, *Nitrosomonas europaea* dominated the low DO reactors (Park and Noguera, 2004; Arnaldos *et al.*, 2013; Liu and Wang, 2013), whereas in others *Nitrosomonas oligotropha*-like organisms were the prevalent AOB (de Bie *et al.*, 2001; Gieseke *et al.*, 2001; Bellucci *et al.*, 2011; Fitzgerald *et al.*, 2015). The mechanistic basis for the adaptation to low DO in AOB is uncertain and might include both a greater

affinity for DO (a lower  $K_{DO}$ ), as well as a modification in the metabolism of those nitrifying bacteria. The conflicting reports of the identity of AOB in low DO could be a consequence of different sludge retention time (SRT) or substrate concentrations used in those studies. Moreover, we cannot discount that the possible biases in the culture-independent techniques or sequencing analysis used to detect these AOB may have affected previous studies. Such techniques could influence the identification of the rare AOB species (Ross *et al.*, 2013; Sims *et al.*, 2014).

There is some evidence of mixotrophic growth in AOB in low DO reactors, in particular Bellucci *et al.* (2011) observed an increase in growth yield in AOB. AOB normally have the relatively low yield that are characteristic of chemolithotrophs and that must fix their own carbon. The increase cell yield coefficient could be indicative of the energy benefits conferred by the use of organic matter as carbon source. But it is still not known how and why AOB would shift its carbon source to survive in DO deprived environments. For many years the nitrifying organisms were considered to be obligate chemolithoautotrophs (Koops *et al.*, 2006; Sayavedra-Soto and Arp, 2011). However, in the absence of oxygen or in poorly oxygenated environments, pure cultures of AOB are able to use pyruvate or lactate as the only carbon source (Beyer *et al.*, 2009; Schmidt, 2009). In addition, some NOB can grow heterotrophically (Bock, 1976; Watson *et al.*, 1986; Daims, Nielsen, *et al.*, 2001; Starkenburg *et al.*, 2008).

In present day, engineers are wanting to know how long it will take for a WWTP to adapt to a change in DO concentrations. Adaptation is a difficult process and still something of mystery. In this study, we investigate the adaptation of nitrifying community to a very low DO concentration, in particular the acclimation of the AOB species. We hypothesize that DO concentrations influence not only the selection of AOB community but also the metabolism of the AOB growth. The AOB abundance, diversity and performance were assessed to evaluate how these organisms adapt under such circumstances. Different sequencing strategies were used to deeply characterize the AOB population under low DO in order to observe a shift in that community. Moreover, we performed a two specie model to estimate the dynamics of the AOB population when decreasing the aeration. Finally, we quantified NOB to determine whether or not nitrification is completed under low DO.

## 3.2 Materials and Methods

### 3.2.1 Continuous reactor

Four laboratory-scale reactors were inoculated with 3 L of recirculated activated sludge (50%) from the municipal WWTP in Tudhoe Mill (County Durham) and fed with sterile synthetic wastewater media (50%). Two of the reactors (R1\_L and R2\_L) were maintained at low DO concentrations and the other two (R3\_H and R4\_H) units at high DO (Figure 3.1). Low and high oxygen values were achieved by continuously bubbling a gas mixture (nitrogen-oxygen) containing 2.0% and 21.0% oxygen. Mixing was provided with a stirrer (IKA®, South Africa) at 120 rpm and it was supplied a constant air flow rate of 0.05 L per min. Synthetic wastewater, adapted from Knapp and Graham (2007), contained 293 mg/L  $(\text{NH}_4)_2\text{SO}_4$ , 320 mg/L peptone (LabM, UK), 190 mg/L meat extract, 30 mg/L yeast extract (Sigma, UK), 30 mg/L urea, 28 mg/L  $\text{K}_2\text{HPO}_4$ , 2 mg/L  $\text{CaCl}_2 \cdot 2\text{H}_2\text{O}$ , 2 mg/L of  $\text{MgSO}_4 \cdot 7\text{H}_2\text{O}$ , 5 mM Pyruvate, 1 ml/L of trace element solution (0.75 g/L  $\text{FeCl}_3 \cdot 6\text{H}_2\text{O}$ , 0.075 g/L  $\text{H}_3\text{BO}_3$ , 0.015 g/L  $\text{CuSO}_4 \cdot 5\text{H}_2\text{O}$ , 0.09 g/L KI, 0.06 g/L  $\text{MnCl}_2 \cdot 4\text{H}_2\text{O}$ , 0.03 g/L  $\text{NaMoO}_4 \cdot 2\text{H}_2\text{O}$ , 0.06 g/L  $\text{ZnSO}_4 \cdot 7\text{H}_2\text{O}$ , 0.075 g/L  $\text{CoCl}_2 \cdot 6\text{H}_2\text{O}$ , 0.5 g/L EDTA, and 1 ml/L concentrated hydrochloric acid), and 1.1 mg/L  $\text{NaHCO}_3$ . The concentrated feed medium was autoclaved and trace elements solution was sterilised by passing through a 0.2  $\mu\text{m}$  filter (MERCK KGaA, Germany) and stored at 4°C before adding into the bulk medium. The influent flow rate in each reactor was 0.6 L/day, corresponding to a fixed 5 days SRT and hydraulic retention time (HRT). Influent ammonium, Total Kjeldahl Nitrogen (TKN) and chemical oxygen demand (COD) was  $67.5 \pm 6.2 \text{ mg N/L}$ ,  $133.2 \pm 13.5 \text{ mg N/L}$  and  $776.5 \pm 58.7 \text{ mg/L}$ , respectively. In this study high  $\text{NH}_3$  concentrations were used to maximize the AOB abundance under low DO concentration. The reactors operated for 276 days.

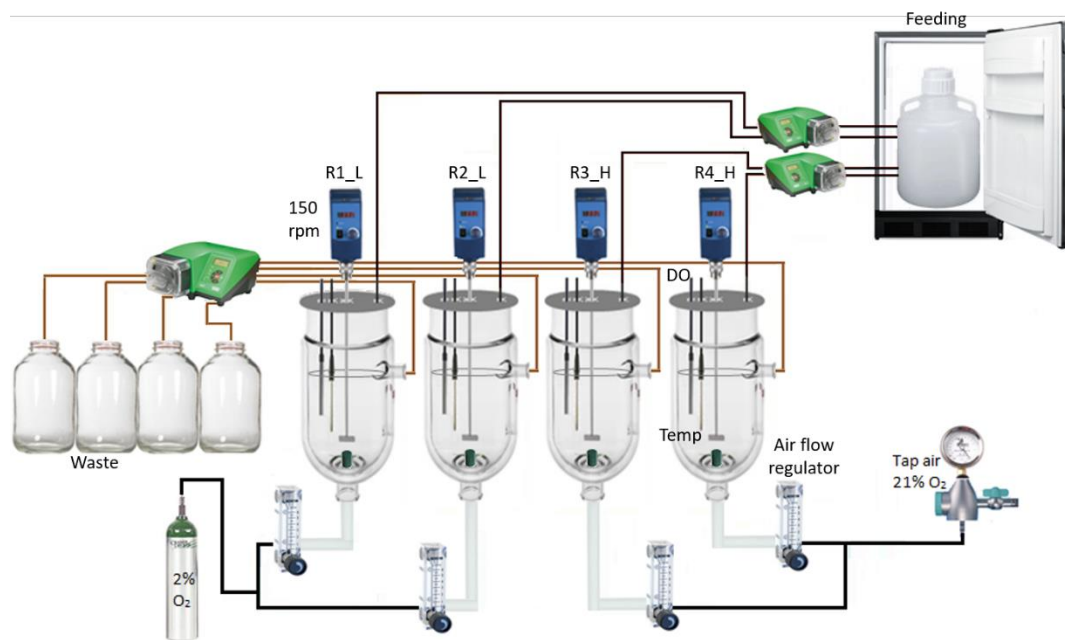


**Figure 3.1** Design of the four laboratory bioreactors set-up.

### 3.2.2 Monitoring and sample preparation

All the reactors were monitored with specific probes for pH (Broadley Technologies Ltd, CA, USA), DO (FireSting O<sub>2</sub>, Aachen, Germany) and temperature (Pico Tech, St Neots, UK). Around 150 mL sample from each reactor and from feed medium was collected every 3 days and, after 17 days, every week for physicochemical analysis. Ammonium and COD levels were determined using Ammonium Cell Test Kit and COD cell test, respectively, (MERCK KGaA, Germany), according to the manufacturer's instructions. NO<sub>2</sub><sup>-</sup> and NO<sub>3</sub><sup>-</sup> were measured by ion chromatography (Dionex DW-1000 ion chromatograph; Dionex Corp., Sunnyvale, CA, USA). The ion chromatograph was fitted with an IonPac AS14A analytical column and a 25-μL injection loop. It operated at a flow rate of 1 mL/min with 8.0 mM Na<sub>2</sub>CO<sub>3</sub>-1.0 mM NaHCO<sub>3</sub> as eluent. All these compounds were determined after sample filtration from a 0.2 μm syringe filter. Total suspended solids (TSS), volatile suspended solids (VSS), TKN and alkalinity were determined according to standard methods (APHA, 1998). All chemical and physical analysis were duplicated. Biomass samples were saved for molecular analysis. Four times 2 mL samples were collected per reactor for DNA extraction and stored at -20°C. Also, further tubes containing 2 mL samples were collected for future analyses of RNA and metagenomics.

### 3.2.3 DNA extraction

Four mL of the biomass samples collected at several days (0, 3, 12, 17, 23, 30, 37, 44, 66, 86, 100, 127 and 143) were centrifuged at 10,000 g for 3 min, and the supernatant was removed down to a volume of 250 µL. The DNA was extracted from the final volume using the FastDNA® SPIN Kit for Soil (MP-Biomedicals, CA, USA) in accordance with the manufacturer's instructions. Samples were placed into 2 ml tubes containing MT buffer and sodium phosphate buffer a mixture of ceramic and silica particles to lyse cells. Cell were then centrifuged to pellet cell debris and lysing matrix and the supernatant was purified using SPIN filters. DNA was then eluted into 50 µl of DNase Free water. We confirmed the presence of intact DNA on 1.5% agarose gel electrophoresis. The DNA was stored at -20°C until further analysis.

### 3.2.4 Preparing standards for quantitative PCR

Standards used in the quantitative PCR (qPCR) assays were prepared from circular plasmids containing the target fragment of DNA. Standards used for *nxrB* genes were previously obtained in Technical University of Denmark (DTU), by cloning of the PCR amplified genes into TOPO® (Invitrogen, CA, USA) vectors. For *amoA* gene, we obtained clones prepared with TOPO®. We cultured up *E. coli* clones containing the specific fragment and extracted the plasmid DNA using the Roche High Pure Plasmid Isolation Kit following the manufacturer's instructions. The specificity of each extracted plasmid assay was confirmed using 1.5% agarose gel electrophoresis. The concentration of DNA of plasmids containing the inserted *amoA* gene was previously determined by Quant-it Picogreen Assay Kit (Invitrogen, CA, USA). The total weight in grams per copy of extracted plasmid was determined on the basis of the Avogadro's number by the following equation:

(3.1)

$$\text{Number of } \frac{\text{copies}}{\mu\text{L}} = \frac{6.022 \times 10^{23} \left( \frac{\text{molecules}}{\text{moles}} \right) \times \text{DNA concentration} \left( \frac{\text{g}}{\mu\text{L}} \right)}{\text{Number of bases pairs} \times 660 \text{ daltons}}$$

After determining the DNA standard gene abundance/ µL, standards were serially diluted in molecular grade water to give a range of concentration from 10<sup>2</sup> to 10<sup>8</sup> target sequence copies/µL.

### 3.2.5 Quantitative PCR of nitrifiers

To evaluate the abundance of AOB and NOB, we performed qPCR reactions using a CFX96 real-time PCR detection system (Bio-Rad, UK) with an iCycler iQ fluorescence detector and software version 2.3. Table 3.1 provides information on the primers used for the different organisms. Specific primer to the *amoA* gene, amoA-1F\* and amoA-2R (Rotthauwe *et al.*, 1997), was used in these reactions (Table 3.1). Meanwhile, NOB abundance was investigated by quantifying two different sets of primers: one specific to the  $\text{NO}_2^-$  oxidoreductase (*nxrB*) gene for *Nitrospira* (nxrB169f–nxrB638r, (Pester *et al.*, 2014) and the other specific to the *nxrB* gene for *Nitrobacter* (NxrB-1F and NxrB-1R, (Vanparry *et al.*, 2007). Each sample contained 3 $\mu\text{L}$  of template DNA, 0.5  $\mu\text{L}$  of forward and reverse primer (10  $\mu\text{M}$ ), 5  $\mu\text{L}$  of SsoFast EvaGreen Supermix (BioRad, UK), and 1  $\mu\text{L}$  of molecular biology grade water. The reaction conditions used for the *amoA* gene specific primers consisted of the initial denaturation step: 95°C for 4 min, followed by 35 cycles at 95°C for 1 min, 57°C for 45 s and 72°C for 1 min and a final extension step of 72°C for 7 min. The conditions used for the *nxrB* gene were: 95°C for 5 min, followed by 35 cycles at 95°C/40 s, 56°C/40 s and 72°C/1.5 min and extension at 72°C for 10 min (*Nitrospira*); or 95°C for 10 min followed by 40 cycles at 95°C/1 min, 55°C/1 min and 72°C/2 min and extension at 72°C for 12 min. (*Nitrobacter*). The template used to construct standard curves was a circular plasmid containing the target fragment of DNA. Standard curves were made by using serial dilutions (10<sup>2</sup> to 10<sup>8</sup> copies per  $\mu\text{L}$ ) and added every run. A blank was also added to test potential contaminations. The qPCRs were run in triplicate for the *amoA* assay and in duplicate for both *nxrB* assays. PCR efficiency ranged from 90% to 110% with  $r^2$  values over 0.99 for all calibration curves.

**Table 3.1** Description of the primers used for the qPCR and sequencing analysis.

Target gene	Primer name	Sequence (5'-3')	Reference
<i>amoA</i> -AOB	amoA-1F	GGGGTTTCTACTGGTGTT	Rotthauwe <i>et al.</i> (1997)
	amoA2R	CCCCTCKGSAAAGCCTTCTTC	
<i>nxrB</i> - <i>Nitrospira</i>	nxrB169f	TACATGTGGTGGAAACA	Pester <i>et al.</i> (2014)
	nxrB638r	CGGTTCTGGTCRATCA	
<i>nxrB</i> - <i>Nitrobacter</i>	NxrB-1F	ACGTGGAGACCAAGCCGGG	Vanparry <i>et al.</i> (2007)
	NxrB-1R	CCGTGCTGTTGAYCTCGTTGA	
16S rRNA	F515	GTGCCAGCMGCCGCGTAA	Caporaso <i>et al.</i> (2011)
	R806	GGACTACHVGGGTWTCTAAT	

### 3.2.6 Calculation of AOB biomass, fraction and yield

The cells per  $\mu\text{L}$  obtained in qPCR were converted in biomass expressed as mg per mL following the equation below:

(3.2)

$$X_{\text{AOB}}(\text{mg/L}) = \frac{\text{AOB (cells}/\mu\text{L}) \times \text{Volume} \times \text{density} \times \text{diameter}}{10^9}$$

where the volume is equal to  $0.523 \mu\text{m}^3$ , the diameter and total density of an AOB cell is  $1 \text{ m}$  and  $0.636 \text{ g/cm}^3$ , respectively. Subsequently, AOB percentage was inferred by dividing the  $X_{\text{AOB}}$  (mg VSS\_AOB/L) by the total VSS. In order to calculate the growth yield ( $Y_{\text{AOB}}$ ) the equation previously described by Rittmann *et al.* (1999) was used and solved:

(3.3)

$$X_{\text{AOB}} = \left[ Y_{\text{AOB}} \frac{1 + (1 - f_d) \times b_{\text{AOB}} \times \theta}{1 + b_{\text{AOB}} \times \theta} \right] \Delta \text{NH}_3\text{-N}$$

where  $\theta$  is the solid retention time (5 days),  $b$  is the endogenous respiration rate ( $0.15 \text{ day}^{-1}$ ),  $f_d$  is the fraction of the active biomass that is biodegradable (0.8), and  $\Delta \text{NH}_3\text{-N}$  is the  $\text{NH}_3$  consumption. The maximum  $Y_{\text{AOB}}$  value obtained from each reactor was consider as the largest yield that can be reached by AOB under low and high DO concentrations.

### 3.2.7 Modelling AOB dynamics at low DO

The AOB enrichment was characterized by an exponential growth according to the equation:

(3.4)

$$N(t) = N_0 \times e^{\mu t}$$

where the increase in AOB cells ( $N$ ) is represented through time,  $N_0$  is the initial quantity,  $t$  is time, and  $\mu$  is the specific growth rate (Tchobanoglous *et al.*, 2003).

We also adapted a simple mathematical model developed by (Ofițeru and Curtis, 2009), which is an adaptation of the resource ratio theory (RRT) of Tilman (1982), where two AOB species are to consume two resources ( $\text{NH}_3$  and oxygen) (Appendix 8.2). We simulated the adaptation of the AOB community to low DO employing the same operational parameters as were used in the experimental work for simulations (130 mg  $\text{NH}_3\text{/L}$  inlet, 0.2 mg  $\text{O}_2\text{/L}$  and

5 day SRT) and simulating different AOB initial abundances. The kinetic parameters are summarized in Table 3.2, according to (Park and Noguera, 2007).

**Table 3.2** Kinetic parameters for the AOB species.

Species	Parameters		
	$\mu$ ( $d^{-1}$ )	K <sub>DO</sub> (mg/L)	K <sub>NH<sub>3</sub></sub> (mg/L)
<b>AOB1</b>	0.66±0.09	0.24±0.13	1.62±0.97
<b>AOB2</b>	0.66±0.09	1.22±0.43	0.48±0.35

### 3.2.8 Amplicon sequencing

#### 3.2.8.1 PCR reactions and sequencing preparation

In order to assess the AOB diversity and relative abundances, we used two different primer sets (Table 3.1) for library preparation for the sequencing runs. All primers were ordered as HPLC grade primers from Thermo Fisher Scientific GmbH (Darmstadt, Germany) and were diluted to 10 µM working stock.

For Ion torrent sequencing, we analysed samples collected from reactors at low and high DO (R1\_L and R3\_H) at different times (0, 3, 6, 8 and 10 days, in duplicate). PCR amplification was carried out with universal primers set which target the V4–V5 region of the bacterial and archaeal 16S rRNA genes (515F: 5'-GTGNCAGCMGCCGCGTAA-3'; 926R: 5'-CCGYCAATTYMTTTRAGTT-3'). All forward primers contained a Golay indexed sequencing tails. These PCR reactions were carried out in 25 µL reaction mixture containing: 0.5 µL (10 µM) of each primer, 0.5 µL (10 mM) of deoxynucleoside triphosphates (dNTPs), 2.5 µL of FastStart HiFi 10x Buffer #2 (Roche Diagnostics Ltd., UK), 0.25 µL of FastStart HiFi Polymerase (5 U/µl; Roche Diagnostics Ltd., UK), 20.25 µL of molecular biology grade water (Sigma–Aldrich, UK) and 0.5 µL of extracted DNA using an automated thermal cycler (Techne, UK). The thermal PCR conditions consisted of the initial denaturation (95°C, 2 min), followed by 30 cycles (95°C for 30 s, 56°C for 30 s and 72°C for 45 s) and a final extension at 72°C for 7 min. Samples were purified twice using 1.1x AMPure XP beads (Beckman Coulter, CA, USA). The concentration of the purified DNA was quantified by a dye based method, Qubit® kit (Invitrogen, CA, USA) using a Qubit® 2.0 Fluorometer, following the manufacturer's protocols. Samples were then pooled in equimolar amounts further purified using a Pippin Prep System (Life Technologies, CA, USA) following the manufacturer's protocol.

For Illumina sequencing, two PCR-based approaches were evaluated in the samples collected from all the reactors at day 0, 3, 17, 30, 37, 44 and 66 (in duplicate): 16S rRNA

gene and *amoA* gene. Primers used for the two libraries are described in Caporaso *et al.* (2011) and Rotthauwe *et al.* (1997) (Table 3.1). The V4 region of 16S was designed to amplify a 254 base pairs (bp) insert with primer pair F515 and R806 (Caporaso *et al.*, 2011). Particulate *amoA* genes were PCR amplified from total DNA extracted with primers amoA-1F and amoA2R (Rotthauwe *et al.*, 1997). For 16S rRNA work, the DNA extracts were provided to the Centre for Genomic Research (CGR, <http://www.liv.ac.uk/genomic-research>) in the University of Liverpool for library construction using HiFi HotStart ReadyMix (2X, KAPA, MA, USA). The two step PCR reactions were carried out, according to the 16S dual index nested PCR protocol, with the following parameters: initial denaturation at 98°C for 2 min, followed by 10 or 15 cycles (first and second PCR, respectively) of 95°C for 20 s, 65°C for 15 s, and 70°C for 30 s with a final extension at 72°C for 5 min. For *amoA* library preparation, we performed the first PCR reaction which contained a mixture of 2.5 µL of extracted DNA, 0.5 µL of each primer (10 µM), 12.5 µL of HiFi HotStart ReadyMix (2X) and 9 µL of molecular biology grade water, making a total volume of 25 µL. The PCR mixtures were held at 94°C for 5 min, followed by 35 cycles at 94°C/30 s, 56°C/30 s and 72°C/30 s and a final DNA extension step of 5 min at 72°C. The next steps of the library preparation were conducted in CGR, where a second PCR was performed to attach Illumina sequencing adapters sequences following the Nextera® XT protocol. They cleaned up all PCR products with AMPure XP beads (Beckman Coulter, CA, USA) and quantified with Qubit® kit (Invitrogen, CA, USA) before pooling samples.

### **3.2.8.2 Ion torrent and Illumina high-throughput sequencing**

Ion torrent sequencing was conducted at Newcastle University (Newcastle upon Tyne, UK) using Ion Torrent Personal Genome Machine System (Life Technology, CA, USA) on an Ion 316 chip according to the manufacturer's protocols.

Illumina sequencing was performed by CGR in Liverpool using the Illumina Nextera XT primers-based PCR protocol in the HiSeq2500 platform (Illumina, CA, USA). All samples were multiplexed and sequenced in a single lane on the HiSeq using 2 × 300 bp paired-end sequencing.

### **3.2.8.3 Processing of sequencing data from Ion Torrent**

Processing of sequencing 16S rRNA sequences from Ion Torrent was performed with the Quantitative Insights Into Microbial Ecology toolset (QIIME - version 1.7.0) (Caporaso *et al.*, 2010), using the pipeline available from [https://github.com/greggiceton/qiime\\_pipeline](https://github.com/greggiceton/qiime_pipeline). Initially, 16S rRNA raw sequences were demultiplexed according to the sample barcode, then filtered to remove poor quality bases (minimum phred quality score = 20; minimum length = 100 base pairs). Cleaned reads were clustered into operational taxonomic units (OTUs) with the pick\_open\_reference\_otus.py workflow in QIIME, with centroid uniqueness determined with the UCLUST algorithm (usearch v5.2.32) (Edgar, 2010) at 97% similarity. The resulting representative sequences were aligned using PyNast (Caporaso *et al.*, 2010), and taxonomic assignments were performed with the Ribosomal Database Project (RDP) naïve Bayesian rRNA classifier (Wang *et al.*, 2007) and SILVA reference database version 123 (Yilmaz *et al.*, 2014).

### **3.2.8.4 Processing of sequencing data from Illumina**

Sequences of *amoA* and 16S rRNA genes from Illumina were trimmed by CGR. Cutadapt version 1.2.1 (Martin, 2011) was used to remove the presence of Illumina adapter sequences. Reads were further quality trimmed using Sickle version 1.200 (Joshi and Fass, 2011) with a minimum quality score of 20 and reads shorter than 10 bp were discarded. We ran the DADA2 pipeline (v.1.1.1, <http://benjneb.github.io/dada2/tutorial.html>) using R (version 3.2.2) on *amoA* and 16S rRNA sequencing samples. The post-processed sequences were quality checked, filtered and trimmed further, as suggested in DADA2 pipeline. Trimming and filtering were performed on both forward and reverse reads for 16S rRNA sequences, but only on the forward reads for *amoA* sequences, since the reverse reads had poor quality, with the default parameters (truncate length: 240; maximum of two expected errors per read (maxEE = 2)). Cleaned reads were then dereplicated for efficiency, and processed with the DADA2 algorithm to determine true biological sequences. Taxonomy assignment was performed with the DADA implementation of the RDP classifier (Wang *et al.*, 2007) and SILVA reference database (Yilmaz *et al.*, 2014) for the 16S rRNA samples. A custom AOB database (Koops *et al.*, 2006) was used as reference data base for AOB. The total numbers of classified biological sequences after processing with DADA were 17,191 and 2,691 for 16S rRNA and *amoA*, respectively. Further analysis was carried out using R

packages phyloseq (McMurdie and Holmes, 2013) and ampvis v.1.9.2 (<http://bioconductor.org/biocLite.R>), where samples were rarefied (depth = 10,000) and low abundant species were filtered to perform principal component analysis (PCA) was conducted.

### **3.2.8.5 Bioinformatic analysis**

The microbial and AOB communities in the reactors samples were analysed in PRIMER (version 7.0.11, (Clarke and Gorley, 2015)). The impact of both treatments in the AOB community was tested on PCA and on the Bray-Curtis dissimilarity indices was used to calculate a distance matrix for non-parametric analyses of similarity (ANOSIM).

### **3.2.9 Statistical analysis**

All statistical analyses were conducted in Minitab® software (version 17.1.0, Minitab Inc., PA, USA) and Rstudio (version 1.0.136). Parameters measured in the reactors were analysed by checking the normality with Anderson- Darling test. Descriptive, analysis of variance (ANOVA) and paired-t test analysis were conducted. Abundance data was log-transformed before statistical tests and comparisons were done in order to evaluate the influence of DO concentration.

## **3.3 Results and Discussion**

### **3.3.1 Effect of DO concentration on nitrification performance**

#### **3.3.1.1 Reactors performance**

Nitrification was monitored in four chemostat reactors operated at low and high oxygen concentrations for 276 days (Figure 3.2). Complete nitrification was observed in the two high DO reactors from the beginning of the experiment (Figure 3.2.b), there being no significant differences in the TKN removal between duplicates and throughout the experiment ( $98.6 \pm 3.1\%$ , nested ANOVA:  $p$ -value = 0.6,  $\alpha = 0.05$ ). On day 151, an incorrect amount of NH<sub>3</sub> and sodium bicarbonate was added to the feed. This episode was followed by a loss of NH<sub>3</sub> oxidation in one of the reactors at high DO (R4\_H). The reactor recovered after 13 days. Although oxygen supply rates were the same in the duplicate systems, the DO concentration was slightly different being  $6.3 \pm 0.7$  mg/L and  $6.6 \pm 0.9$  mg/L in R3\_H and R4\_H,

respectively (Paired t-test:  $p$ -value < 0.05,  $\alpha = 0.05$ ). In the low DO reactor, the oxygen concentrations were constant at  $0.2 \pm 0.1$  mg/L and indistinguishable (Paired t-test:  $p$ -value = 0.9,  $\alpha = 0.05$ ) throughout the experiment. TKN accumulated for the first 58 days of operation but then TKN removal gradually increased (Figure 3.2a). The TKN removal in the low DO reactors were different,  $72.3 \pm 15.5\%$  and  $56.2 \pm 12.7\%$  in R1\_L and R2\_L, respectively (nested ANOVA:  $p$ -value < 0.05,  $\alpha = 0.05$ ). The average temperature was in all configurations  $22.3 \pm 1.4^\circ\text{C}$ .

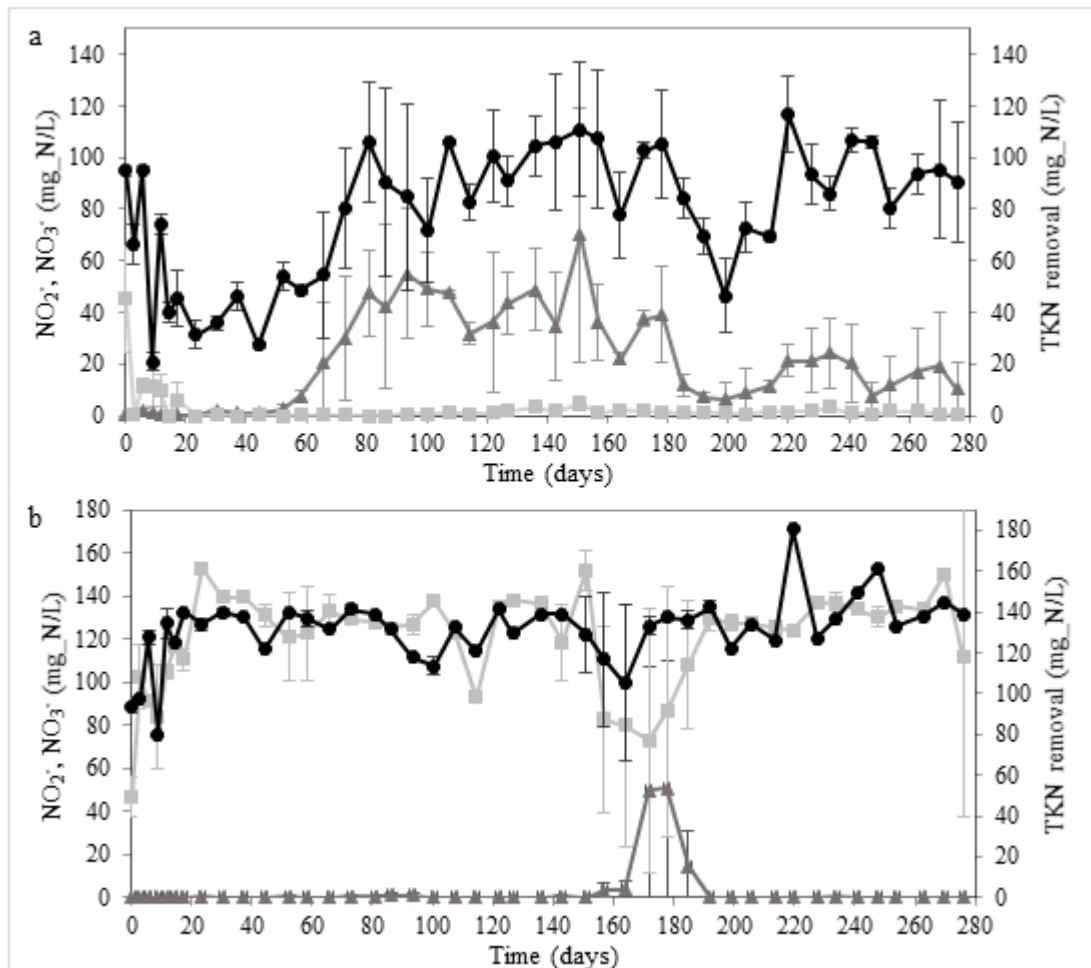


**Figure 3.2** Nitrification performance in laboratory-scale chemostat reactors operated at low and high DO conditions. TKN removal (black circles),  $\text{NO}_2^-$  concentration (dark grey triangles) and  $\text{NO}_3^-$  concentration (light grey squares) in reactors with low aeration (a) and high aeration (b).

As expected, DO concentration near saturation level ensured almost complete nitrification with very little  $\text{NO}_2^-$  accumulation ( $0.6 \pm 3.2$  mg/L on average) in the high DO reactors. By contrast,  $\text{NO}_2^-$  accumulated in the two low DO systems ( $28.1 \pm 22.3$  mg/L) and  $\text{NO}_3^-$  concentrations were modest ( $1.3 \pm 1.3$  mg/L), suggesting that low aeration levels may have prevented complete nitrification. This finding contrasts with previous reports which

found no  $\text{NO}_2^-$  accumulation in similar reactors with DO concentration of less than 0.5 mg/L (Park and Noguera, 2004; Bellucci *et al.*, 2011; Arnaldos *et al.*, 2013; Liu and Wang, 2013; Fitzgerald *et al.*, 2015). Since NOB have a lower affinity for oxygen than the ammonium oxidizers ( $K_{\text{DO}} = 0.43 \text{ mg/L}$  against to  $K_{\text{DO}} = 0.03 \text{ mg/L}$ ) (Blackburne *et al.*, 2008), the accumulation of  $\text{NO}_2^-$  oxidation is to be expected at low aeration (Picioreanu *et al.*, 1997; Tchobanoglous *et al.*, 2003). In addition, it has also been reported that high concentrations of  $\text{NH}_3$  favour AOB over NOB and can lead to  $\text{NO}_2^-$  accumulation (Blackburne *et al.*, 2008).

At the beginning of the experiment,  $\text{NH}_3$  accumulated in the low DO reactors and even after the acclimation more than 30% of  $\text{NH}_3$  was not oxidized. As a consequence, the amount of free  $\text{NH}_3$  (FA) increased up to 6.6 mg/L (concentration calculated according to equation 8.1, Appendix 8.1) in the medium, raising the pH up to  $8.5 \pm 0.2$  (against  $7.04 \pm 0.5$  in the high aeration) (Figure 3.3). It is thought that the inhibition of  $\text{NO}_2^-$  oxidation starts at FA in the range of 0.1 – 1.0 mg/L of  $\text{NH}_3$  (Anthonisen *et al.*, 1976), and therefore it is likely that nitrite-oxidizers activity could be reduced due to the presence of high FA concentration.

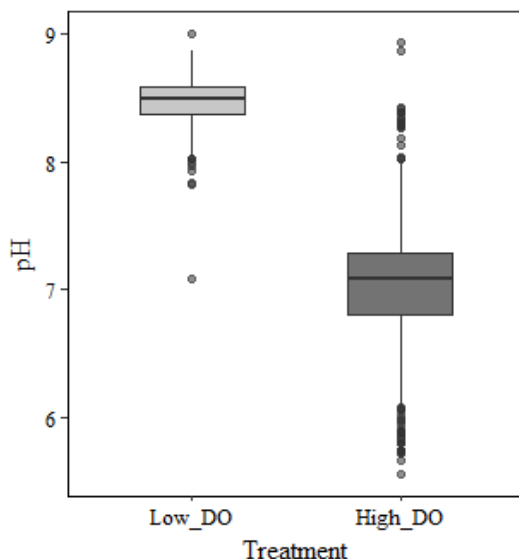


**Figure 3.3** Average pH measured in the reactors at low and high aeration.

### 3.3.2 Nitrifying community adapted under low DO

#### 3.3.2.1 Adaptation of AOB in the low and high DO nitrifying reactors

In the high DO reactors, there was a short initial period in which the numbers of AOB declined falling from  $4.4 \times 10^6$  to  $8.1 \times 10^5$  cells /mL. But after 17 days, the AOB number had recovered and stabilised in a range of  $1.3 \times 10^6$  –  $2.1 \times 10^7$  cells/mL (Figure 3.4b).

In the low DO reactors, the total AOB declined exponentially for 17 days, falling from  $2.2 \times 10^7$  to  $6.9 \times 10^4$  cells/mL. However, after day 17 an increase in the numbers of AOB bacteria was observed eventually reaching  $3.6 \times 10^7$  of cells/mL by day 66, three order of magnitude higher than the nadir (Figure 3.4a). From then on, the numbers of AOB in the low and high DO reactors were indistinguishable (nested ANOVA between reactors:  $p$ -value = 0.9,  $\alpha = 0.05$ ; Paired t-test between time:  $p$ -value = 0.3,  $\alpha = 0.05$ ), ranging from  $8.1 \times 10^5$  to  $3.6 \times 10^7$  of cells/mL. Though the TKN removal improved after day 58 in the low DO reactors, it did not attain the levels seen in the high DO reactors (Figure 3.4) despite the AOB numbers being comparable. This implies some difference in the ecology of the AOB at low and high DO conditions.

The adaptation of the AOB can occur by three mechanisms: selection of a particular AOB within the community, arrival of a new species into the community or the physiological adaptation of the existing AOB community. Some authors have related the selection of a specific AOB with DO concentrations (Park and Noguera, 2004; Bellucci *et al.*, 2011; Liu and Wang, 2013; Fitzgerald *et al.*, 2015). Nevertheless, Arnaldos *et al.* (2013) did not link the acclimation to low DO conditions to the selection of a specific AOB, since the population size changed randomly in both reactors operated at low and high oxygen concentrations. They thought that AOB could adapt to strict DO concentrations due to an enhanced expression of a heme protein, but they still have not identified the protein type and thereby its biochemical role (Arnaldos *et al.*, 2014; Arnaldos and Pagilla, 2015). Also, Liu and Wang (2013) attributed the decrease of nitrifier endogenous decay rates in low DO concentrations to the recovery of nitrifiers and nitrification performance. In the next sections, we hypothesise that the adaptation of AOB could be attributed to the selection of a chemolithoheterotrophic or chemoorganoheterotrophic subpopulation.

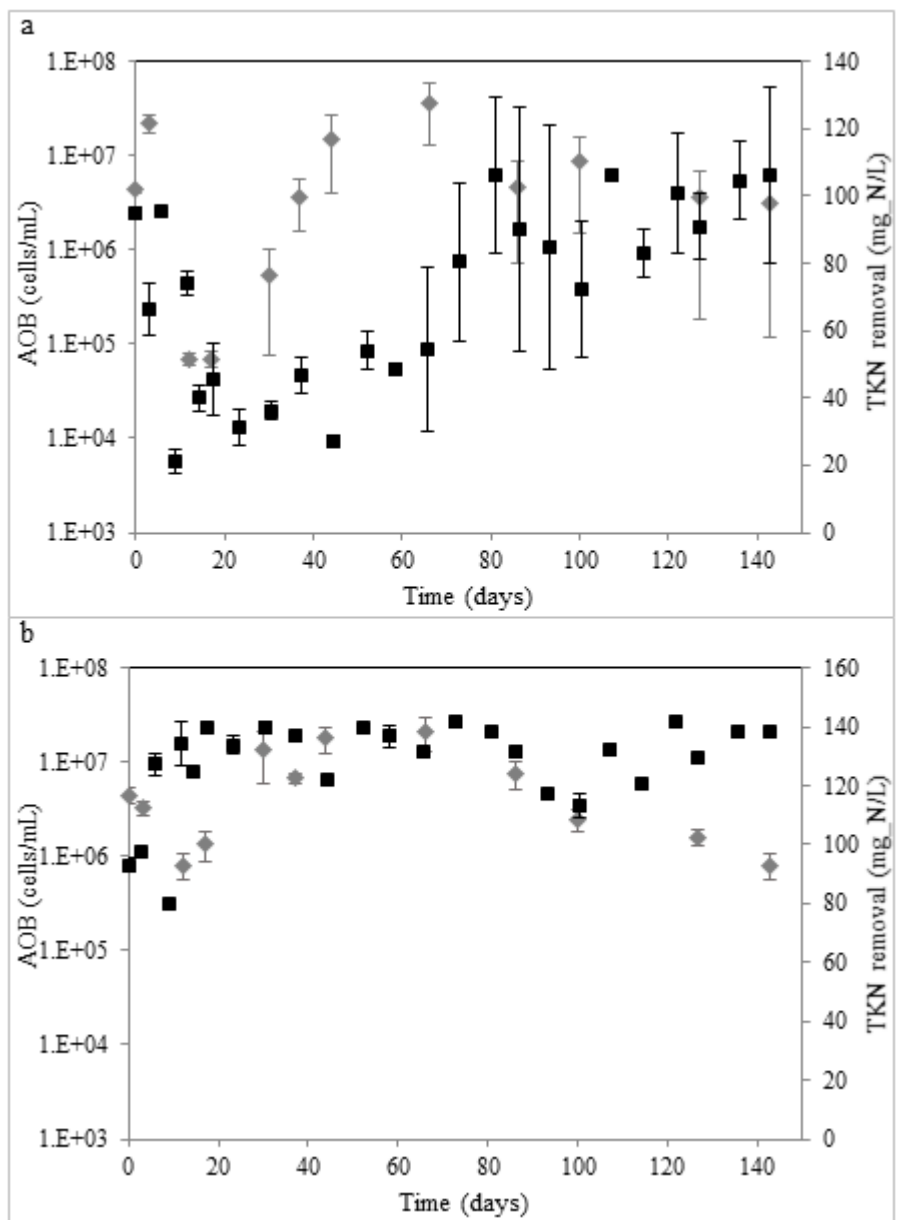


**Figure 3.4** AOB cell abundances (grey diamond) obtained from qPCR in the reactors under low (a) and high (b) DO concentrations and their respective TKN consumption (black square) over 143 days.

### 3.3.2.2 Underlying Dynamics

The enrichment achieved by AOB can be characterized as a transient period of exponential growth of a low DO tolerant subpopulation of the bacteria that could have come from either inside or outside the system. The simplest way to understand the increase in AOB concentration ( $N$ ) is using the exponential growth equation. Therefore, we can estimate the initial number of the tolerant AOB present in the activated sludge and determine how long these cells will take to adapt to very low DO levels. Modelling the exponential growth (Figure 3.5), we estimated that the specific net growth rate of the adapted AOB was  $0.2 \text{ d}^{-1}$  and its  $N_0$  was therefore about  $2 \times 10^3 \text{ cells/mL}$ , corresponding to 0.04% of the total AOB community

( $p$ -value < 0.05 for the slope and in the intercept,  $r^2 = 0.9$ ). Since  $N_0$  is greater than zero, the increase of certain AOB population occurred within the inoculum and not from immigration. This result was expected given that the method was applied to laboratory-scale reactors, but this information could be useful for the management of full-scale treatment plants.

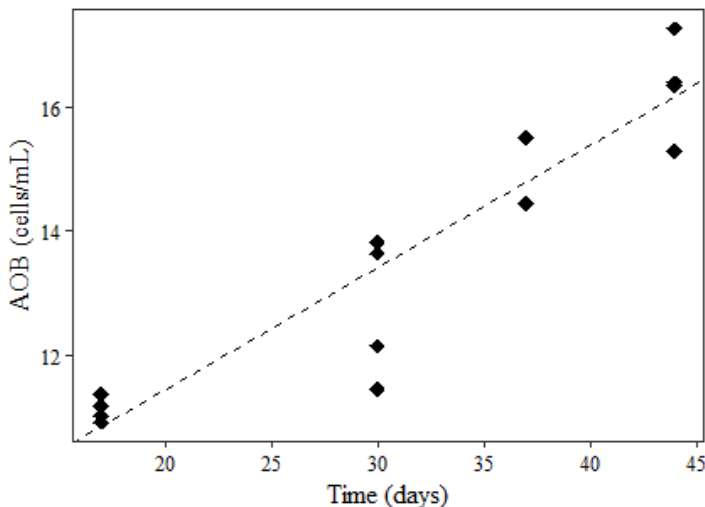


**Figure 3.5** Exponential regression curve of the AOB cell abundance under low DO. The slope of the line represents the specific growth rate of the adapted AOB following an exponential growth ( $r^2 = 0.9$ ).

We can support this analysis developing a simple two species model to evaluate the dynamic of different AOB populations at low DO concentrations (Figure 3.6a). The simulation result was very similar to our data: the rate of increase in total AOB was a mixture of the increase AOB2 abundance (with higher affinity for oxygen) and the decrease AOB1 abundance (with lower affinity for oxygen). In the initial phase, we observed that the growth rate of AOB2 decreased before actually growing exponentially to dominate the system. The estimated  $N_0$  using an exponential growth was presumably underestimated. During the adaptation period, the number of AOB was lower and therefore the consumption of  $\text{NH}_3$  was little. Similar result was observed in the experiment where only  $31.7 \pm 6.9\%$  of the TKN was removed in the initial period. The simulation showed that the adaptation of the subpopulation of AOB community to extreme low DO conditions was around two months (the same time in the laboratory experiments). The model suggested that the time to adaption was dependent of the initial concentration of the selected AOB (AOB2): the higher the initial concentration, the shorter the time of acclimation and vice-versa (Figure 3.6). And, once acclimated, AOB abundance and  $\text{NH}_3$  removal was almost at the same efficiency as in high DO reactors. Adaptation is a function of time and the species rarity present in reactors. The adaptation of nitrifying bacteria has been already correlated to long term periods at low DO (Arnaldos and

Pagilla, 2015), suggesting that prolonged operation allowed sufficient time for AOB acclimatization.

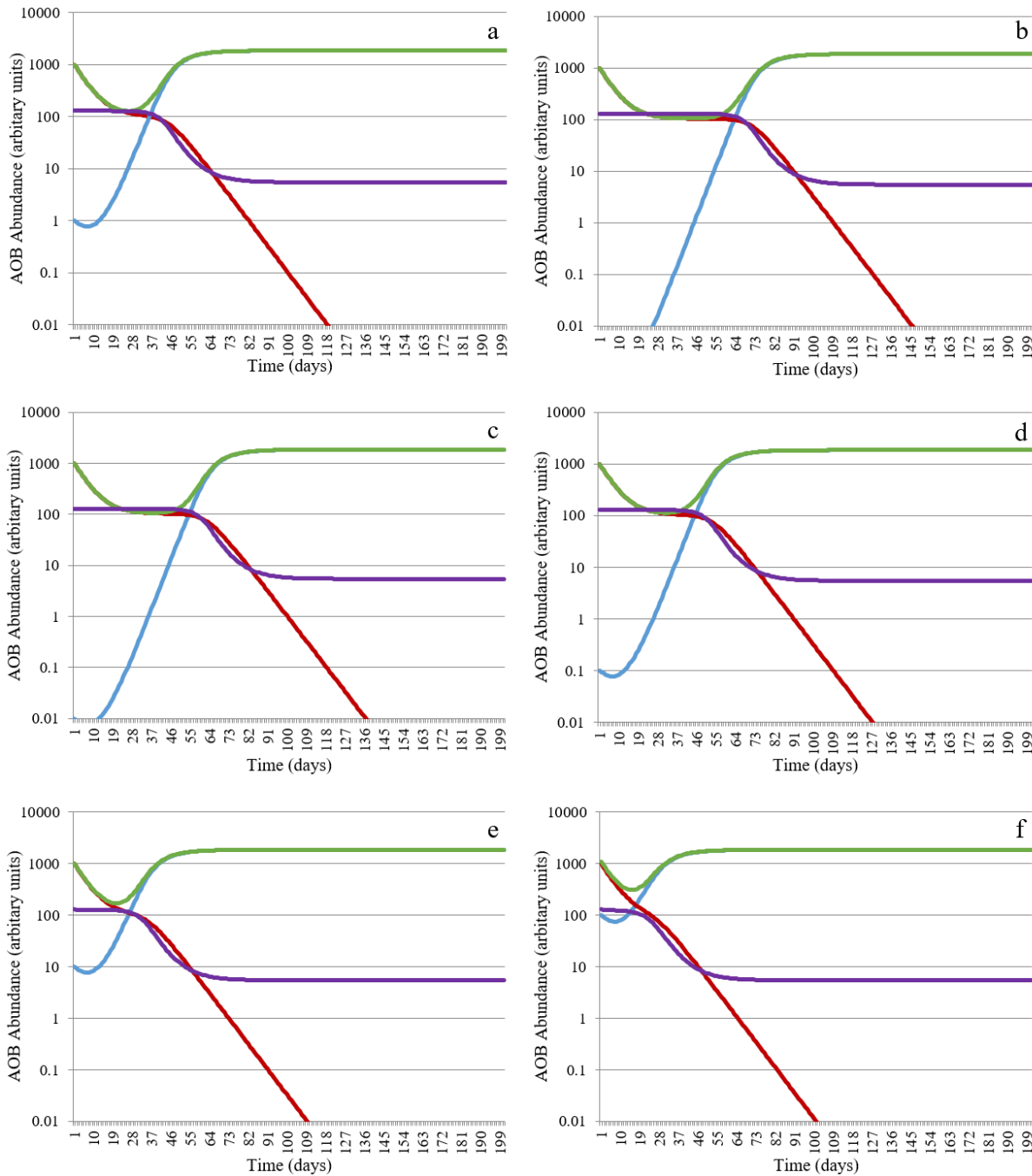


**Figure 3.6** Model for two species (AOB1 – red; and AOB2 – blue; total AOB – green) with the experimental parameters: 130 mg/L of NH<sub>3</sub> in the inlet (purple) and 0.2 mg/L of DO. Initial concentrations of the two species were modelled with arbitrary values in which the concentrations of AOB2 varied: 1 (a), 0.001 (b), 0.01 (c), 0.1 (d), 10 (e) and f (100).

### 3.3.2.3 AOB composition and diversity

Ion torrent and Illumina high-throughput sequencing (HTS) were used to characterize the composition of nitrifiers community in low and high DO conditions throughout the operation. After trimming the 16S rRNA amplicon sequences from Ion torrent platform, the 9 samples contained a total of 137,421 reads assigned to 8189 OTUs. The sequences obtained were not long enough to identify the species level of AOB. Only 3 OTUs were identified as *Nitrosomonas* and *Nitrosospira*. Within these OTUs, only the genus *Nitrosomonas* was found at low DO concentrations and they had a relative abundance of 0.0003% in the samples collected at the beginning of the experiment. No known AOB were detectable during the first 30 days of operation and therefore comparison between different conditions over time was not possible. Identification of rare species in a microbial community is problematic even using HTS technologies (Zhan and MacIsaac, 2015). Sample preparation (PCR amplification), DNA sequencing and computational analysis (genomics alignment and assembly) introduce bias and can lead to distorted coverage of the relevant gene (Sims *et al.*, 2014).

To improve the sequencing data and increase the coverage depth of rare species in order to detect AOB, we sequenced several samples collected at times 0, 3, 17, 23, 30, 37, 44 and 66 days from the 4 reactors (with replicates) and ran in HiSeq 2500 sequencer. Two different genes were targeted to improve the chances of capturing the highest number of AOB organisms: 16S rRNA gene (targeting all bacteria and archaea) and *amoA* gene specific to ammonia-oxidizers.

Using 16S rRNA sequencing, 73,055,533 reads were grouped into 17,191 unique sequences. Cluster analysis of the total population was performed on rank of similarities to compare differences between oxygen conditions, reactors and time. There was a significant difference between low and high DO reactors (ANOSIM:  $r^2 = 0.4$ ,  $p$ -value = 0.001), but no differences between duplicate reactors (R1\_L and R2\_L – ANOSIM:  $r^2 = 0.04$ ,  $p$ -value = 0.2; R3\_H and R4\_H – ANOSIM:  $r^2 = -0.03$ ,  $p$ -value = 0.7). Phylogenetic analysis of the 16S rRNA sequences showed that between 0.02 and 0.7% of the unique sequences were AOB with affiliation to *N. europaea/Nc. mobilis* lineage (cluster 7) and *N. oligotropha* lineage (cluster 6a). Although, changes of AOB community with oxygen concentration were detected by similarity analysis (ANOSIM:  $r^2 = 0.3$ ,  $p$ -value = 0.001), differentiation of those organisms over time was not possible (Figure 3.7). A very low proportion of sequences mainly in the initial samples were identified as AOB, but sequencing analysis grouped the *N. europaea/Nc. mobilis* cluster-7 in the low DO reactors and *N. oligotropha* cluster-6a in the high aeration mode. The total diversity in all the reactors was higher at the beginning of the operation

(Figure 3.8), and therefore, rare species would require millions of reads to be detected (Sims *et al.*, 2014).

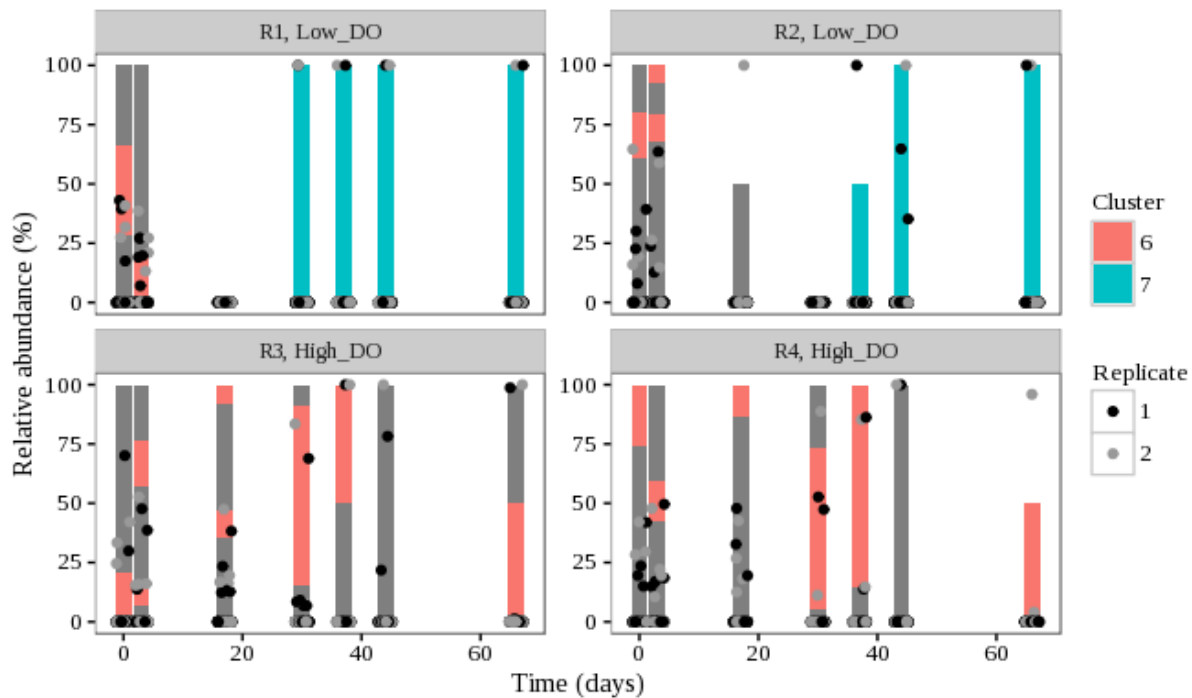


**Figure 3.7** Relative abundance of the AOB close related sequences from 16S rRNA sequencing in the reactors at low and high DO over 66 days. Each bar represents the sample collected at a certain time and condition and all the different clusters are represented by colours: cluster 6 (red) and cluster 7 (blue). Each sample was run in duplicate: replicate 1 (black) and 2 (grey). The grey bars represent the sequences with no species assignments.

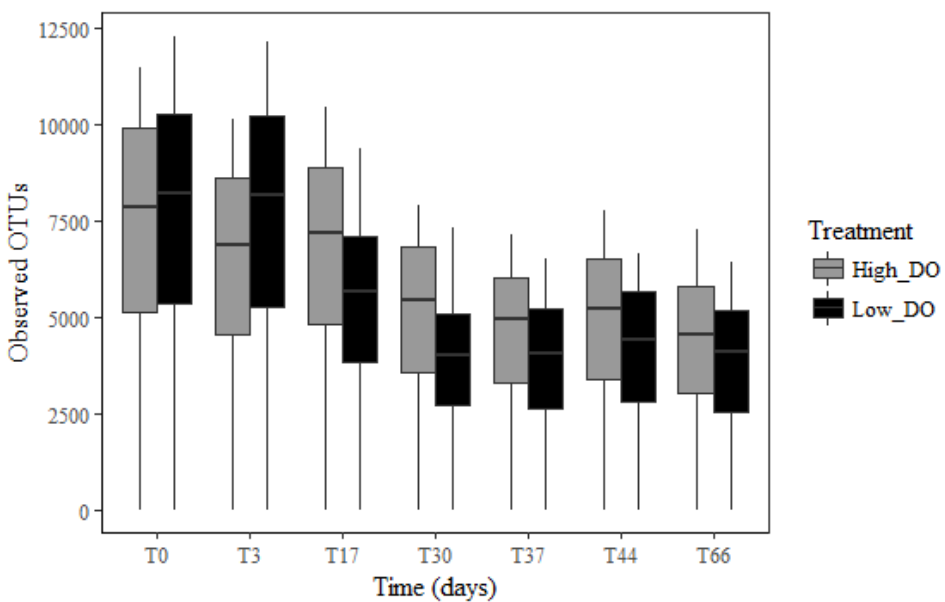


**Figure 3.8** Observed OTUs average at times 0, 3, 17, 30, 44 and 66 days in low and high DO.

We also sequenced and analysed the *amoA* gene fragment to get a more detail information of the AOB community changes at different aerations. A total of 2691 unique sequences were generated from 20,457 *amoA* sequences. Figure 3.9 illustrates a PCA plot based on the similarities between the recovered sequences at low and high DO. PCA analyses revealed that the AOB community composition diverged between the low and high DO reactors. This was further confirmed by an ANOSIM of the four reactors ( $r^2 = 0.5$ ,  $p$ -value = 0.001). Again, no differences between duplicate reactors (R1\_L and R2\_L – ANOSIM:  $R^2 = -0.002$ ,  $p$ -value = 0.4; R3\_H and R4\_H – ANOSIM:  $r^2 = -0.032$ ,  $p$ -value = 0.7). Sequencing the *amoA* gene provided additional information about the AOB community in the initial samples.

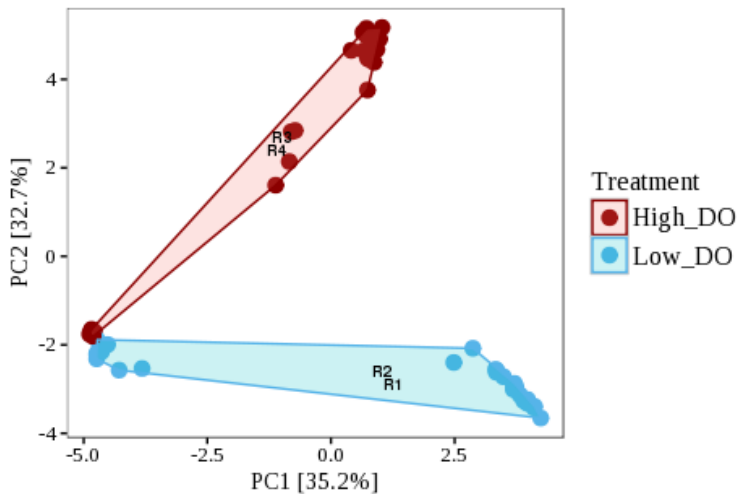


**Figure 3.9** PCA analysis based on the Bray Curtis similarity of the OTUs derived from Illumina sequencing *amoA* gene. Clusters are separated by oxygen treatment and reactors: low DO (blue – R1\_L and R2\_L) and high DO (red – R3\_H and R4\_H).

Duplicate reactors showed a parallel divergence of *amoA* clusters over time (Figure 3.10). Initially, all samples from both configurations comprised *N. oligotropha* lineage (cluster 6a), *N. europaea/Nc. mobilis* lineage (cluster 7), and *Nitrosospira* lineage (cluster 0 and 2), with  $98.8 \pm 1.6\%$ ,  $0.7 \pm 1.4\%$ ,  $0.4 \pm 0.3\%$  of relative abundance, respectively. By day 17, the four reactors had diverged into two lineages and the characteristic AOB community persisted through all the experiment. While *N. oligotropha* cluster-6a and *Nitrosospira* cluster-0 dominated the reactors at high DO concentration with a relative abundance of  $53.6 \pm 15.6\%$  and  $15.6 \pm 11.9\%$ , respectively, the *amoA* sequences in low DO were dominated ( $99.9 \pm 0.03\%$ ) by *N. europaea/Nc. mobilis* cluster-7. This difference suggested that the low DO might have promoted the selection of *N. europaea/Nc. mobilis* lineage from within the AOB community. Although there is disagreement about the AOB found in reactors operated under

low DO (de Bie *et al.*, 2001; Gieseke *et al.*, 2001; Park and Noguera, 2004; Bellucci *et al.*, 2011; Arnaldos *et al.*, 2013; Liu and Wang, 2013; Fitzgerald *et al.*, 2015), the results presented here agree with the study done by Park & Noguera (2004). They reported that *N. europaea* was found in an oxygen limited chemostat, whereas *N. oligotropha* appeared to be prevalent at higher oxygen levels. They subsequently isolated and characterized AOB strains grown in reactors at 0.12 – 0.24 mg O<sub>2</sub>/L (Park and Noguera, 2007). In the phylogenetic analysis in low DO, we did not see *N. oligotropha* lineage in our study, which could be explained by the low oxygen affinity of this bacteria. However, the high oxygen affinity for *N. europaea* lineage reported in their work and the possible low tolerance for high NH<sub>3</sub> concentrations of these organisms might explain their survival in the our low DO reactors and the incomplete NH<sub>3</sub> consumption (only 64.3 ± 16.3% consumed).

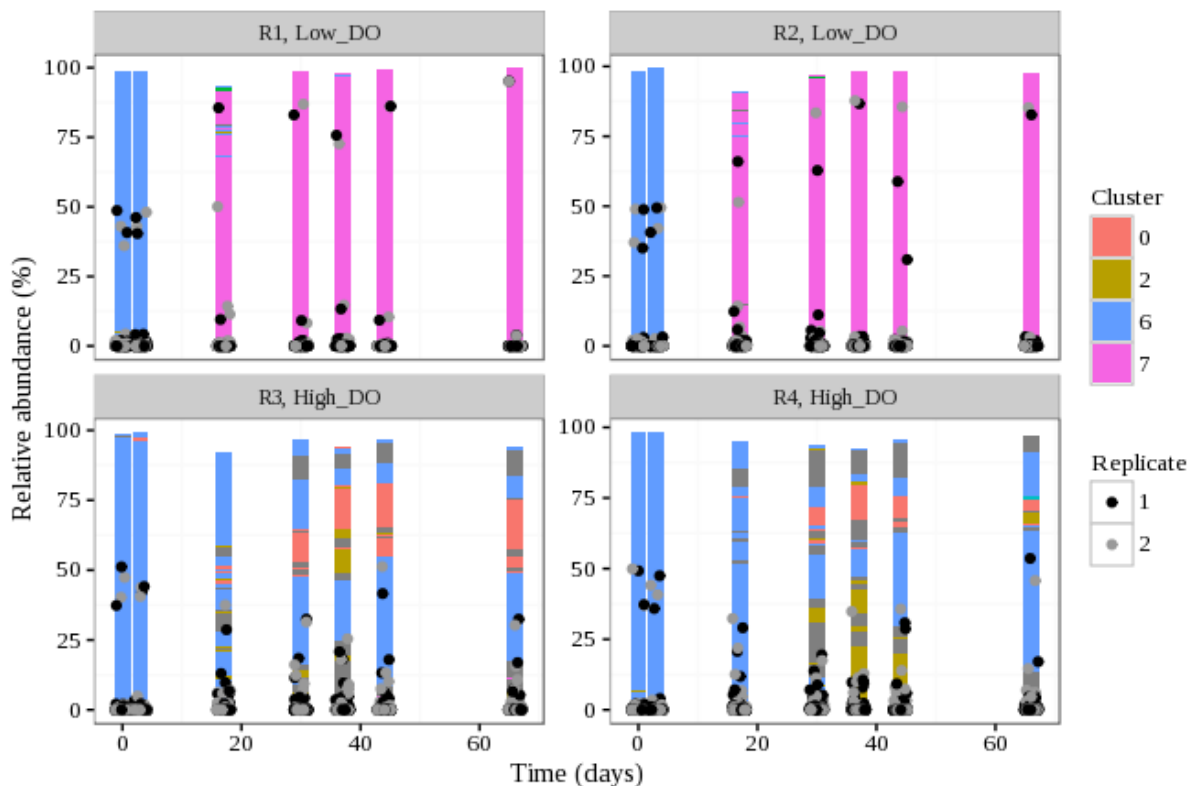


**Figure 3.10** Relative abundance of the 100 most abundant AOB close related sequences from *amoA* gene sequencing in the reactors at low and high DO over 66 days. Each bar represents the sample collected at a certain time and condition and all the different clusters are represented by colours: cluster 0 (red), cluster 2 (gold), cluster 6 (blue) and cluster 7 (purple). Each sample was run in duplicate: replicate 1 (black) and 2 (grey). The grey bars represent the sequences with no species assignments.

### 3.3.2.4 Adaptation of NOB in the low DO nitrifying reactors

The reactors operated under low DO concentration had very low amount of  $\text{NO}_3^-$  production ( $1.3 \pm 1.3 \text{ mg/L}$ ). Functional gene *nxrB* encoding the  $\text{NO}_2^-$  oxidoreductase enzyme was amplified to quantify *Nitrospira* and *Nitrobacter* in the different reactors at different time points (Figure 3.11).

Surprisingly, the cell number of NOB remained relatively high throughout the experiment, even in the oxygen limiting system. NOB growth declined in the initial phase of the experiment in the low DO reactors, decreasing by 2 orders of magnitude from  $1.7 \times 10^7$  to  $6.6 \times 10^5$  cells/mL and  $1.2 \times 10^8$  cells/mL to  $5.8 \times 10^6$  for *Nitrospira* and *Nitrobacter*, respectively. After day 30, the *Nitrospira* cells remained in a range of  $1.6 \times 10^6 - 4.7 \times 10^7$  cells/mL (nested ANOVA between reactors:  $p$ -value = 0.6,  $\alpha = 0.05$ ; Paired t-test between time:  $p$ -value = 0.2,  $\alpha = 0.05$ ). In both configurations the *Nitrobacter* cell numbers were (after an initial reduction) relatively stable in a range of  $1.5 \times 10^6 - 2.8 \times 10^7$  (nested ANOVA between reactors:  $p$ -value = 0.9,  $\alpha = 0.05$ ; Paired t-test between time:  $p$ -value = 0.9,  $\alpha = 0.05$ ) (Figure 3.10). The results suggested that none of the taxa quantified were dominant in the four reactors through all the experiment. The low oxygen concentration was expected to limit both NOB, since both *Nitrospira* and *Nitrobacter* are thought to have similar low affinity for oxygen ( $K_{DO} = 0.54 \text{ mg/L}$ , (Blackburne *et al.*, 2007)). Interestingly, in the initial phase in the low DO reactors, the NOB abundance decreased by 2 orders of magnitude compared to the 3 orders of magnitude decrease seen in the AOB number. This result suggested that the NOB population being selected was more abundant in the biomass used to seed the reactor than the AOB population.

$\text{NO}_2^-$  oxidation was incomplete in the low DO reactors with the accumulation of  $\text{NO}_2^-$  and only modest amounts of  $\text{NO}_3^-$  in the system. This was surprising as the NOB population only dipped briefly at low DO concentration (when the reactors were initiated) and quickly recovered to levels comparable to those seen at high DO concentrations. Previous studies reported complete  $\text{NO}_2^-$  consumption in reactors under DO concentrations between 0.2 – 0.5 mg/L, suggesting that the activity of NOB was not inhibited by low DO (Park and Noguera, 2004; Bellucci *et al.*, 2011; Arnaldos *et al.*, 2013; Liu and Wang, 2013; Fitzgerald *et al.*, 2015). Also, Liu and Wang (2013) related the survival of these organisms to the selection of NOB sublineage with the highest affinity for oxygen.

There are at least two explanations that can be attributed to the adaptation of NOB in the oxygen limited reactors. The presence of low amounts of  $\text{NO}_3^-$  in the presence of abundant NOB suggests simultaneous nitrification and denitrification (heterotrophic and nitrifier

denitrification). In this case, the production of  $\text{NO}_3^-$  by NOB is followed immediately by the reduction of this compound, by denitrifiers, to  $\text{N}_2$  leaving the small residual  $\text{NO}_3^-$  concentration observed.

The hypothesis of simultaneous nitrification and denitrification is supported by the difference in the amount of biomass seen under low and high DO conditions. The biomass concentration stabilised at an average of  $133.3 \pm 43.7$  and  $362.7 \pm 110.2$  mg/L in low and high DO reactors, respectively. The putative heterotrophs (around 90 – 97 % of the total biomass) had 37.4% less biomass in the low DO reactors, but most of the influent COD ( $94.4 \pm 4.6\%$ ) was removed in both configurations (Figure 3.12), even using an extra carbon source (pyruvate). The consumption of similar amounts of COD did not result in similar amounts of biomass. The smaller amount of biomass implies a lower yield in the putative heterotrophic biomass under low DO. That is consistent with our hypothesis of simultaneous nitrification and denitrification by assuming the presence of facultative aerobes denitrifiers (Rittmann and McCarty, 2001; Guo *et al.*, 2009).

Alternatively, associated to the low oxygen level, the reactors were fed with an extra organic carbon (pyruvate), and therefore it is possible that there was a change in the metabolism of NOB. These bacteria may have been able to consume simple organic carbons, such as pyruvate, to synthesise biomass and/or generate energy. Recently, mixotrophic growth in the presence of  $\text{NO}_2^-$  was detected in *Nitrobacter* and *Nitrospira* species, but only in aerobic conditions (Bock, 1976; Watson *et al.*, 1986; Daims, Nielsen, *et al.*, 2001; Starkenburg *et al.*, 2008).

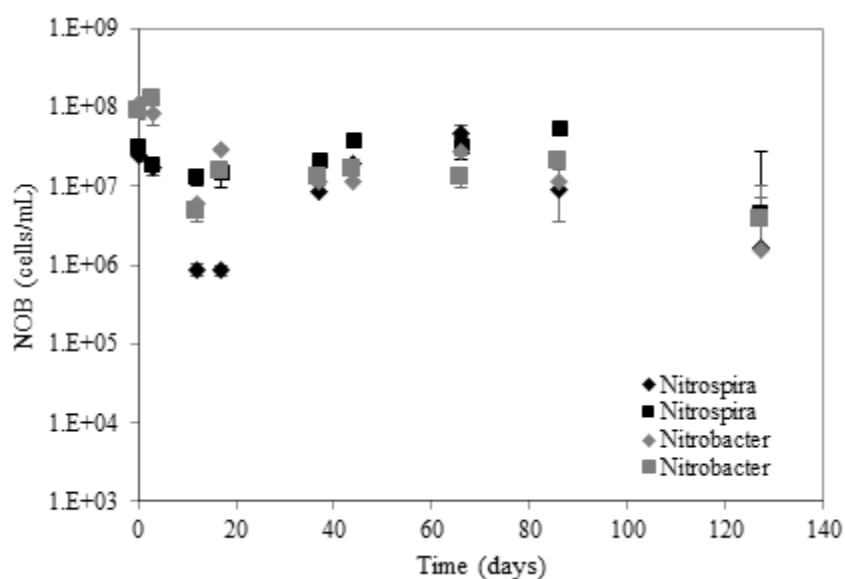


**Figure 3.11** *Nitrospira* (black) and *Nitrobacter* (grey) cell abundances (cells/mL) obtained from qPCR in the reactors under low DO (diamond) and high (square) conditions over 127 days.

### 3.3.3 Possible metabolic pathways of AOB

The alkalinity was largely consumed ( $92.1 \pm 10.3\%$ ) in the reactors at high DO and actually accumulated during the adaptation time in the low aeration reactors (Figure 3.12). The increase in alkalinity at low DO concentrations presumably reflected the low consumption of carbon dioxide ( $\text{CO}_2$ ) by AOB. A drop (by day 58) in alkalinity in the low DO reactors co-occurred with a period of  $\text{NH}_3$  consumption (Figure 3.12 and 3.2), but only  $51.8 \pm 18.5\%$  of alkalinity was removed. Each AOB cell consumed on average around  $6.1 \times 10^{-8}$  and  $3 \times 10^{-7}$  mg of alkalinity in low and high DO, respectively.

This result is difficult to reconcile with the AOB abundances determined by qPCR, since both low and high DO configurations had similar amount of AOB after reaching the steady state (on average  $6.9 \times 10^6$  for high DO and  $1.1 \times 10^7$  cells/mL for low DO), but consume different amounts of alkalinity/ $\text{NH}_3$ . Thus, the maximum growth yields were higher in the low DO ( $0.36 \pm 0$  mg AOBVSS/mg N) reactor than in high DO reactor ( $0.1 \pm 0$  mg AOBVSS/mg N).

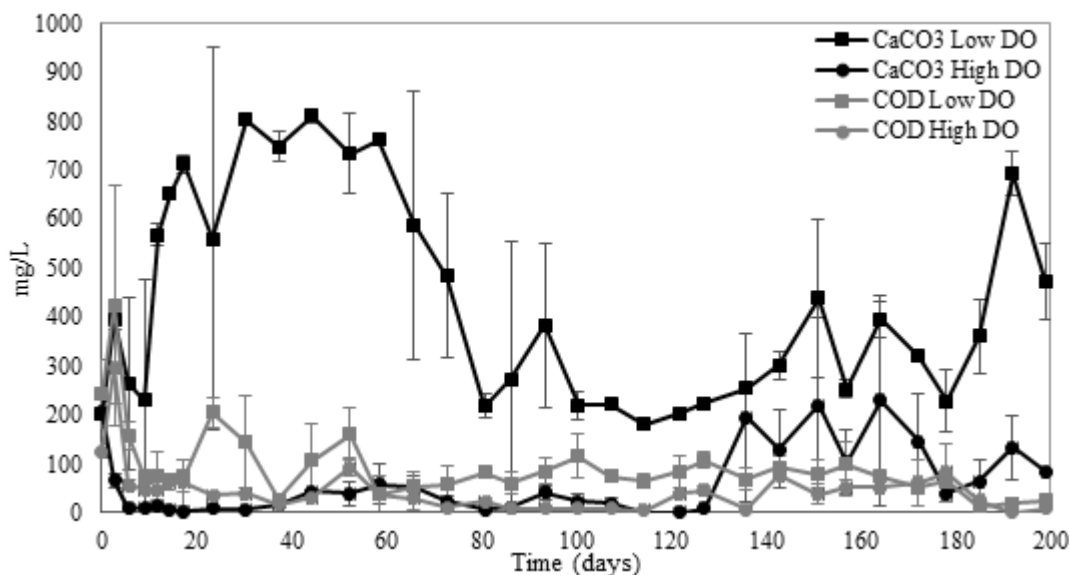


**Figure 3.12** COD (grey) and alkalinity (black) concentration measured in the low aeration (squares) and high aeration (circles).

We suggest that under low DO concentrations the AOB subpopulation (*N. europaea/Nc. mobilis* lineage) adopted a mixotrophic metabolism that are able to use organic matter (probably pyruvate) as a carbon source and/or electron donor. A switch from inorganic to an organic carbon source would reduce the energetic cost of obtaining  $\text{CO}_2$  and the

electrons required to form new biomass (Hommes *et al.*, 2003). Also, the use of organic matter as electron donor would be energetically favourable.

Such proposal is based on this study, where the low concentration of oxygen was associated with a low yield of putative heterotrophs (high COD consumption) and an increased yield in the AOB (higher growth). Bellucci *et al.* (2011) also observed higher yields in the AOB under low DO concentrations. They also hypothesised that AOB adopted a chemolithoorganotrophic metabolism: replacing CO<sub>2</sub> fixation with the uptake of organic carbon compounds. Moreover, a theoretical model, considering no losses of energy in proton translocations or in the ATP formation, estimated higher yields for AOB (0.35 g Bio/g N-NH<sub>3</sub>) when pyruvate was the only carbon source (González-Cabaleiro *et al.*, in preparation). The maximum growth yield using an autotrophic growth should be around 0.13 g Bio/g N-NH<sub>3</sub>, which is half of the observed value at low DO in this study. Moreover the incomplete NH<sub>3</sub> removal in this study could suggest that AOB adopted an organotrophy metabolism. The obligate lithotrophy growth of AOB is explained by the incomplete tricarboxylic acid (TCA) cycle due to the absence of 2-oxoglutarate dehydrogenase expression. However, the activity of this enzyme was detected in anaerobic reactors implying the completion of the TCA cycle and thus organotrophic growth (Beyer *et al.*, 2009). Chemoorganoheterotrophic growth in pure cultures of AOB, such as *N. europaea* (the subpopulation adapted under low DO in this study), has been reported under anoxic/anaerobic conditions with pyruvate as electron donor and energy source and NO<sub>2</sub><sup>-</sup> as electron acceptor (Beyer *et al.*, 2009; Schmidt, 2009).

### 3.4 Conclusions

In the present work, we observed the acclimatization of the nitrifying bacteria to low DO concentration. The adaptation of AOB took place through the selection of very rare taxa present in the original seed. This result was further confirmed by simulating two AOB species under low DO. We observed that the time to adapt to such conditions appeared to be dependent on the initial concentration of the selected bacteria in the seed. Members of the *N. europaea/Nc. mobilis* lineage were found in reactors at low DO. This selected AOB had high yields and consumed less alkalinity (CO<sub>2</sub>) and NH<sub>3</sub> than those seen at high DO concentrations supporting a hypothesis of chemolithoheterotrophic or chemoorganoheterotrophic metabolism by AOB at low DO. There were no significant differences in the NOB abundance at low and high DO concentrations, suggesting that these organisms may have oxidized NO<sub>2</sub><sup>-</sup> and

Chapter 3. Adaptation of nitrifying bacteria at low dissolved oxygen conditions

denitrification have occurred. We conclude that nitrifying bacteria can adapt to low DO concentrations in full-scale treatment plants, but the NH<sub>3</sub> and carbon metabolism may change.

## **Chapter 4. Impact of nitrous oxide emissions in activated sludge operated at low dissolved oxygen concentrations**

### **4.1 Introduction**

Energy consumption and the concomitant release of GHGs is a major concern for the water industry (U.S. Environmental Protection Agency, 2006). GHG emissions during the aeration of activated sludge account for around 3% of the UK annual total (Ofwat, 2010). The UK water industry released around 374 million tonnes of GHG carbon dioxide equivalents (CO<sub>2</sub>e) to the atmosphere in 2016 (DBEIS, 2017). Although aeration control is an effective means of reducing the energy demand of activated sludge plants, when these plants operate under anoxic or low DO conditions substantial amounts of N<sub>2</sub>O can be produced (Tallec *et al.*, 2006; Kampschreur *et al.*, 2008). N<sub>2</sub>O is a long-lived (~114 years) (Montzka *et al.*, 2002) trace gas which contributes significantly to atmospheric radiative forcing, having a global warming potential ~300 times that of CO<sub>2</sub> (Myhre *et al.*, 2013), and is the largest sink for stratospheric ozone (O<sub>3</sub>), via NO production (Ravishankara *et al.*, 2009). Anthropogenic activities account for ~ 40% of total N<sub>2</sub>O emissions (Ciais *et al.*, 2013) and wastewater treatment may account for ~8% of anthropogenic N<sub>2</sub>O (U.S. Environmental Protection Agency, 2006). Sustainable activated sludge treatment should minimise N<sub>2</sub>O production; this requires an understanding of the mechanisms involved in its production.

The production of N<sub>2</sub>O during wastewater treatment has been associated with both heterotrophic denitrification and nitrifier denitrification (Law *et al.*, 2012). In heterotrophic denitrification, under typical anaerobic conditions, N<sub>2</sub>O arises as an obligate intermediate during the sequential reduction of NO<sub>3</sub><sup>-</sup> to N<sub>2</sub> (NO<sub>3</sub><sup>-</sup> → NO<sub>2</sub><sup>-</sup> → N<sub>2</sub>O + NO → N<sub>2</sub>) coupled to organic substrate oxidation (Bonin *et al.*, 2002). Transient N<sub>2</sub>O accumulation can result via the inhibition of N<sub>2</sub>O reductase by low DO. In nitrifier denitrification NH<sub>3</sub> is first oxidized to NO<sub>2</sub><sup>-</sup> by AOB, followed by NO<sub>2</sub><sup>-</sup> reduction to NO, N<sub>2</sub>O and finally N<sub>2</sub> (Bock *et al.*, 1995). It is enhanced at low DO and high NO<sub>2</sub><sup>-</sup> concentrations (Kampschreur *et al.*, 2008). AOB can also produce N<sub>2</sub>O as a byproduct during the incomplete oxidation of hydroxylamine (NH<sub>2</sub>OH) to NO<sub>2</sub><sup>-</sup> (Hooper and Terry, 1979; Chandran *et al.*, 2011). These latter two pathways have both been identified as major contributors to the conversion of NH<sub>3</sub> to N<sub>2</sub>O in activated sludge (Itokawa *et al.*, 2001; Bonin *et al.*, 2002; Tallec *et al.*, 2006).

The sensitivity of N<sub>2</sub>O production to DO results in higher emissions being reported during intermittent aeration or aerobic/anoxic cycling (Yu *et al.*, 2010; Kosonen *et al.*, 2016). In addition to elevated NO<sub>2</sub><sup>-</sup> and NH<sub>3</sub> concentrations, low C/N ratio, low pH, and short SRTs can also promote N<sub>2</sub>O production (Hanaki *et al.*, 1992; Thörn and Sörensson, 1996; Colliver and Stephenson, 2000).

To date, studies of the performance of activated sludge at low DO concentrations have focused on the degree of NH<sub>3</sub> oxidation and microbial diversity in the activated sludge (Park and Noguera, 2004; Bellucci *et al.*, 2011; Liu and Wang, 2013; Fitzgerald *et al.*, 2015). Nevertheless, N<sub>2</sub>O emissions have been typically neglected. Even so, high N<sub>2</sub>O emissions have been observed at low DO values (between 0.1 to 2 mg/L) in batch experiments using biomass from a full-scale activated sludge plant. Emissions were highest at 1 mg O<sub>2</sub>/L (Tallec *et al.*, 2006). Stenström *et al.* (2014) showed that DO reduction below 1.0–1.5 mg/L during nitrification resulted in high N<sub>2</sub>O emissions in water and off-gas from a sequencing batch reactor treating digester supernatant. However, in both cases the biomass was acclimated to high DO and this may have increased the N<sub>2</sub>O emissions. The operation of bio-reactors at low DO concentrations with an acclimated biomass may reduce the possible N<sub>2</sub>O production. Also, even such production may increase during the low aeration systems, it is still not known if N<sub>2</sub>O will have a serious impact on net GHG emissions in activated sludge plants.

In this study we investigated N<sub>2</sub>O production in small-scale laboratory reactors containing activated sludge and operated at preselected (low and high) DO concentrations. The outcome of this work will be relevant to the evaluation of N<sub>2</sub>O emissions during the operation of full-scale activated sludge plants under low DO concentrations and thus will have implications for the reduction of operational costs and the contribution from activated sludge treatment to the atmospheric N<sub>2</sub>O inventory.

## 4.2 Materials and methods

### 4.2.1 Setup and operation of continuously stirred bioreactors

The reactor operation is described in detail elsewhere (Chapter 3.2.1). Briefly, four, three litre continuous reactors were established. Two were maintained at 0.2 mg O<sub>2</sub>/L and two at 6.3 – 6.6 mg O<sub>2</sub>/L and each reactor employed a synthetic medium with a SRT and HRT of 5 days. The reactors were operated for 276 days prior to the batch test. The reactor was inoculated with biomass (activated sludge) collected from the Tudhoe Mill (County Durham,

UK) domestic WWTP. Concentrations of the different variables measured in the medium and sludge reactor through the experiment are shown in Table 4.1.

**Table 4.1** Characteristics of the laboratory-scale reactors operated at different DO concentrations.

Variables	Average ( $\pm$ Standard deviations)	
	Low DO	High DO
<b>Volatile Suspended Solids (VSS) (mg/L)</b>	133.3 $\pm$ 33.6	362.7 $\pm$ 77.9
<b>Chemical Oxygen Demand (COD) removal (mg/L)</b>	692.1 $\pm$ 54.7	727.7 $\pm$ 58.5
<b>DO (mg/L)</b>	0.2 $\pm$ 0.1	6.3 $\pm$ 0.5 – 6.6 $\pm$ 0.6
<b>pH</b>	8.46 $\pm$ 0.1	7.04 $\pm$ 0.4
<b>CaCO<sub>3</sub> removal (mg CaCO<sub>3</sub>/L)</b>	310.8 $\pm$ 77.5	534.7 $\pm$ 86.2
<b>Total Kjeldahl Nitrogen (TKN) removal (mg/L)</b>	88.7 $\pm$ 16.8	128 $\pm$ 14.7
<b>NO<sub>2</sub><sup>-</sup> (mg/L)</b>	27.4 $\pm$ 15.9	0.2 $\pm$ 0.2
<b>NO<sub>3</sub><sup>-</sup> (mg/L)</b>	1.3 $\pm$ 0.9	125 $\pm$ 14.8
<b>AOB average (cells/mL)</b>	5 x 10 <sup>6</sup>	3.1 x 10 <sup>6</sup>
<b>NOB average (cells/mL)</b>	1.9 x 10 <sup>7</sup>	3 x 10 <sup>7</sup>

## 4.2.2 Batch experiments

Twelve samples were collected from each reactor, sequentially over 48 hours. In each case, around 20 mL of activated sludge was collected at steady state condition and placed in a 60 mL serum vial, leaving a notional 40 mL headspace (total 96 vials) (Figure 4.1). All vials initially contained ambient air and were closed with PTFE red rubber through which the gases were later sampled. For the low DO reactor samples, the vials were first flushed with pure N<sub>2</sub> gas to exclude all atmospheric air. Liquid samples collected from the reactors were injected into the vacuum vials which were agitated using an orbital shaker at 130 rpm to achieve liquid-gas phase equilibration and incubated at room temperature. At each sequential time point, the gas was extracted from a vial head space using a syringe and analysed by gas chromatography following an established method (Upstill-Goddard *et al.*, 1996). In brief, N<sub>2</sub>O was separated isothermally (60°C) on a 5m x 1.75 mm id., 80-100 mesh Porapak Q column, and passed over Mg(ClO<sub>4</sub>)<sub>2</sub> and NaOH to remove H<sub>2</sub>O vapour and CO<sub>2</sub>. Carrier gas (flow rate ~ 25 mL/min) was ultra-high purity (UHP) N<sub>2</sub>. Analysis of N<sub>2</sub>O used a 63Ni Electron Capture Detector operated at 350°C. Calibration was with a mixed secondary standard prepared by pressure dilution in UHP N<sub>2</sub> (Upstill-Goddard *et al.*, 1996) and pre-calibrated against a commercially sourced mixed standard (300 ppbv N<sub>2</sub>O in N<sub>2</sub>) certified to

an accuracy of  $\pm 1\%$  (Air Products). Analytical precision was  $\pm 0.8\%$  based on analysis of the standard.

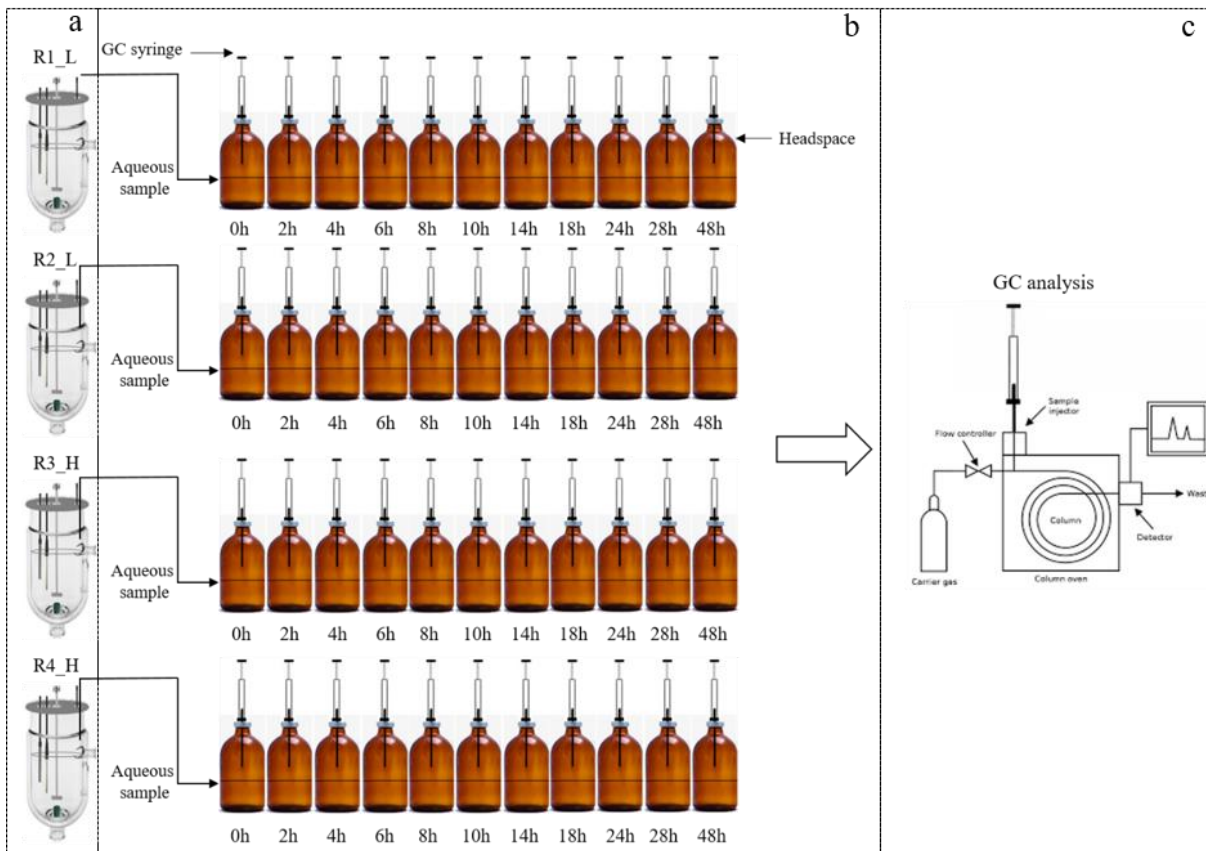


**Figure 4.1** Schematic diagram of the experimental system: four laboratory-scale bioreactor operated at low (R1\_L and R2\_L) and high (R3\_H and R4-H) DO (a); Batch experiments (b); GC analysis for N<sub>2</sub>O analysis (c).

NO<sub>2</sub><sup>-</sup> and NO<sub>3</sub><sup>-</sup> were analysed by ion chromatography (Dionex DW-1000 ion chromatograph; Dionex Corp., Sunnyvale, CA, USA) following 0.2  $\mu\text{m}$  filtration (syringe filters) at times 0, 2, 3, 5, 8, 10, 14, 28 and 48 h. The ion chromatograph was fitted with an IonPac AS14A analytical column and a 25- $\mu\text{L}$  injection loop. It operated at a flow rate of 1 mL/min with 8.0 mM Na<sub>2</sub>CO<sub>3</sub>-1.0 mM NaHCO<sub>3</sub> as eluent.

#### 4.2.3 Calculation of N<sub>2</sub>O production rate

The total amount of N<sub>2</sub>O in each vial is the sum of N<sub>2</sub>O in the gaseous (headspace) and aqueous phases, the relative amounts in each being driven by solubility-dependent phase partitioning, as determined by the relative phase volumes and N<sub>2</sub>O solubility at the sample temperature (Upstill-Goddard *et al.*, 1996). A phase partitioning correction was therefore applied using solubility values derived from Weiss and Price (1980), as detailed in Upstill-

Goddard *et al.* (1996). The N<sub>2</sub>O production rate in each replicate was determined by applying linear fit to the time-dependent N<sub>2</sub>O concentration for each oxygen concentration. The fraction (Y<sub>N<sub>2</sub>O</sub>) of the N<sub>2</sub>O production rate (rN<sub>2</sub>O) arising from nitrogen (TKN) consumption was estimated using equation 4.1:

(4.1)

$$Y_{N_2O} = \frac{rN_2O}{rTKN} \times 100$$

where rTKN is the TKN consumption rate.

#### 4.2.4 Statistical analysis

Significant differences in the results were examined using nested analysis of variance (ANOVA) and paired t-test analysis in RStudio (version 1.0.136). The linear regression analysis and statistics were conducted in R.

### 4.3 Results and Discussion

#### 4.3.1 N<sub>2</sub>O production at different oxygenation levels

The nitrogen mass balance based on TKN, NO<sub>2</sub><sup>-</sup> and NO<sub>3</sub><sup>-</sup> (Table 4.1) revealed incomplete nitrification, indicated by the accumulation of NO<sub>2</sub><sup>-</sup>, and an apparent loss of total nitrogen. About 68% of the ammonium nitrogen input consumed was not accounted for in the mass balance. Under oxygen limiting conditions, AOB are thought to trigger a defensive mechanism that overcomes the negative effect of high NO<sub>2</sub><sup>-</sup> concentrations caused by inhibition of the activity of NOB at low DO concentrations (Poth and Focht, 1985; Stein and Arp, 1998). By using NO<sub>2</sub><sup>-</sup> as a terminal acceptor, AOB conserve oxygen for the initial step in NH<sub>3</sub> oxidation, remove a toxic product and decrease their need to compete with NOB for oxygen (Poth and Focht, 1985). Thus, AOB shift to an nitrifier denitrification pathway, using NO<sub>2</sub><sup>-</sup> as an electron acceptor and producing N<sub>2</sub>O with hydrogen, hydroxylamine or organic carbon (pyruvate, lactate) as an electron donor (Abeliovich and Vonshak, 1992; Bock *et al.*, 1995; Schmidt *et al.*, 2004). This is consistent with the work of Tallec *et al.* (2006) in microcosms from full-scale treatment plants who found N<sub>2</sub>O production to vary with the oxygen concentration and that the highest N<sub>2</sub>O emissions occurred at low DO concentrations (from 0.1 to 2 mg/L).

To investigate the N<sub>2</sub>O production in all the reactors, we performed batch experiments. In these experiments N<sub>2</sub>O production occurred during the first 14 h, when oxygen would have still been available (Figure 4.2a). After this point N<sub>2</sub>O declined, presumably due to denitrification being favored in the absence of oxygen. The NO<sub>2</sub><sup>-</sup> and NO<sub>3</sub><sup>-</sup> concentrations were always constant over time at both oxygen concentrations (paired t-test: *p*-value = 0.2 and 0.1 for NO<sub>2</sub><sup>-</sup> and NO<sub>3</sub><sup>-</sup> in low DO; *p*-value = 0.4 for NO<sub>2</sub><sup>-</sup> and NO<sub>3</sub><sup>-</sup> in high DO,  $\alpha = 0.05$ ; nested ANOVA: *p*-value = 0.4 for both low and high DO reactors).

In the biomass from the high DO reactors, there was a small, but statistically significant increase in N<sub>2</sub>O concentration with time (slope *p*-value was  $< 0.05$ ,  $r^2 = 0.3$ , intercept *p*-value = 0.8) (Figure 4.2b) corresponding to an estimated mean production rate of 11.2 nmol/L.h. A very small proportion of TKN, 0.03%, was removed as N<sub>2</sub>O (Table 4.2). By contrast, at high DO concentration all the TKN removed was converted to NO<sub>3</sub><sup>-</sup>.

At a DO of about 0.2 mg/L there was a statistically significant linear relationship between production rate and time (slope *p*-value was  $< 0.05$ ;  $r^2 = 0.8$ , intercept *p*-value 0.9) (Figure 4.1). At lower oxygen concentrations, the mean production rate of N<sub>2</sub>O increased to 402.1 nmol/L.h, but this represented only 1.5% of the total oxidized TKN (Table 4.2). This could be because we operated the reactors at low DO concentration for 276 days prior to our experiment: it has been suggested that steady-state oxygen limitation favours lower N<sub>2</sub>O production than transient anoxic-aerobic disturbances (Ahn *et al.*, 2011).

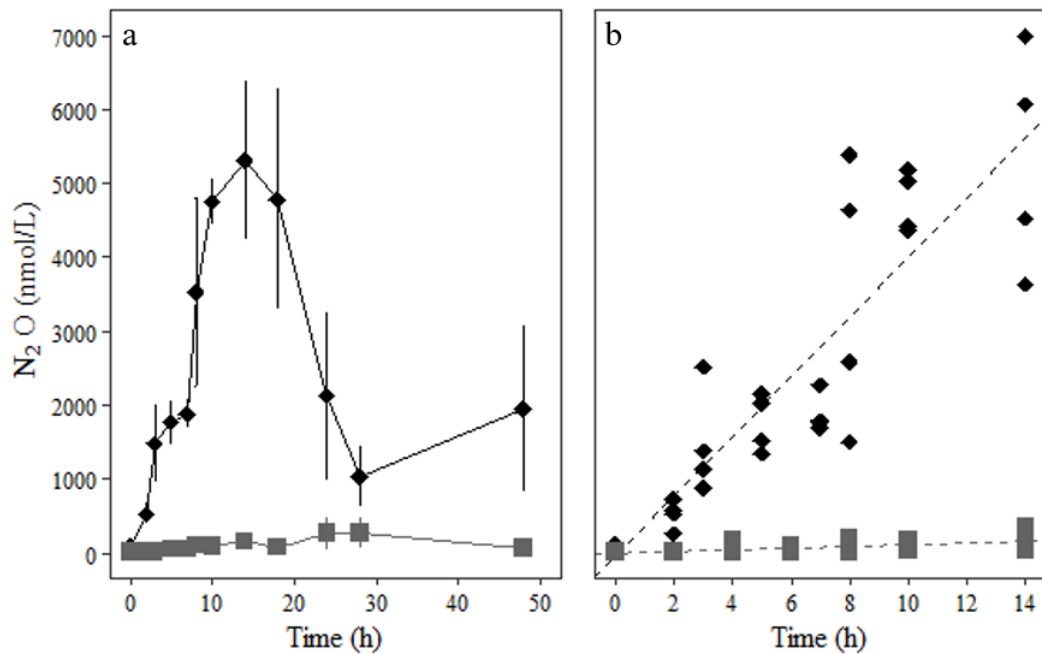


**Figure 4.2** N<sub>2</sub>O emissions for each batch experiment operated at different times and different oxygen concentrations (a): low DO (black diamond) and high DO (grey square). These analyses enabled to calculate the N<sub>2</sub>O production rate by linear regression (b).

**Table 4.2** Nitrogen removal (TKN) and production (NO<sub>2</sub><sup>-</sup>, NO<sub>3</sub><sup>-</sup>, N<sub>2</sub>O) rate and percentage of N<sub>2</sub>O emission in activated sludge laboratory-scale reactors operated at low and high DO.

DO (mg/L)	TKN removal (nmol/L.h)	NO <sub>2</sub> <sup>-</sup> (nmol/L.h)	NO <sub>3</sub> <sup>-</sup> (nmol/L.h)	N <sub>2</sub> O (nmol/L.h)	% N <sub>2</sub> O (N-N <sub>2</sub> O)	% Loss of N
<b>0.2</b>	<b><math>5.3 \times 10^4</math></b>	<b><math>1.6 \times 10^4</math></b>	<b><math>7.7 \times 10^2</math></b>	<b><math>4 \times 10^2</math></b>	<b>1.5</b>	<b>66.1</b>
<b>6.3 – 6.6</b>	<b><math>7.6 \times 10^4</math></b>	<b><math>1.2 \times 10^2</math></b>	<b><math>7.4 \times 10^4</math></b>	<b><math>1.1 \times 10^1</math></b>	<b>0.03</b>	<b>2.1</b>

Although we observed higher N<sub>2</sub>O production in the low DO batch experiments, the amount of N<sub>2</sub>O produced was clearly insufficient to account for the observed loss of total nitrogen. The additional “missing” 66.1% of oxidized TKN (Table 4.2) could most plausibly be explained by the production of gaseous N<sub>2</sub> or NO as the final product (Kuai and Verstraete, 1998; Tallec *et al.*, 2006). If so, 97.7% of total gas production would have been accounted for by these gases, which is in agreement with a dominant production of N<sub>2</sub> reported previously (Tallec *et al.*, 2006). Neither N<sub>2</sub> or NO (neither of which is greenhouse active) was measured in our reactors so this interpretation cannot be directly tested. Results reported by Ahn *et al.* (2010) showed that under anoxic conditions the majority of the N<sub>2</sub>O formed was dissolved in the liquid phase, where it was converted to N<sub>2</sub> which was then released to the gas phase. The release of N<sub>2</sub> in this study under low DO conditions was probably a consequence of

simultaneous heterotrophic denitrification and nitrifier denitrification coupled with COD consumption. The presence of NOB in the reactors at low DO (Table 4.1) would explain the oxidation of  $\text{NO}_2^-$  to  $\text{NO}_3^-$ , which would then become available to, and consumed by, denitrifying bacteria. Denitrification can also occur at low oxygen levels, resulting in conversion of  $\text{NO}_3^-$  and/or NO and  $\text{N}_2\text{O}$  produced by AOB, to  $\text{N}_2$  (Schmidt *et al.*, 2003; Jia *et al.*, 2013). *Nitrosomonas* strains have been shown to denitrify despite the absence of *nosRZDFYL* genes involved in  $\text{N}_2$  metabolism (Zart and Bock, 1998; Chain *et al.*, 2003; Schmidt *et al.*, 2004). A red copper protein (nitrosocyanin) identified in AOB may play an important role in the denitrification metabolism, since nitrosocyanin shares significant sequence similarity with the electron donor copper region of  $\text{N}_2\text{O}$  reductase (Whittaker *et al.*, 2000).

Three factors could also have contributed to the observed low  $\text{N}_2\text{O}$  production. Firstly, it is known that limiting organic carbon increases  $\text{N}_2\text{O}$  emission during denitrification (Hanaki *et al.*, 1992; Itokawa *et al.*, 2001). The addition of pyruvate to the reactors could aid reduction of  $\text{N}_2\text{O}$  and thereby increase the fraction of gaseous nitrogen emitted to the atmosphere as  $\text{N}_2$ . Secondly, high pH in low DO reactors might have facilitated the low  $\text{N}_2\text{O}$  production. Thörn and Sörensson (1996) observed the formation of  $\text{N}_2\text{O}$  at pH lower than 6.5 and Hanaki *et al.* (1992) reported an increase in  $\text{N}_2\text{O}$  when pH fell from 8.5 to 6.5 in a denitrifying laboratory reactor. Finally,  $\text{N}_2\text{O}$  can be reduced by denitrifiers. During nitrification  $\text{NO}_2^-$  can increase the concentration of  $\text{N}_2\text{O}$  (Hanaki *et al.*, 1992; Schultheiss *et al.*, 1995; Tallec *et al.*, 2006; Kampschreur *et al.*, 2009). However, in our study  $\text{NO}_2^-$  accumulation was observed with no concomitant increase in  $\text{N}_2\text{O}$  production. Denitrifiers probably had a significant role in the reduction of  $\text{NO}_2^-$  to  $\text{N}_2$ , preventing the inhibition of  $\text{N}_2\text{O}$  reductase and the release of  $\text{N}_2\text{O}$  to air.

### 4.3.2 Contribution of DO to $\text{N}_2\text{O}$ emissions from WWTP

Even though only a small amount of TKN was released as  $\text{N}_2\text{O}$ , even in the low DO reactors with incomplete nitrification, the high global warming potential of  $\text{N}_2\text{O}$  (Myhre *et al.*, 2013) will amplify its warming effect. The fraction of  $\text{N}_2\text{O}$  emitted from full-scale WWTPs varies from 0 to 25% of the nitrogen load (Law *et al.*, 2012) and presumably this wide range reflects a wide variability in reactor configurations and their operational conditions (Tallec *et al.*, 2006; Law *et al.*, 2012).

In principle, it should be possible to accept the release of N<sub>2</sub>O caused by running the reactor at low DO concentrations if the GHG impact is offset by a reduction in CO<sub>2</sub>e emissions arising from the reduction in power demand. Therefore, to evaluate the sustainability of nitrification in treatment plants with low aeration, we converted the N<sub>2</sub>O/m<sup>3</sup> of treated wastewater to CO<sub>2</sub>e/m<sup>3</sup> and the equivalent kWh/m<sup>3</sup>.

Our low and high DO reactors produced  $2.1 \times 10^{-3}$  and  $5.9 \times 10^{-5}$  kg N<sub>2</sub>O/m<sup>3</sup> of treated wastewater respectively (in accordance to 5 days HRT used in our reactors). Considering an atmospheric warming impact of 1 kg of N<sub>2</sub>O equivalent to ~ 310 kg of CO<sub>2</sub>, the equivalent CO<sub>2</sub> emissions for our reactors would be 0.66 and 0.02 kg CO<sub>2</sub>e/m<sup>3</sup>, at low and high DO respectively. In 2016, the CO<sub>2</sub> emission factor for electricity generated in the UK was estimated at 0.41 kg CO<sub>2</sub>e/kWh (GOV UK, 2016). Converting our CO<sub>2</sub>e concentrations of N<sub>2</sub>O by the conversion factor, the electricity associated would be 1.6 kWh/m<sup>3</sup> (low DO) and 0.04 kWh/m<sup>3</sup> (high DO). The specific electricity consumption in municipal WWTPs was reported as 0.274 kWh/m<sup>3</sup> for COD only and 0.452 kWh/m<sup>3</sup> for both COD removal and nitrification (Shi, 2011), meaning that the N<sub>2</sub>O production in our low DO reactors would have a substantial impact on GHG emissions.

However, it is relevant to scale the N<sub>2</sub>O production from our study to a real wastewater treatment scenario. Thus two approaches for evaluating N<sub>2</sub>O impact should be considered: we can either assume (i) that the reactors emit a constant amount of N<sub>2</sub>O per unit of reactor volume irrespective of the nitrogen load or (ii) that, for any given DO concentration, the reactor emits a constant fraction of the NH<sub>3</sub> oxidized.

Assuming release per unit volume and HRT of 12 hours (mostly used in WWTPs), we estimated the N<sub>2</sub>O production of treated wastewater to be about  $2.1 \times 10^{-4}$  and  $5.6 \times 10^{-6}$  kg /m<sup>3</sup> in low and high DO reactors respectively. Consequently, the CO<sub>2</sub>e emissions would be 0.07 and  $1.8 \times 10^{-3}$  kg/m<sup>3</sup> equivalent to 0.16 and  $4.5 \times 10^{-3}$  kWh/m<sup>3</sup> in low and high DO, respectively. Under this scenario the energy converted of N<sub>2</sub>O production at low DO is below the range of energy consumed in wastewater treatment and hence the CO<sub>2</sub>e emissions would be lower. This results implies that engineers should save at least 0.16 kWh/m<sup>3</sup> to compensate the amount of N<sub>2</sub>O released and thus achieve neutral climate impact. Since this approach assumes a constant N<sub>2</sub>O release per unit of reactor volume, shorter retention times (and thus higher NH<sub>3</sub> loadings) would be estimated to produce less GHGs.

Alternatively, we can assume that, for any given DO concentration, the reactor emits a constant fraction of the NH<sub>3</sub> oxidized as N<sub>2</sub>O. The N<sub>2</sub>O production and equivalent energy would increase proportionally to the amount of NH<sub>3</sub> oxidized. In our study 0.03% of the NH<sub>3</sub>

oxidized was estimated as N<sub>2</sub>O at high DO and 1.5% at low DO. Using the latter figure and assuming an NH<sub>3</sub> effluent concentration of 2 mg/l we can relate target energy saving to the influent NH<sub>3</sub> concentration (Figure 4.3). In our study around 88 mg\_N/L was oxidized and consequently a substantial amount of N<sub>2</sub>O was estimated to be produced. However, most domestic WWTPs have less than 40 mg NH<sub>3</sub>/L, meaning that the amount of N<sub>2</sub>O produced and the electricity would be lower (0.69 kWh/m<sup>3</sup>) than the values estimated in our reactors. This method suggests that at least 0.02 kWh/m<sup>3</sup> must be saved for each mg of NH<sub>3</sub> oxidized and thus is likely to balance the release of N<sub>2</sub>O and CO<sub>2</sub> for plants with low strength influents.

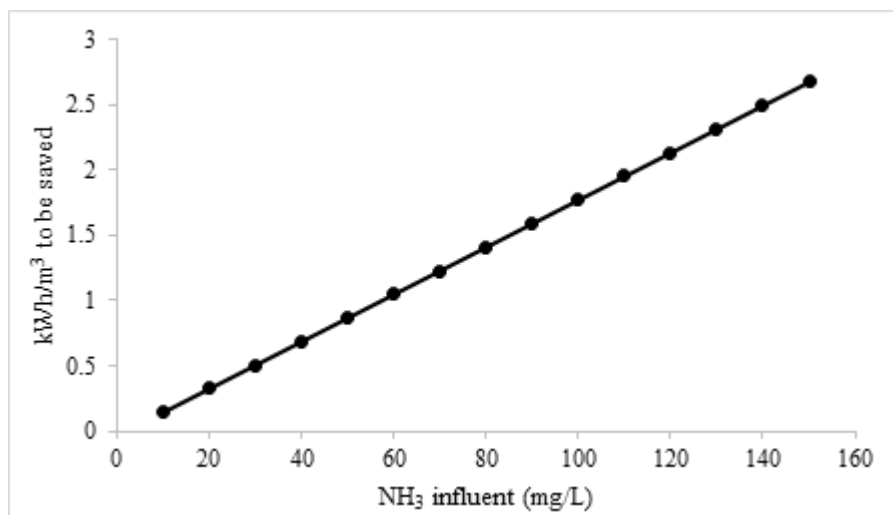


**Figure 4.3** Variation of electricity equivalent estimated from a constant NH<sub>3</sub> fraction at different NH<sub>3</sub> influent assuming an effluent of 2 mg NH<sub>3</sub>/L.

Reduced aeration can decrease CO<sub>2</sub> emissions and plant operational costs. In this study the potential contribution to global warming impact (Myhre *et al.*, 2013) arising from the associated N<sub>2</sub>O emissions from WWTPs may be acceptable for conventional nitrifying systems maintained at constant low DO concentrations. Nevertheless, the impact of operating at lower DO will depend on the reduced energy demand and the associated CO<sub>2e</sub> and the actual energy saving (and CO<sub>2</sub> saving) will depend on the characteristics of the wastewater plant and the aeration system used. We recommend further investigations on monitoring N<sub>2</sub>O and CO<sub>2</sub> emissions overall a continuous experiment at low DO, along with continued studies of AOB and NOB. Any instability in the biomass of nitrifying bacteria or their metabolism caused by low DO or high NH<sub>3</sub> concentrations could impact the removal of NH<sub>3</sub> and NO<sub>2</sub><sup>-</sup>, and thus increase N<sub>2</sub>O emissions. We assume that reactors operating in the long-term at low DO conditions will achieve steady-state with respect to effluent composition. These studies

are required to improve our process understanding and should ideally be at the full-scale of a WWTP to corroborate our findings.

#### **4.4 Conclusion**

Total nitrogen removal was evaluated in laboratory-scale activated sludge reactors at different DO concentrations, accompanied by estimates of N<sub>2</sub>O emission derived from the results of batch experiments. The estimated mean production rate of N<sub>2</sub>O was much higher at low aeration (402.1 nmol/L.h) than at high aeration (11.2 nmol/L.h). The estimated N<sub>2</sub>O emissions were only 1.5% and 0.03% respectively of the TKN removal at low and high DO conditions, implying that the large majority of the nitrogen deriving from NH<sub>3</sub> oxidation was released to air as N<sub>2</sub>, either by denitrification or nitrifier denitrification. The estimations of N<sub>2</sub>O emissions from WWTPs showed the equivalent CO<sub>2</sub> emissions to be similar or higher than is estimated in a real plant. Our results highlight a need to balance the effect of low DO operation against the corresponding power saving to evaluate fully GHG emissions. Striking this balance will require a detail understanding of the stability and performance of nitrifying bacteria.

## **Chapter 5. Detection and isolation of ammonia-oxidizing bacteria grown under low dissolved oxygen by fluorescence in situ hybridization - flow cytometry cell sorting protocol**

### **5.1 Introduction**

Nitrifying activated sludge systems are operated with a high level of aeration due to the aerobic metabolism of AOB with implications in the operational cost and carbon footprint (Bellucci *et al.*, 2011) of this industry. Preliminary studies demonstrated that complete nitrification can be achieved in a chemostat with DO lower than 0.5 mg/l (Park and Noguera, 2004; Bellucci *et al.*, 2011; Arnaldos *et al.*, 2013; Liu and Wang, 2013; Fitzgerald *et al.*, 2015). Such conditions seem to promote the selection of AOB communities with a high yield growth rate (1.5 mg AOB-VSS/mg NH<sub>4</sub><sup>+</sup>-N). This high yield was also observed in our previous study that found the *Nitrosomonas europaea*/*Nitrosococcus mobilis* lineage dominating the low DO reactors.

AOB have been characterized as chemoautotrophic organisms that can fix carbon dioxide via the Calvin Cycle (Wood, 1986; Head *et al.*, 1993; Hommes *et al.*, 2002; Chain *et al.*, 2003; Koops *et al.*, 2006). However, the ability of AOB species to grow with high yields and to survive under anoxic or anaerobic conditions could be because the AOB have a mixotrophic metabolism. Under anoxic conditions pure cultures of *N. europaea* and *Nitrosomoas eutropha* were capable of growing chemoorganoheterotrophically in the presence of pyruvate and lactate as carbon and energy source (Beyer *et al.*, 2009; Schmidt, 2009). Genomic profiles of the sequenced AOB revealed genes encoding enzymes involved in catabolic pathways of several simpler organic compounds, but transporters for most of these compounds have not been identified (Chain *et al.*, 2003). This may mean that AOB which will have grown chemoheterotrophic will have only modest uptake rates for such compounds and thus low growth rates.

We cannot know if this organism, with this metabolism, was present in the seed or if it acquired these properties in the low DO reactors. Whereas a pure culture is by definition composed of clones of a single organism, microbes in real communities may be able to adapt to extreme conditions by increasing the mutation rate or facilitating the incorporation of novel DNA (through horizontal gene transfer or absorbing free DNA) (Galhardo *et al.*, 2012; Roller

*et al.*, 2013; Cordero and Polz, 2014). Thus the conditions in WWTPs, in this study the DO concentrations, may promote the selection or expression of the genes necessary for chemoheterotrophic metabolism.

At present, there is not enough information available on the influence of oxygen on AOB to predict their response to low oxygen concentrations in mixed cultures. This group of organisms are not easily cultivated and isolated in pure culture (due to their slow growth rates and fastidious growth requirements (Head *et al.*, 1993)). Culture-independent molecular techniques could allow us to access the genomes of uncultivated microorganisms (Head *et al.*, 1993; Podar *et al.*, 2007), such as AOB. However, their low abundance limits addressing this gap by using shotgun genome sequencing to create genome assemblies and thus metabolic reconstruction (Podar *et al.*, 2007; Gomez-Alvarez *et al.*, 2009). The less abundant organisms tend to be underrepresented in PCR amplification (Wallner *et al.*, 1997).

If it were possible to select and sequence targeted DNA from a complex microbial consortium it would be likely to avoid the challenges of assembling small DNA fragments into large contigs (DeLong, 2005; DeLong and Karl, 2005). One possible way to do this is the combination of fluorescent *in situ* hybridization (FISH) with flow cytometry equipped with a cell sorting to target and sort specific groups from mixed microbial communities for the purpose of genome sequencing (Müller and Nebe-von-Caron, 2010; Haroon *et al.*, 2013). Fluorescence-activated cell sorting (FACS) is a powerful tool for the rapid identification and separation of single cells from a heterogeneous cell suspensions based on a combination of several parameters. These two techniques can be useful for single-cell genomics and to establish links between phylogeny composition of a specific organism and the metabolic activity. Such method has already been applied to recover anaerobic methanotrophic archaea genomes from a bioreactor performing anaerobic oxidation of methane coupled with denitrification or to access the metabolically active microorganisms in biogas reactor samples (Haroon *et al.*, 2013; Nettmann *et al.*, 2013).

The combination of these two techniques will be valuable to create an isolation method and a genome reconstruction from a metagenomic assembly of AOB genome grown under low DO conditions. Therefore, we will be able to confirm if low aeration promotes the selection of AOB communities with a mixotrophic metabolism. The aim of this study was to expand our knowledge about the AOB genomes under different oxygen concentrations and subsequently helping to define the best conditions for the nitrification process. We used FISH-FACS to obtain the genome sequences of AOB species from activated sludge cultivated at low (R1\_L and R2\_L) and high DO (R3\_H and R4\_H). In the first step, we optimized the

Chapter 5. Detection and isolation of ammonia-oxidizing bacteria grown under low dissolved oxygen by fluorescence in situ hybridization - flow cytometry cell sorting protocol standard FISH protocol by modifying the fixation step and evaluated the best sonication conditions to break up cell aggregates. In the second step, we used flow cytometry to perform multiparametric assays in combination with cell sorting in order to access single AOB cell genomes.

## 5.2 Materials and Methods

### 5.2.1 Fixation test

An in solution FISH protocol based on Amann, Krumholz, *et al.* (1990) and Coskuner *et al.* (2005) study was applied for the recovery of unmodified nucleic acids. To evaluate the labelling efficiency of oligonucleotide FISH probes specific for AOB bacteria, different fixative agents at different hybridization incubation times (1h, 2h and overnight) were tested. 50 mL of fresh sample from a full-scale nitrifying activated sludge plant treating mostly domestic wastewater in Tudhoe Mill (County Durham) were collected and stored at different fixative agents (paraformaldehyde, glycerol and ethanol). Samples stored in glycerol (20% v/v) and ethanol (50% v/v) were immediately fixed at the treatment plant. Samples stored in 8% paraformaldehyde were initially kept in ethanol (1:1 ratio) and transported to the laboratory at approximately 4°C and fixed as described by (Amann, Binder, *et al.*, 1990). After fixation, all samples were stored at -20°C.

### 5.2.2 FISH hybridization and DNA staining

Whole-cell hybridization was carried out at 46°C for all of the probes with 35% formamide. All oligonucleotide probes were purchased from Thermo Fisher Scientific GmbH (Germany) (Table 5.1). Nso1225 probe was used for the detection of AOB. A positive control, consisting of a mixture of the three universal bacteria probes (Bact338I, Bact338II, and Bact338III) was added to validate the technique used in the present study and to measure the total number of bacteria cells in the sample. Two negative controls were used: no probe and a nonsense probe (Anti-Bact338) controls to check the autofluorescence and nonspecific binding in the sample, respectively. The hybridization efficiency of each test was measured using a Leica TCS SP2UV confocal laser scanning microscope (CLSM; Leica Microsystems, Ltd., UK) at X 630 amplification (X 63 objective lens). Images were captured and analysed using LEICA TCS software (version 2.00 build 0770) and a total of five fields of view (FOV) were randomly acquired using a transect method across an image spot and optical sections of

Chapter 5. Detection and isolation of ammonia-oxidizing bacteria grown under low dissolved oxygen by fluorescence in situ hybridization - flow cytometry cell sorting protocol

1- $\mu$ m thickness. We exported and analysed the images using the software ImageJ (version 1.6.0\_24). For each image, the ratio of the area of cells stained with Cy3 (targeting AOB) and FITC (targeting the bacterial probes) was determined by filtering the colour threshold and then measuring the area. Statistical analysis of the AOB abundances measured in the fixative agent tests was conducted in RStudio (version 1.0.136) applying a two-way analysis of variance (ANOVA).

After this initial microscopy test, several combinations of different dye probes were hybridized and tested by flow cytometry to optimize the simultaneous detection of AOB (Cy3 and Cy5) and total bacteria/DNA (FITC – FISH dye, SYTO 9 (Molecular Probes®, OR, USA)). Four glycerol fixed samples were hybridized, two with Cy3 dye and two with Cy5 dye, and combined with FITC and SYTO 9 dyes. Samples fixed in ethanol and paraformaldehyde were tested with one combination, Cy5 and SYTO 9.

**Table 5.1** Oligonucleotide probes and primers used in this study.

Probe	Position	Probe sequence (5'-3')	Target	Reference (s)
<b>Bac338I</b>	338–355	GCTGCCTCCCGTAG GAGT	Domain <i>Bacteria</i> (positive control)	Amann, Krumholz, <i>et al.</i> (1990); Daims <i>et al.</i> (1999)
<b>Bac338II</b>	338–355	GCAGGCCACCCGTA GGTGT	Domain <i>Bacteria</i> (positive control)	Daims <i>et al.</i> (1999)
<b>Bac338III</b>	338–355	GCTGCCACCCGTAG GTGT	Domain <i>Bacteria</i> (positive control)	Daims <i>et al.</i> (1999)
<b>Anti- Bac338</b>	338–355	ACTCCTACGGGAG GCAGC	None (negative control)	Daims <i>et al.</i> (1999)
<b>Nso1225</b>	1225– 1244	CGCCATTGTATTAC GTGTGA	Ammonia-oxidizing betaproteobacteria	Mobarry <i>et al.</i> (1996)
<b>Nsv443</b>	444–462	CCGTGACC GTTCG TTCCG	<i>Nitrosolobus multiformis</i> , <i>Nitrosospira briensis</i> , and <i>Nitrosovibrio tenuis</i>	Mobarry <i>et al.</i> (1996)
<b>Nsm156</b>	156–174	TATTAGCACATCTT TCGAT	<i>Nitrosomonas C-56</i> , <i>Nitrosomonas europaea</i> , <i>Nitrosomonas eutropha</i> , and <i>Nitrosococcus mobilis</i>	Mobarry <i>et al.</i> (1996)
<b>amoA- AOB</b>	332–349	GGGGTTTCTACTGG TGGT	amoA-1F	Rotthauwe <i>et al.</i> (1997)
	802–822	CCCCTCKGSAAAGC CTTCTTC	amoA2R	Rotthauwe <i>et al.</i> (1997)

### **5.2.3 Sonication**

Prior to flow cytometry, the ability of mechanical treatment to disrupt cell aggregates was tested using a sonicating water bath and ultrasonicator. Both were performed with 2 mL FISH labelled samples at different times. The bath sonicator was an Ultrasonic bath USC 300 TH (45 kHz, VWR International LTD, UK) and was operated for 2, 4, 6 and 8 min. The ultrasonicator was a 250 Digital Ultrasonifier (Branson, CT, USA) equipped with a horn tip (3 mm), being run at 20 kHz for 30 s at 25 W and 15 s and 30 s at 74 W. Each sample was sonicated twice with 30 s break between each cycle. During ultrasonication, the samples were kept on ice to avoid cell lysis caused by the increase of temperature. The dispersed samples were filtered through cell strainers (pore size 35 µm) to remove large cell aggregates and then diluted at 1:100. The combination of FISH dyes with the DNA staining occurred after probe hybridization and sonication in the bacterial suspensions, where one millilitre of these samples were stained with 5 µM/mL of SYTO 9 and incubated at room temperature in the dark.

### **5.2.4 Flow cytometry and Sorting**

Test analysis were carried out using a LSRFortessa™ X-20 (BD, NJ, USA) with Blue 488 nm, Yellow/Green 561 nm and Red 635 nm lasers for detection of probes labelled with FITC/SYTO 9 (~488 nm), Cy3 (~550 nm) and Cy5 (~650 nm), respectively. Blue and green fluorescent emissions were collected with a bandpass filter of 530/30 nm and 582/15, respectively, while the red fluorescence was collected by a longpass filter (670/30 nm). Forward scatter (FSC) and side scatter (SSC) and negative controls were used to distinguish total population from electronic noise and debris. When performing analyses on glycerol fixed samples, sorting was done using scattergrams of SSC and Cy3/Cy5. Using ethanol and paraformaldehyde fixed samples, the population of interest was gated and sorted by scattergrams of SYTO 9 versus Cy5. At least 50,000 events were analysed for each cytogram and all data analysed in BD FACSDiva™ software (BD, NJ, USA) and FlowJo™ software (LLC, OR, USA). Sorting was undertaken with a MoFlo® Astrios™ (Beckman Coulter, CA, USA) and the bandpass filters were 530/30 and 671/30 nm for the blue and red fluorescent emissions, respectively. We ran samples using a 100 µm nozzle at a frequency of around 50,000 Hz. Up to  $10^4$  cells were sorted and stored into 1.5 mL centrifuge tubes containing 500 µL 1X phosphate buffered saline solution and stored at -20°C.

### **5.2.5 DNA extraction and amplification**

Sorted populations were extracted by cycles of freezing and thawing described in Head *et al.*, (1993). The cells were centrifuged and the pellet was resuspended in 100 µL of lysis buffer (TE buffer - 10 mM-Tris/HCl, 1 mM-EDTA, pH 8.0 – containing 1 %, v/v, Tween 80). After 1 min on a heating block at 98°C, the cell suspension was snap-frozen in dry ice. We repeated this procedure three times and the genomic DNA solution was amplified using multiple displacement amplification (MDA) kit (Illustra GenomiPhiV2 DNA amplification kit, GE Healthcare Life Sciences, Sweden) according to the manufacturer's instructions. For purification, spin columns from Isolate II DNA Genomic DNA kit (Bioline, MA, USA) were used to clean up the amplified DNA. To provide the optimum chemical environment for the binding of the DNA to the columns, we diluted the DNA in the buffers provided in the kit according to the manufacturer's instructions. The concentration of the purified DNA was quantified by a dye based method, Qubit® kit (Invitrogen, CA, USA) using a Qubit® 2.0 Fluorometer, to ensure sufficient amounts for sequencing. The ratio of absorbance at 260/280 nm and 260/230 nm were used to access the purity of the DNA using a Nanodrop 3300 (Thermo Fisher Scientific, DE, USA). A ratio around 1.8 and 2.0 was accepted for DNA.

### **5.2.6 Amplification of amoA gene by PCR**

The presence of AOB in the sorted cells was verified by amplifying the functional *amoA* gene using PCR. In this reaction, we used specific primer amoA-1F and amoA2R (Table 5.1, Rotthauwe *et al.* (1997)). All the reactions were carried out in 50 µL reaction mixtures containing 47 µL of PCR buffer (MegaMix-Blue; Microzone Ltd., UK), 0.5 µL of each primer (10 µM), and 1 µL of DNA template. The thermal profile for *amoA* gene amplification was: initial denaturation at 94°C for 5 min, followed by 35 cycles of denaturation at 94°C for 30s, annealing at 56°C for 30s, and elongation at 72°C for 30s. The final extension step was conducted at 72°C for 5 min. The PCR products were visualized by agarose gel at 1.5% using a ladder with 50 - 2,000 base pairs (bp).

### **5.2.7 DNA library preparation, sequencing and post-processing**

DNA extracts were sent to the Centre for Genomic Research (CGR, <http://www.liv.ac.uk/genomic-research>) in the University of Liverpool for shotgun library construction using Illumina TruSeq Nano DNA sample preparation kit (insert sizes: 550 bp). A paired-end sequencing of 2x150 bp was applied and multiplexed onto 1 lane of the Illumina HiSeq 4000 platform (Illumina, CA, USA) generating 400M clusters. Cutadapt version 1.2.1 (Martin, 2011) was used to remove the presence of Illumina adapter sequences. Reads were further quality trimmed using Sickle version 1.200 (Joshi and Fass, 2011) with a minimum quality score of 20 and reads shorter than 100 bp were discarded. After trimming we used SPAdes v3.9.0 (Bankevich *et al.*, 2012) with default parameters to assemble the metagenomics data. Two different strategies were used to assemble the data: combined replicate samples (RL\_1 and RL\_2; RH\_3 and RH\_4) and individual samples.

### **5.2.8 Extract reads associated with AOB**

We considered two methods for scaffold binning. For the combined assembly, we used the multi-metagenome workflow (Albertsen *et al.*, 2013):

<https://github.com/MadsAlbertsen/multi-metagenome>) to extract the genomes by utilizing differential coverage binning of samples RL\_1 and RL\_2 and samples RH\_3 and RH\_4. The read coverage was estimated individually by mapping each library to de novo assembled scaffolds using Burrows-Wheeler Aligner (BWA) (Li and Durbin, 2010), generating two abundance estimates (coverages) per scaffold. Open reading frames (ORFs) were predicted in the assembled scaffolds using Prodigal (Hyatt *et al.*, 2010) and 107 essential single copy genes were screened against the predicted ORFs using HMMER3 (<http://hmmer.janelia.org/>) and Hidden Markov model (HMM) (Dupont *et al.*, 2012). BLASTP was used for the taxonomy classification of the identified proteins against the RefSeq protein database (v. 52), and MEGAN (Huson *et al.*, 2011). Individual genome bins were extracted from metagenomes using RStudio (version 3.3.2, RStudio, Inc., MA, USA). Initially, the two coverage estimates per each condition (low and high DO) were plotted against each other for all scaffolds and bin selection was executed by colouring scaffolds (containing essential genes) according to their taxonomy affiliation. The extracted scaffold subsets were further refined by a principal component analysis of tetranucleotide frequencies and scaffolds were coloured by GC content.

In the second method the individual sample assemblies were analysed according to the following protocol. The SPAdes assembly graph (fastg) files were loaded into Bandage v0.07 (Wick *et al.*, 2015), after which BLAST searches for *amoCAB* motifs and reference ammonia monooxygenase sequences from *N. europaea* (GCA\_000009145.1) were performed.

Significant BLAST hits (>60% similarity, e-value < 1e<sup>-10</sup>) were then used to guide the extraction. Briefly, the read coverage for each *amoCAB* contig was determined, and all nodes with a coverage lower than 10% of the *amoCAB* node(s) discarded. The effect is to remove the low coverage sequencing errors that join the ammonia oxidizing genome to the rest of the meta-genome, and extract as much of the ammonia oxidizing associated genome as possible.

Gene prediction of the extracted genomes was performed using PROKKA (Seemann, 2014) v1.11. A phylogenetic tree was generated by maximum likelihood method with 1,000 resampling bootstrap analysis. The alignments were created using a multiple sequence alignment program, MAFFT, and the tree was obtained using Randomized Axelerated Maximum Likelihood (RAxML, version 8.0.0).

## 5.3 Results and Discussion

### 5.3.1 Hybridization efficiency and detection of AOB by flow cytometry

A combination of FISH and FACS was used to recover AOB from activated sludge sample for subsequent genome sequencing. The standard FISH protocol permeabilizes and stabilizes the cell integrity by fixing samples with paraformaldehyde (Amann, Binder, *et al.*, 1990). However, this compound makes the cell wall rigid by cross-linking proteins and nucleic acids and thus makes DNA extraction more difficult (Pernthaler and Amann, 2004). In order to develop a fixative protocol that would facilitate subsequent DNA recovery, glycerol and ethanol were evaluated (at different concentrations and hybridization times) and the hybridization efficiency compared to that of paraformaldehyde (Figure 5.1).

In the microscopy test, all three agents (glycerol, paraformaldehyde and ethanol) demonstrated a positive signal at different hybridization times, indicating the penetration of the fluorescent probes into the cells. There were no statistical differences in average brightness between the different methods (ANOVA: p > 0.05), indicating that both ethanol and glycerol could be used as an effective fixative agent at a minimum hybridization time of 2 h.

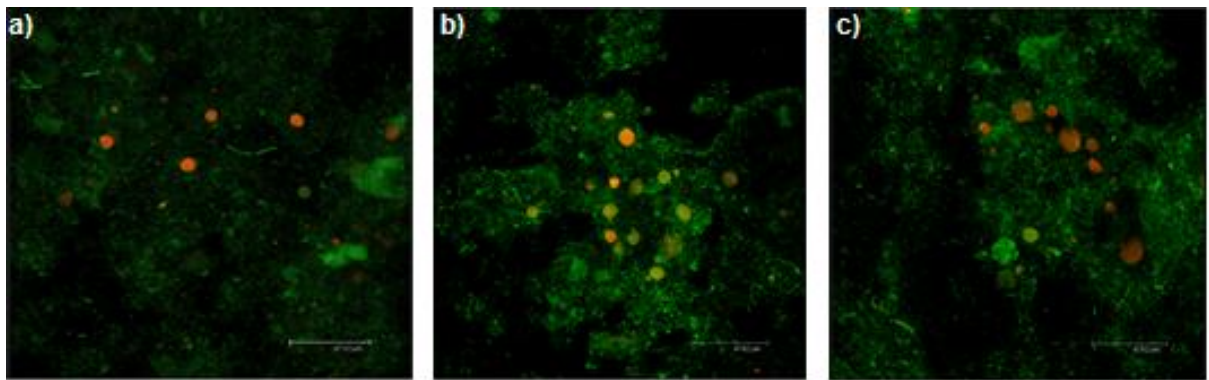


**Figure 5.1** AOB and all bacteria labelled with Cy3 (red) and FITC (green), respectively after a hybridization time of 2h. Cells were fixed in paraformaldehyde (a), glycerol (b) and ethanol (c). Bar, 4.5 mm.

A multiparameter flow cytometry strategy was used to identify and gate the purest AOB cells from total population. To access AOB labelling we used scattergrams of FSC versus SSC, FSC versus FITC/SYTO 9, FITC/SYTO 9 versus Cy5/Cy3 and SSC versus Cy5/Cy3.

Analyses of the three fixative agents using flow cytometry showed paraformaldehyde as one of the best fixative agents, since it had a strong fluorescent signal and the best gating separation (tested with Cy5 and SYTO 9) mainly when compared with samples stored in glycerol (Figure 5.2 a, b). However, as expected, the DNA could not be extracted, presumably due to the paraformaldehyde interactions with the cell wall (Pernthaler and Amann, 2004).

When samples were preserved in glycerol, a different gating and sorting strategy was used to access AOB. FISH probes versus SSC pattern distributions revealed the presence of two populations combining several dyes, Cy3 and Cy5 for AOB and FITC and SYTO 9 for respectively total bacteria and DNA (Figure 5.2a (I – IV)). Cells were sorted using the defined gate. However, the AOB 16S rRNA gene was not detected even though the AOB clusters were clearly present using microscope (Figure 5.1b). Presumably, the fluorochrome signal of the probe targeting AOB was insufficient to be detected in flow cytometry and the high intensity of the instrument background noise (debris, organic and inorganic particles) contributed to false negatives (Foladori, Tamburini, *et al.*, 2010; Nettmann *et al.*, 2013). These difficulties in flow cytometry detection were probably also related to the low abundance of AOB present in the complex samples. In contrast to this result, fresh samples from sludge bioreactor communities stored in glycerol virtually guaranteed effective hybridization and sorting when targeting a bacterial and archaeal population in previous reports (Yilmaz *et al.*, 2010; Haroon *et al.*, 2013).

On the other hand, ethanol fixed samples also gave positive AOB signal in samples stored after 2, 6 and 24 months (Figure 5.2c (I, II and III)) and could be used to preserve cells in activated sludge from full treatment plants and laboratory-scale reactors. We chose to hybridize samples with Cy5 and SYTO 9 for further analysis and sorting since this combination allowed a reliable separation of AOB from the total population and cell debris, minimizing the number of false positive and false negative events. Staining the DNA with SYTO 9, we got a brighter and distinguished separation to the background noise of the flow cytometry. In addition, the emission wavelength of Cy5 (670 nm) is higher than Cy3 (570 nm), which avoids the spectral overlap between the cells labelled with SYTO 9 (488 nm).

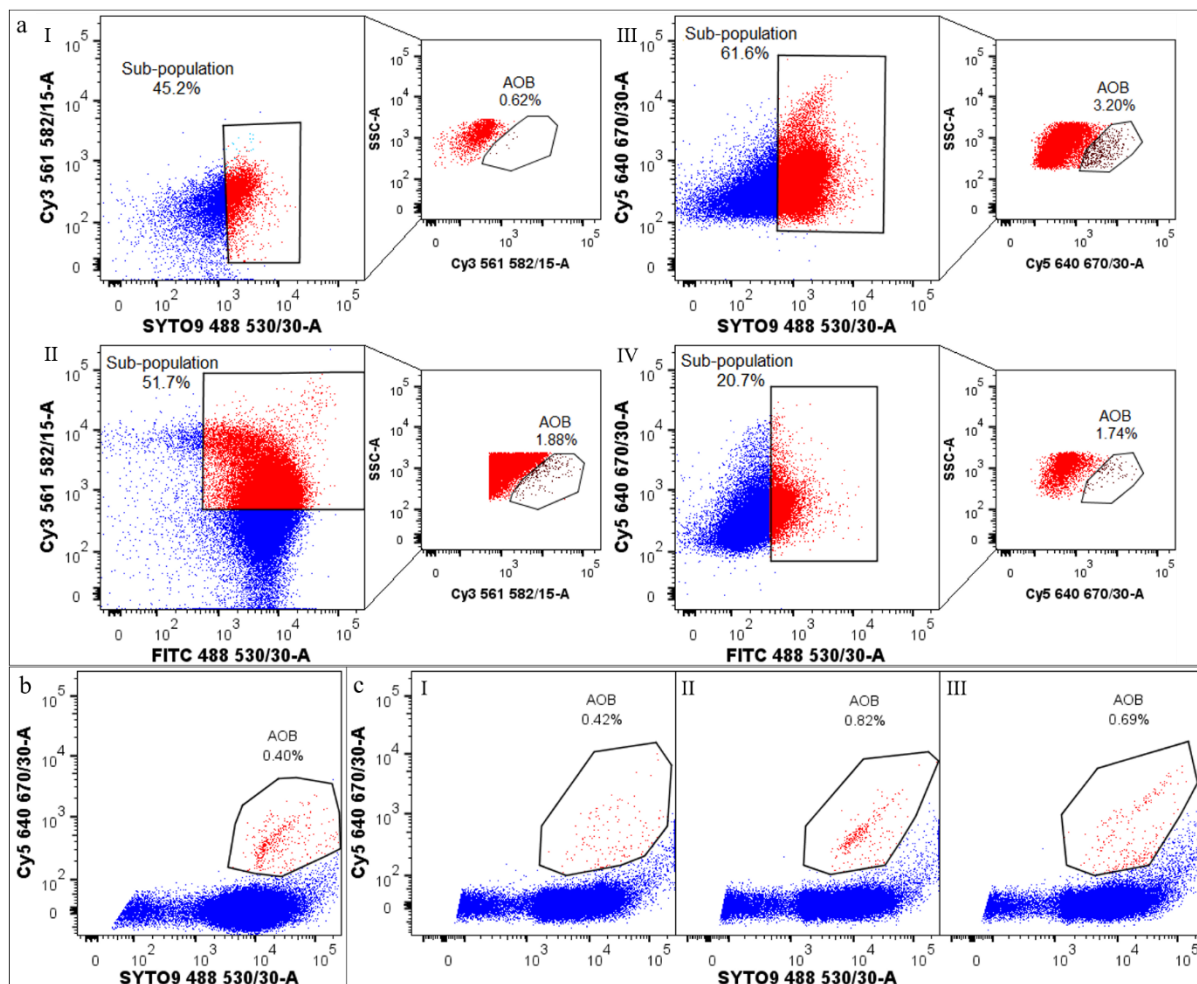


**Figure 5.2** Flow cytometry outputs of bacteria cells from activated sludge samples fixed with glycerol (a), paraformaldehyde (b) and ethanol (c). Cells fixed in glycerol were hybridized with: Cy3 and SYTO 9 (I), Cy3 and FITC (II), Cy5 and SYTO 9 (III) and Cy5 and FITC (IV); AOB cell clusters were selected using scattergrams of Cy3/Cy5 versus FITC/SYTO 9 (big square) and sorted using the respective subsets plotted by SSC versus Cy3/Cy5 (small square). Cells fixed in ethanol were tested at different times: 24 months (I), 6 months (II), 2 months (III). The different colours indicate the different populations: glycerol fixation - regions with a red dark outline indicate the target population with the respective percentage relative to the sub-

Chapter 5. Detection and isolation of ammonia-oxidizing bacteria grown under low dissolved oxygen by fluorescence in situ hybridization - flow cytometry cell sorting protocol population with red light; ethanol and paraformaldehyde fixation – regions with a red outline indicate the target population with the respective percentage relative to total DNA with blue colour.

### 5.3.2 Effect of sonication on AOB

Wastewater samples are a complex matrix and highly aggregated (Foladori, Bruni, *et al.*, 2010). In order to obtain a homogenous suspension of mostly single cells and to prevent clogging of the flow cytometry fluidic system during analysis, the samples were pre-treated in a sonicating water bath and an ultrasonicator. Despite performing two replicated tests for each of the different treatments, we have only presented the results of the first such test. We suspect that there were insufficient AOB in the activated sludge samples to permit detection by flow cytometry in the second run.

The sonication time of the two pre-treatment methods was varied to minimize cell lysis. Flow cytometry cytograms for bath sonication over shorter time periods (2 and 4 min) detected a small number (~0.25%) of AOB events (Figure 5.3a (I and II)). In activated sludge, bacterial cells are mainly attached to aggregates and probably the low dispersion of cells and therefore, the existence of big clusters had limited the probe hybridization (Falcioni *et al.*, 2006). Increasing the sonication time to 6 and 8 min (Figure 5.3a (III and IV)), increased the number of events detected in the bacterial gated population ( $\approx 0.5\%$  of the total population). This result suggests that the sonication time was sufficient to allow greater disaggregation of flocs and thus greater release of bacteria from the matrix. The separation of the cells may have led to an increase in the probe hybridization and therefore detection by flow cytometry.

Ultrasonication has been effectively applied to disrupt biomass in environmental samples (Falcioni *et al.*, 2006; Foladori, Bruni, *et al.*, 2010; Ma *et al.*, 2013). The ultrasonication pre-treatment decreased the total population events by around 10% compared with the shorter bath sonication (Figure 5.3b (I)). However, when we applied a lower ultrasonic power (25 W), the number of the gated events increased to 1.3% (Figure 5.3a (V)), but not at 74 W (Figure 5.3b (II)). The strongest ultrasonication increased the cell disintegration but also increased the number of spread cells and the electronic noise (which interfered with the separation of populations). Previous studies have demonstrated that ultrasonic treatment contributes to the floc disaggregation and increases the number of bacterial cells detected (Epstein and Rossel, 1995; Falcioni *et al.*, 2006). Nevertheless the fine balance between the power applied to achieve detachment of cells while avoiding cell lysis has to be considered (Buesing and Gessner, 2002). The ultrasonication at 25 W was deemed

Chapter 5. Detection and isolation of ammonia-oxidizing bacteria grown under low dissolved oxygen by fluorescence in situ hybridization - flow cytometry cell sorting protocol

to be the best pre-treatment based on both the greatest separation of the two labelled populations and the largest increase in AOB number detection in flow cytometry.

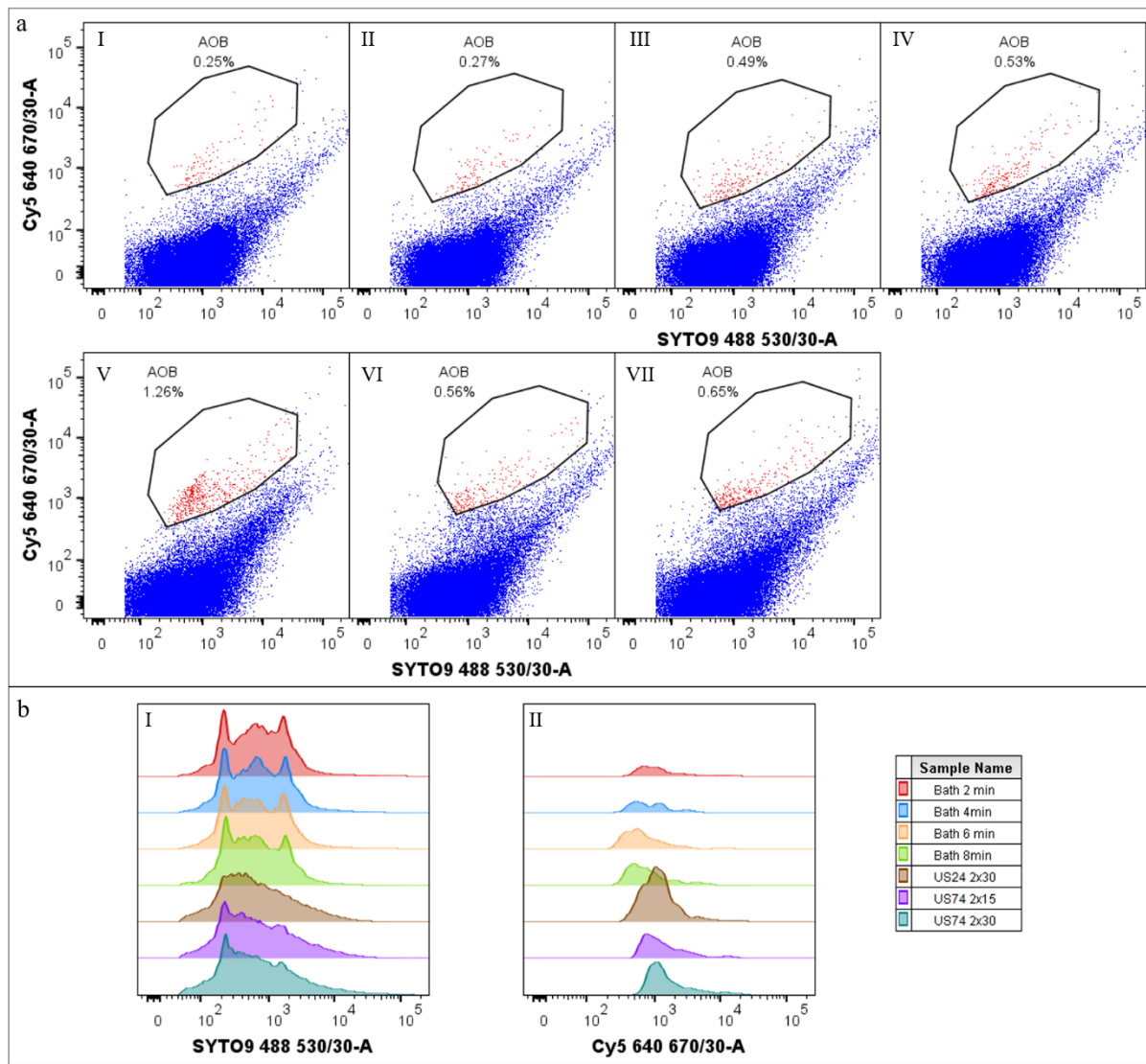


**Figure 5.3** Flow cytometry outputs of the sonication test applied to samples from activated sludge. (a) Scattergrams of the different pre-treatments showing SYTO 9 versus Cy5: bath sonication for 2 (I), 4 (II), 6 (III), and 8 (IV) min and ultrasonication for 2x30 s at 25 W (V), 2x15 s at 74 W (VI) and 2x30 s at 74 W (VII). The different colours indicate the different populations: regions with a red outline indicate the target population with the respective percentage relative to total DNA with blue colour. (b) Histograms of SYTO 9 (I) and Cy5 (II) for all different pre-treatments.

### 5.3.3 Sorting of AOB and whole genome amplification

Cells from four nitrifying reactors operated at different DO concentrations (two reactors operated at 0.2 mg O<sub>2</sub>/L and the other two at 6.5 mg O<sub>2</sub>/L) were hybridized with

FISH probes and sorted by FACS using the optimized procedure. The optimised gating strategy was applied. First, we ran a negative control and discarded contamination determined by the FSC and SSC scattergram versus SYTO 9. Then a sample hybridized with a probe targeting all DNA (SYTO 9) was run and a threshold gate for DNA events only was defined. Finally, a scattergram of Cy5 versus SYTO 9 was applied to gate AOB, and subsequently sort the targeted population. In total between  $1 \times 10^9$  and  $2 \times 10^9$  events were detected. We observed that a small part of the population shifted to the Cy5 axis compared to the total population and those cells were gated and sorted in one set to avoid cell loss. Up to  $10^4$  cells were sorted from each reactor, corresponding to 0.1 – 0.2% of the total population (Figure 5.4).

Although the number of cells sorted was low, the mechanical protocol optimized for AOB was able to extract DNA (Figure 5.5). The four samples achieved a concentration of DNA between 40 – 80 ng/ $\mu$ L after purification, where the negative control was lower than 0.2 ng/ $\mu$ L. Attempts to quantify the AOB cells in the sorted populations using qPCR and targeting the *amoA* gene were unsuccessful implying that this gene was below the detection limit ( $10^2$  fragment copies per  $\mu$ L) in the sorted samples. The purified DNA was submitted to shot gun sequencing.

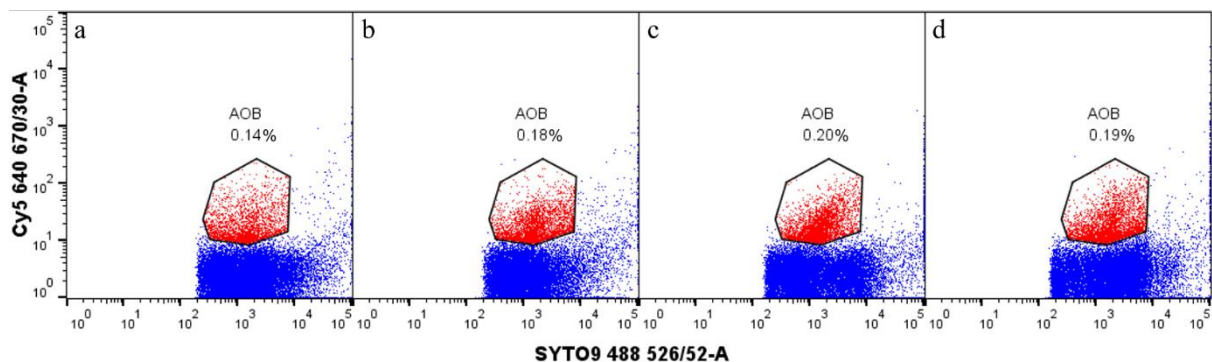


**Figure 5.4** Flow cytometry scattergrams based on SYTO 9 versus Cy5 parameters of the AOB sorting of four bioreactor samples: (a) R1\_L, (b) R2\_L, (c) R3\_H and (d) R4\_H. Each plot contains  $2 \times 10^6$  events and the AOB region of the plot indicates the events gated for sorting. The different colours indicate the different populations: region with a red outline indicate the sorted target population with the respective percentage relative to total DNA with blue colour.

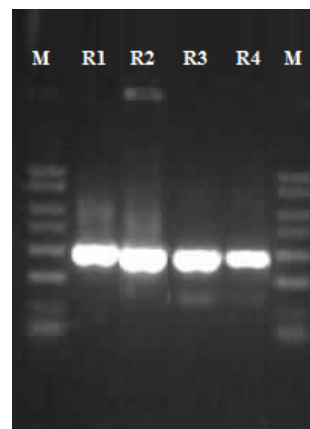


**Figure 5.5** Agarose gel electrophoresis (1.5% agarose) of PCR amplicons of *amoA* gene in the MDA extracts. Lane 1 and 6 represent ladder (50 - 2,000 bp DNA molecular weight ladder) and lane 2, 3, 4 and 5 represent reactor R1\_L, R2\_L, R3\_H and R4\_H, respectively.

### 5.3.4 Sequencing verification of AOB sorted genomes

The enrichment of AOB cultured in laboratory-scale reactors seeded with activated sludge from a full treatment plant was evaluated by shotgun sequencing of the sorted DNA. We applied metagenomics to obtain genome sequence information from AOB growing at different oxygen concentrations. The ratio of AOB sequences to total sequences was different in all samples (Figure 5.6). In total, from all the 16S rRNA sequences, the Nitrosomonadaceae order had over 1500 sequences in reactors R1\_L and R4\_H, 6000 sequences in R3\_H reactor and more than 10,000 in R2\_L reactor. AOB sequences were 3 – 4% of the sorted population in R1\_L and R4\_H reactor samples, and found 14% in reactors R2\_L and R3\_H. No correlation was found between the percentage of AOB within replicate reactor conditions and the percentage of recovery. A large proportion (21 – 30%) of sequences did not match the taxonomy reference dataset.

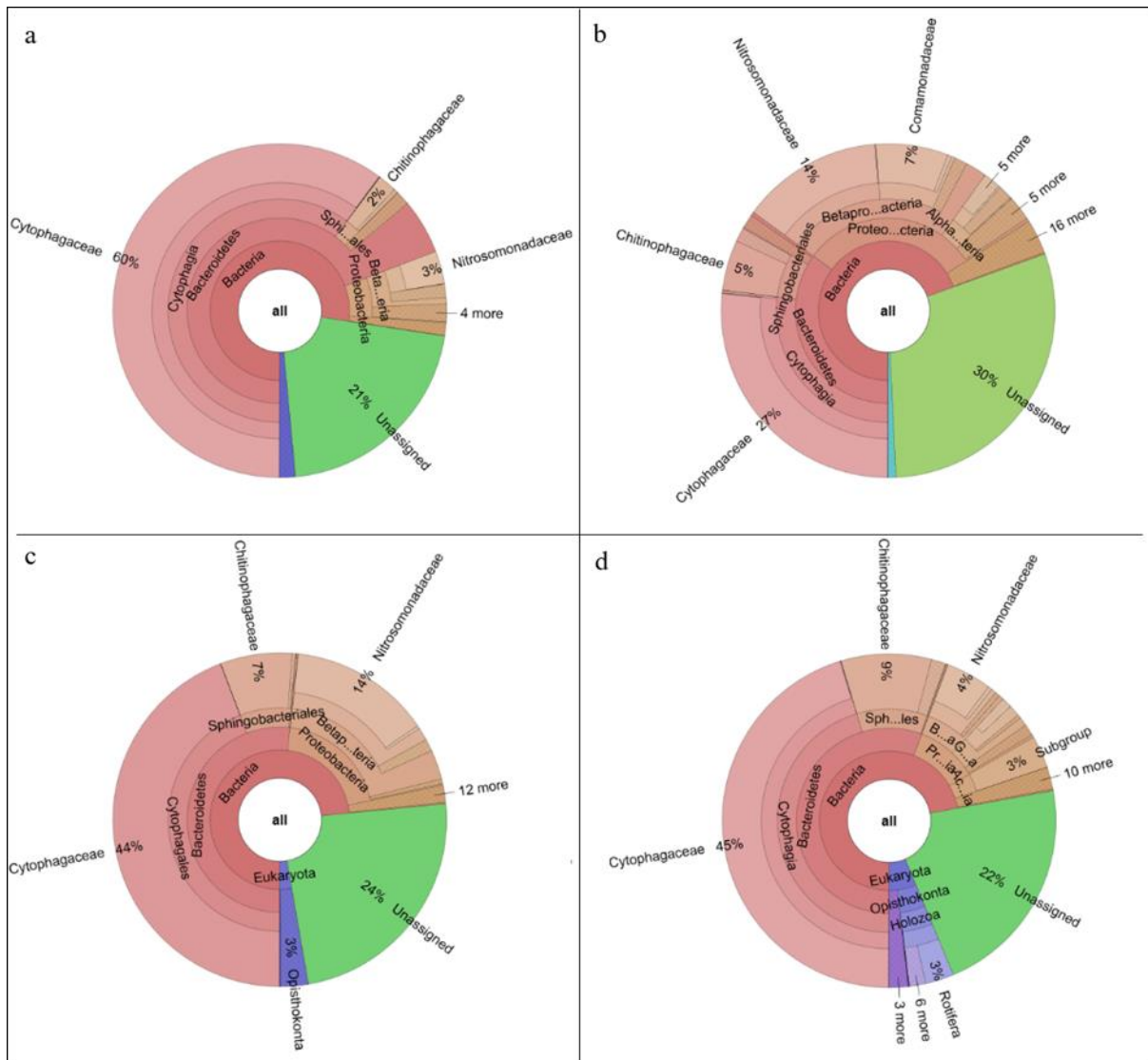


**Figure 5.6** Taxonomic distribution based on 16S gene sequences of the sorted samples: a – R1\_L; b – R2\_L; c – R3\_H; d – R4\_H. The data were visualized using Krona (Ondov *et al.*, 2011). The percentages correlate each phylogeny within the total assigned sequences.

Unexpectedly, the methodology did not appear to successfully select only AOB from laboratory-scale reactors, though when it was applied to a full-scale activated sludge treatment plant AOB comprised 36% of the total sorted population (Figure 8.6, Appendix 8.6). There are some possible explanations for the inability of the FISH-FACS method to enrich sufficient AOB from our bench scale reactors. Comparing cytograms of the laboratory reactor samples with the real activated sludge (Figure 5.2 c and 5.4), the separation between the target species and the background was clearer in the latter. We speculate that some factors, perhaps low fluorescence detection by flow cytometry, might have affected the enrichment of AOB.

The hybridization efficiency of FISH probes is dependent on the cell type and the cellular ribosomal content (Wallner *et al.*, 1993). If the metabolic activity of microbial cells

Chapter 5. Detection and isolation of ammonia-oxidizing bacteria grown under low dissolved oxygen by fluorescence in situ hybridization - flow cytometry cell sorting protocol

was lower in the laboratory-scale reactors, the number of 16S rRNA molecules would be lower and, consequently, the fluorescent signal would be weaker (Nettmann *et al.*, 2013). In each type of sample, the cells may be expressing differing amount of 16S rRNA and thus optimization is a critical step (Milner *et al.*, 2008). Previous studies improved the hybridization conditions for probes targeting AOB (Wagner *et al.*, 1995; Mobarry *et al.*, 1996; Coskuner *et al.*, 2005), but given that a new fixation agent was used (ethanol), those conditions probably need to be revisited. We attempted to increase fluorescence by using two probes labelled with the same dye (Cy3) and targeting different groups of AOB (Table 5.1). The hybridization conditions for probes targeting AOB were tested with different probe concentrations and hybridization times. However, the results were inconclusive (Figure 8.3 and 8.4, Appendix 8.5) and further analysis need to be repeated. Another way to increase signal strength and sensitivity would be the use of multiple FISH probes labelled with multiple fluorochrome molecules that could distinguish rare cells, but it may result in poor or nonspecific binding (Amann, Binder, *et al.*, 1990; Lee *et al.*, 1993). The use of the catalysed reporter deposition-fluorescence in situ hybridization (CARD-FISH) method, which has been applied to increase FISH signal amplification (Pernthaler *et al.*, 2002), might also improve signal intensity and recovery in environmental samples with low rRNA content.

It is also possible that enrichment was affected by the MDA amplification bias. This procedure is known to give differences in coverage between regions (Blainey *et al.*, 2011). This limitation would have led to a greater amplification of certain regions of the genome and the lower coverage in others.

In addition, the detection of AOB using flow cytometry was possibly affected by false positive from other groups of organisms or autofluorescing particles. AOB and heterotrophs coexist and interact and may be bound to each other (Kindaichi *et al.*, 2004; Nogueira *et al.*, 2005; Keluskar *et al.*, 2013). Kindaichi *et al.* (2004) reported that AOB growth supported the survival of heterotrophs by the production of soluble microbial products. This coexistence may explain a high presence of heterotrophs in the selected flow cytometry gate and why the number of AOB cells in that gate was much lower than expected. The improved assessment of false positives would require the collection of more events coupled with a multistage sorting and a refinement of the definition gate. This would however be costly and time consuming. Fujitani *et al.* (2014) developed an isolation method of microcolonies of nitrifying bacteria with FISH-FACS by separating and sorting the microcolonies from heterogeneous aggregates based on their light scattering (FSC versus SSC). A similar strategy of the flow cytometry parameters can be applied in our method to

increase the number of AOB and reduced the false negative signal. Initially a gate is performed based on FSC and SSC signals and a high number of events are sorted followed by a second sorting with a FISH probe (targeting AOB) versus SYTO 9 scattergram.

### 5.3.6 Metagenomics assembly

Because of the low fraction of pure AOB cells, the sequencing data was analysed as a multi genomic species. After the assembling and mapping steps, sequences were binned by two separate methods.

First, metagenomics assembled sequences were submitted to an extraction method based on differential coverage which is based on different abundances of the target organism (Albertsen *et al.*, 2013). In that study, two different DNA extraction methods were applied in two replicated samples. In this study, we used 4 samples from 4 reactors: 2 operated at low DO and other 2 operated at high DO (both containing the target organism – AOB). The DNA of all samples was extracted using the same method and each sample was subsequently sequenced independently followed by a combined assembly of each oxygen condition. Figure 5.7 shows the extracted scaffolds generated by plotting the two coverage estimates of the two oxygen conditions (R1\_L vs R2\_L (a) and R3\_H vs R4\_H (b)) against each other. In total, 3 and 2 population bins were identified as Nitrosomonadales order at low and high DO, respectively. Due to the possible presence of another species, those bins were redefined using principal component analysis of tetranucleotide frequencies and coloured by GC content (Figure 5.8). The 3 population bins identified in the low DO samples had a range of total length of 1.8 – 2.9 Mbp and GC content range (48 – 51%). In the 2 population bins found in the high DO samples, the total length was 3 and 5.1 Mbp, but the GC content (44 – 46%) was lower. Considering that the size of AOB genome is approximately 3 Mbp (Chain *et al.*, 2003), only two of the bin populations extracted had similar size, meaning that probably half of the genome was identified (low DO) or more than one strain was present (high DO).

Chapter 5. Detection and isolation of ammonia-oxidizing bacteria grown under low dissolved oxygen by fluorescence in situ hybridization - flow cytometry cell sorting protocol

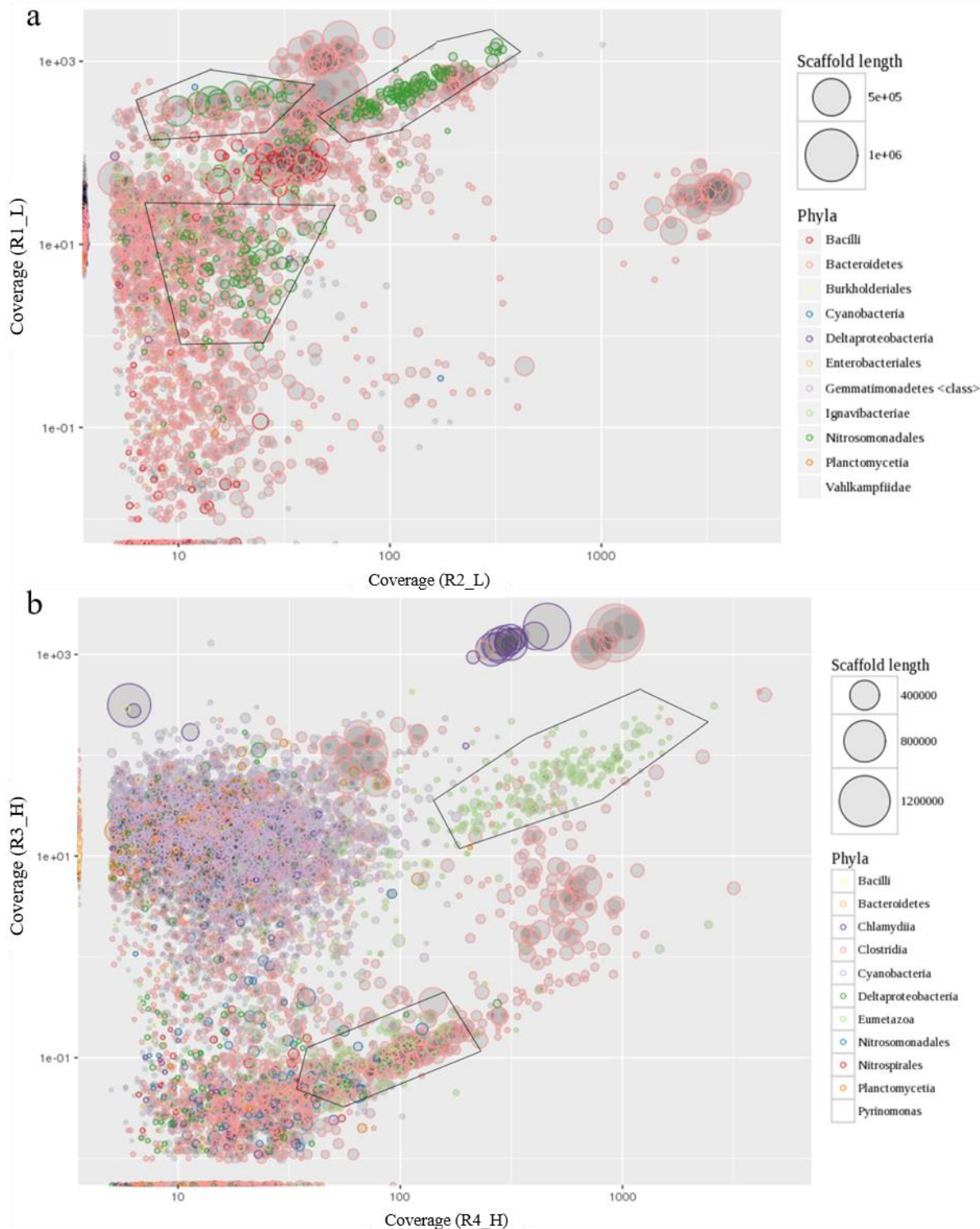


**Figure 5.7** Binning of scaffolds into population genomes from the metagenomes laboratory-scale reactors by differential coverage: (a) R1\_L and R2\_L; (b) R3\_H and R4\_H. Each circle represents a scaffold (only  $\geq 5$  kbp are shown), scaled by the square root of their length and coloured by phylum level assignment of essential genes. The potential genome bins are represented by grouping similarly coloured circles.

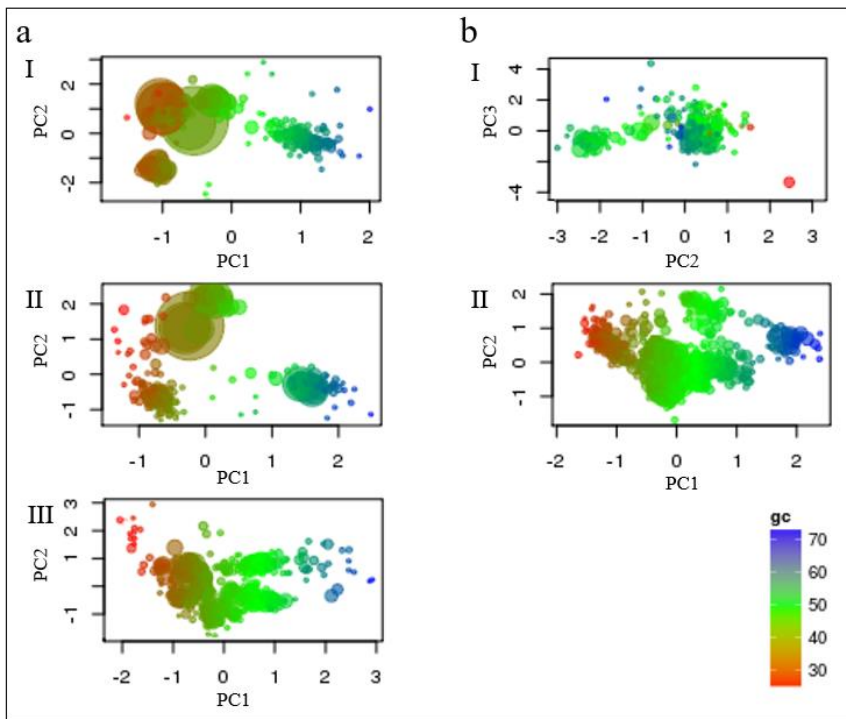


**Figure 5.8** PCA of the subset bins: (a) genome bins 1 (I), 2 (II) and 3 (III) in the low DO samples; (b) genome bins 1 (I), 2 (II) in the high DO samples. The scaffolds are scaled by length and coloured by GC content.

We tried to reassemble all reads within a genome bin, but we ended up with a number of contigs which were not associated with any AOB. Consequently, we cannot be sure that the genes belonged to AOB. These complications were mainly associated with the assembly process.

The process for binning scaffolds from the combining assembly was not able to recover individual AOB genomes from all genomes in the complex samples, a problem related to the amount of short contigs produced in the assembly. As the number of fragments increases, more bins are generated and thus the correct assignment of those bins becomes harder (Dröge and Mchardy, 2012). Even the tracking paired-end reads, which allows the association of short contigs with different coverage from genome and repeat regions with the correct bin (Albertsen *et al.*, 2013), did not improve the AOB genome reconstruction (contigs linking are still mixed between species). The presence of numerous other species may have compromised the binning analysis (Dröge and Mchardy, 2012).

Also, the second binning process based on the GC content may not have perfectly separated the targeted nitrifying bacteria sequences from all genomes. We assumed that there were multiple genomes in the subset bins which had similar GC percentage to AOB (48.5–53.9%) (Klotz and Stein, 2011).

As we previously reported, in low and high DO samples, more than one AOB population bin was detected, meaning that the target organism had different abundances within one sample. The recovery of complete genome bins by differential coverage would be more suitable to duplicated samples (collected from the same reactor) extracted by two different DNA methods, as different abundances of the target organism would be generated in different replicate samples (Albertsen *et al.*, 2013). Although we used two samples from replicate reactors, only one DNA extraction method was applied.

In the individual assembly, a second approach was used to extract AOB genomes by identifying specific genes of these bacteria (*amoCAB*). As described above, this approach requires the identification of key “marker” genes for the individual of interest – in our case the *amoCAB* operon. The assembly graph is then “walked” to identify all associated AOB genes. Using this assembly approach, we could reliably associate genes as belonging to the AOB species. Based on the genome bins containing *amoCAB* genes, phylogenetic annotation was performed to evaluate the AOB species present in each configuration. While the dominant organism in low DO was *N. europaea* (cluster 7) the closest relative specie in the high DO AOB bins was *N. urea* (cluster 6A) (Figure 5.9). These results were also in agreement with the taxonomy analysis of *amoA* amplicon Illumina sequencing (Chapter 3.3.2.3). The apparent indistinguishable genome composition between the two conditions (low and high DO) suggested that are no genetic differentiation to justify the mixotrophic metabolism. However, conclusions cannot be drawn due to the incomplete genome reconstruction and our consequent inability to analyse the metabolic pathways.

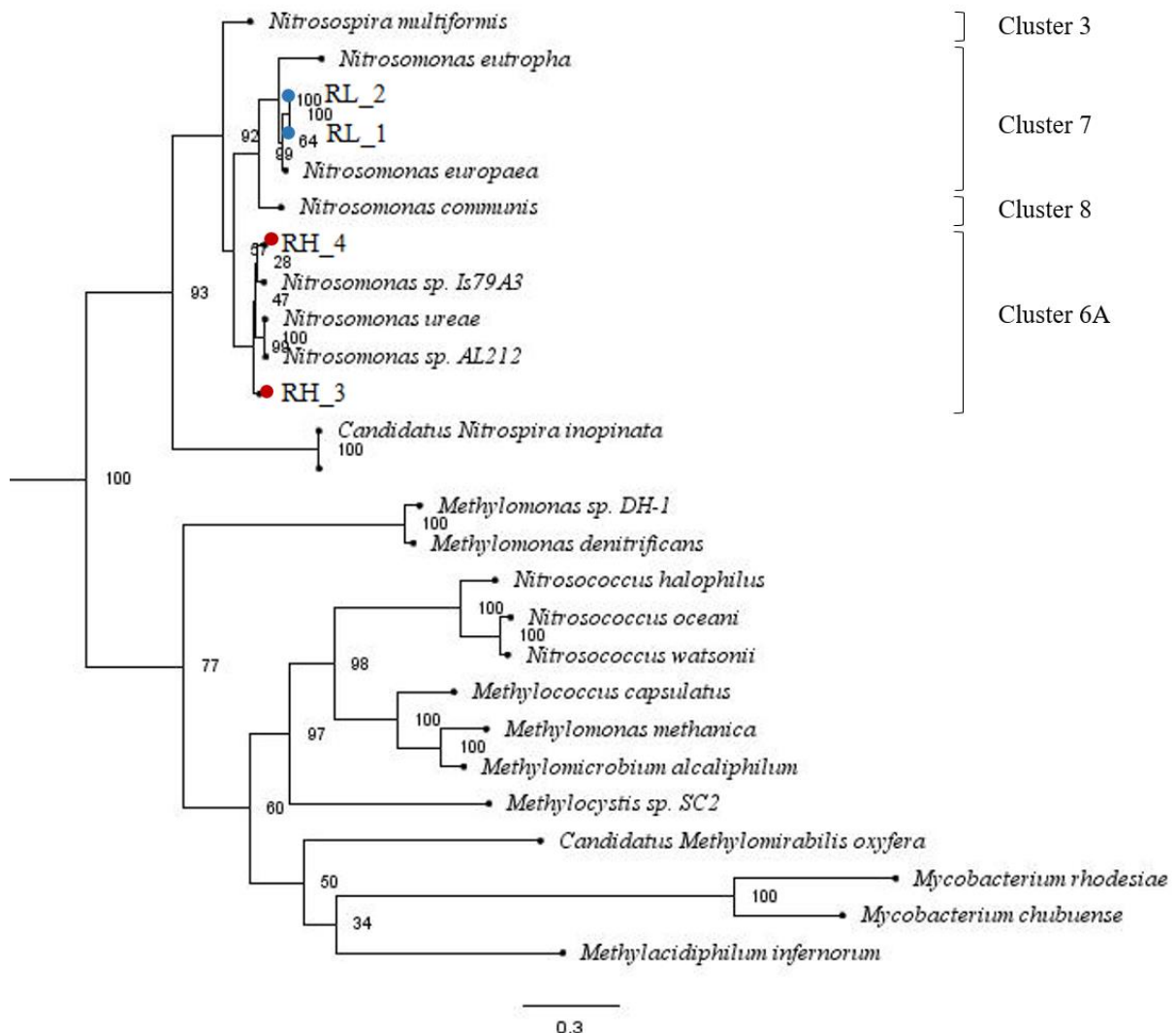


**Figure 5.9** Phylogenetic tree generated from alignment of *amoCAB* sequences obtained by BLAST and the *amoCAB* genes sequences retrieved in the extracted AOB genomes. The tree is based on the maximum likelihood phylogenetic method and shows the relationship between the low (RL\_1 and RL\_2 - blue) and high (RH\_3 and RH\_4 - red) DO reactors. The bootstrap consensus tree was inferred from 1,000 replicates.

Both strategies were not able to produce high quality assemblies and thus a credible reconstruction of AOB genomes was not possible. Poor assembly prejudiced the recovery of long contigs from the mixture of reads that represent part of individual community genomes. The assembly process faces several challenges, including the presence of a diverse taxa community, complex organisms or closely related organisms (Dröge and Mchardy, 2012). The low relative abundance of AOB (3% in some samples) in the total population was a further complicating factor in the assembly and binning of individual genomes. Assembling genomes of low abundant species from a high diversity community is difficult and implies a significant effort in sequencing data (Tringe *et al.*, 2005; Kunin *et al.*, 2008).

Although the AOB enrichment had increased its fraction to more than 10% of the total population in samples R2\_L and R3\_H, it was still not sufficient to achieve a reliable assembly. To reduce the metagenome complexity, improvements of the FISH-FACS method are crucial to recover and sequence the largest possible AOB number and then to accurately assemble and reconstruct their genomes.

## 5.4 Conclusion

In this study, a FISH-FACS protocol was developed to enrich AOB cultivated in bioreactors at different oxygen conditions. The combined method was able to detect AOB using a modification of the traditional fixation step with ethanol. The flow cytometry data suggested that the combination of a specific probe for AOB and the nucleic acid-specific fluorochrome SYTO 9 can easily distinguish these bacteria. The results also demonstrated that pre-treatment incorporating ultrasonication can improve AOB detection. AOB cells were detected and subsequently sorted in samples collected from activated sludge full-scale WWTPs and laboratory-scale reactors. Although, we were able to increase the percentage of AOB from full-scale treatment plant, the enrichment of AOB from bioreactors was not sufficient to permit us to assemble representative genomes. The large bacterial diversity in the sorted sample contributed to the poor assembly of the AOB genomes even when using different assembly strategies. Nevertheless, the optimization of the FISH-FACS protocol will improve the enrichment of AOB and facilitate downstream sequencing and assembly analysis.

## Chapter 6. General conclusions

- Both AOB and NOB adapted to low DO concentrations. TKN removal improved after two months of operation, where 67% of the TKN influent was oxidized. Notwithstanding the incomplete NH<sub>3</sub> and NO<sub>2</sub><sup>-</sup> oxidation in laboratory-scale reactors operated at low DO concentrations, the abundances of AOB and NOB quantified through qPCR were similar to those seen under high DO conditions.
- DO concentration had an effect on the AOB community composition. In the low DO reactors, the selection of a rare AOB cluster (*N. europaea/Nc. mobilis* lineage) from within the seed reduced the adverse effect of low aeration on NH<sub>3</sub> oxidation. The adaptation of this nitrifier community was thought to be related to their high affinity for oxygen and mixotrophic metabolism (higher growth yield), implying the ability to use organic matter as source of carbon or energy.
- Modelling of two AOB species with different oxygen affinities successfully demonstrated the effect of low DO on the AOB community. Adaptation of members with high K<sub>DO</sub> (*N. europaea/Nc. mobilis* lineage) was predicted. Several simulations suggested a dependence of adaptation time with the initial concentration of the selected AOB in the original seed.
- Batch experiments showed higher N<sub>2</sub>O production at low DO than high DO conditions, but this still only represented around 1.5% of the total nitrogen oxidized. The production of N<sub>2</sub>O could have occurred by both AOB and heterotrophic denitrification pathways.
- Complete nitrification might be achieved at long-term low DO (0.2 mg/L), potentially with lower concentration of NH<sub>4</sub> in the influent media. The presence of NOB at the same abundance in all reactors operated at low and high DO and the low concentration of NO<sub>3</sub><sup>-</sup> and N<sub>2</sub>O observed in the low DO conditions suggested the occurrence of simultaneous nitrification and denitrification.

- N<sub>2</sub>O production such that we estimated for a typical full-scale activated sludge plant, led to the recommendation that engineers must save at least 0.16 kWh/m<sup>3</sup> of treated wastewater or 0.02 kWh/m<sup>3</sup> of treated wastewater per each mg of NH<sub>3</sub> oxidized, to balance the possible N<sub>2</sub>O produced with CO<sub>2</sub> emissions saved by aeration at low DO. Although nitrification under low DO can reduce the operational costs, emissions of both gases to the atmosphere should be confirmed in full-scale treatment plants.
- A protocol combining FISH and FACS was successfully developed to detect and subsequently sort AOB. We demonstrated that the hybridization of probes targeting AOB cells was efficient when cells were fixed in ethanol and pre-treated with ultrasonication. Also, we were able to extract DNA from a small concentration of AOB using cycles of freezing and thawing.
- The optimization of the FISH-FACS protocol is required to facilitate the high throughput analysis of low abundant AOB communities in heterogenic samples. Factors, such as low signal intensity, false positive fluorescence signals, complexity and diversity of samples, affected the isolation of AOB from activated sludge operated at low and high DO concentrations and the assembly process analysis.

## Chapter 7. Future work

Although this work has produced important insights into the microbial ecology activated sludge operated at very low oxygen concentrations, further research is strongly recommended into both the adaptation of the community and the evaluation of the possible scale-up of the proposed process conditions.

The adaptation of nitrifying bacteria to low DO demonstrated that both AOB and NOB can grow under low DO. It is likely that the simultaneous activity of nitrifiers and denitrifiers at low DO can lead to the complete removal of the nitrogen. However, it is necessary to evaluate both nitrification and denitrification in a full-scale wastewater treatment process. In particular, it should be worthwhile examining the stability of nitrifiers and their ability to remove both NH<sub>3</sub> and NO<sub>2</sub><sup>-</sup>. In this study NH<sub>3</sub> and NO<sub>2</sub><sup>-</sup> were not completely removed, but lowering nitrogen load will probably reduce the oxygen requirements for these processes and thus allow complete nitrification.

We demonstrated that the adaptation to low DO was occurred by the selection of a rare AOB cluster and this response of AOB with high and low affinities for DO can be modelled. It would be useful to apply this model to simulate the response of AOB species at low DO in full-scale activated sludge in order to predict the time to adaptation. The initial abundance and composition of AOB would need to be required or estimated.

To better understand the metabolism of AOB and NOB under long-term low DO conditions, a deeper analysis of the consumption carbon should be undertaken. For example, stable isotope probing with <sup>13</sup>C-labeled bicarbonate and organic carbon (such as pyruvate) can contribute to monitor and understand the consumption of different carbon sources. This approach can be combined with molecular detection such as DNA or RNA characterization or fluorescence in situ hybridization–microautoradiography (FISH-MAR). Recently, a new technique has been developed to analyse the structure-function of single cells containing stable-isotope-labelled in complex samples: Raman microspectroscopy and FISH. This technique not only can identify microorganisms with a specific activity at the single-cell level, but also quantifies the assimilation of radioactive labelled. Also, Raman-activated cell sorting (RACS) can provide a valuable alternative to sort cells, where Raman microscopy is combined with optical laser tweezers which enables the identification and isolation of the interested single cells according to their Raman spectra and later genome amplification.

Operating at low DO could reduce CO<sub>2</sub>e emissions, but it is necessary to strike at balance between the CO<sub>2</sub>e emissions produced from aeration and the production of N<sub>2</sub>O. Therefore, it is important to directly monitor the GHG emissions in laboratory-scale reactors and later in full-scale plants where the DO has been lowered to 0.2 mg/L.

In order to overcome some of the bias and limitations of the FISH-FACS method, improvements in the hybridization step are crucial and would improve the enrichment of the AOB population in the sorting process. Using a combination of different probes targeting the different species of AOB and having the same dye might substantially increase the fluorescent signal. A different approach of the FISH protocol is the use horseradish-peroxidase (HRP)-labelled oligonucleotide probes combined with CARD of fluorescently labelled tyramides. This method might increase FISH sensitivity and thus increase the signal detected by the flow cytometry.

## Chapter 8. Appendix

### 8.1 FA concentration

FA concentrations can be calculated according to equation 8.1.

$$\text{FA} \left( \frac{\text{mg}}{\text{L}} \right) = \frac{17 \sum \text{NH}_4 - N \left( \frac{\text{mg}}{\text{L}} \right) \times 10^{\text{pH}}}{\frac{k_b}{k_w} + 10^{\text{pH}}} \quad (8.1)$$

### 8.2 Description of the risk based model (Ofițeru and Curtis, 2009)

The model comprises the mass balances for two species and two resources. The form of the mass balances equations is as follows:

$$\frac{dN_i}{dt} = N_i (\mu(R_1, \dots, R_k) - m_i) \quad i=1, \dots, n \quad (8.2)$$

$$\frac{dR_j}{dt} = D(S_j - R_j) - \sum_{i=1}^n Y_{ij} \mu_i(R_1, \dots, R_k) N_i \quad j=1, \dots, k \quad (8.3)$$

$$\mu_i(R_1, \dots, R_k) = \min \left[ \frac{r_i R_1}{K_{1i} + R_1}, \dots, \frac{r_i R_k}{K_{ki} + R_k} \right] \quad (8.4)$$

where  $N_i$  is the population abundance of species  $i$ ,  $R_j$  is the availability of resource  $j$ ,  $m_i$  is the specific mortality rate of species  $i$ ,  $D$  is the dilution rate,  $S_j$  is the influent concentration of resource  $j$ ,  $Y_{ji}$  is the yield of species  $i$  on resource  $j$ . In equation 8.4, the specific growth rate  $\mu_i$  is determined by the most limiting resource,  $r_i$  is the maximum specific growth rate of species  $i$ ; and  $K_{ji}$  is the half-saturation constant for resource  $j$  of species  $i$ .

### 8.3 Calculation of N<sub>2</sub>O production

The N<sub>2</sub>O concentration in the water sample was corrected for solubility-dependent phase partitioning in equilibration. The corrected concentration is:

(8.5)

$$W_i = A_e + [(A_e - A_i) \times \frac{V_a}{V_w \times \alpha_{teq}}]$$

where A<sub>i</sub> is the initial mixing ratio in the equilibrator gas (compressed air), V<sub>a</sub> and V<sub>w</sub> are the headspace and water sample volumes, respectively, and α<sub>teq</sub> is the Ostwald solubility (0.54) at the equilibration temperature (25°C). The concentration of N<sub>2</sub>O in the original sample at *in situ* temperature is calculated in equation 8.3:

(8.6)

$$C_{in situ} = p_{teq} \times \alpha_{teq}$$

where p<sub>teq</sub> is the gas partial pressure at the equilibration temperature with an ambient system pressure mbar (P) and 1013.25 mbar as the standard atmospheric pressure.

(8.7)

$$p_{teq} = W_i \times \left( \frac{1013.25}{P} \right)$$

## 8.4 Estimation of the N<sub>2</sub>O impact in real WWTP conditions

The N<sub>2</sub>O production rate estimated from the experiment was 402 and 11.2 nmol/L.h for low and high DO respectively.

**Table 8.1** Summary of nitrogen compounds concentrations and mass balance.

Low DO			High DO		
NO <sub>2</sub> <sup>-</sup>	1.63E+04	nmol_N/L.h	NO <sub>2</sub> <sup>-</sup>	1.19E+02	nmol_N/L.h
NO <sub>3</sub> <sup>-</sup>	7.74E+02	nmol_N/L.h	NO <sub>3</sub> <sup>-</sup>	7.44E+04	nmol_N/L.h
TKN removal	5.28E+04	nmol_N/L.h	TKN removal	7.62E+04	nmol_N/L.h
N <sub>2</sub> O rate	8.04E+02	nmol_N/L.h	N <sub>2</sub> O rate	2.24E+01	nmol_N/L.h
N <sub>2</sub> O/TKN removed	1.52	%	N <sub>2</sub> O/TKN removed	0.029	%
NO <sub>2</sub> <sup>-</sup> + NO <sub>3</sub> <sup>-</sup> + N <sub>2</sub> O	1.79E+04	nmol_N/L.h	NO <sub>2</sub> <sup>-</sup> + NO <sub>3</sub> <sup>-</sup> + N <sub>2</sub> O	7.46E+04	nmol_N/L.h
(NO <sub>2</sub> <sup>-</sup> + NO <sub>3</sub> <sup>-</sup> + N <sub>2</sub> O)/TKN oxidized	33.9	%	(NO <sub>2</sub> <sup>-</sup> + NO <sub>3</sub> <sup>-</sup> + N <sub>2</sub> O)/TKN oxidized	97.9	%
% of N missed	66.1	%	% of N missed	2.1	%
NO <sub>2</sub> <sup>-</sup> + NO <sub>3</sub> <sup>-</sup>	1.71E+04	nmol_N/L.h			
TKN removal - (NO <sub>2</sub> <sup>-</sup> + NO <sub>3</sub> <sup>-</sup> )	3.57E+04	nmol_N/L.h			
Expected Total amount of gases	3.57E+04	nmol_N/L.h			
N <sub>2</sub> O/total gases	2.25	%			
N <sub>2</sub> + NO	97.7	%			

**Table 8.2** Estimation of N<sub>2</sub>O impact in electricity equivalent at different HRTs.

Low DO			High DO		
N <sub>2</sub> O rate	4.02E+02	nmol/L.h	N <sub>2</sub> O rate	1.12E+01	nmol/L.h
N <sub>2</sub> O rate	4.02E-07	mol/L.h	N <sub>2</sub> O rate	1.12E-08	mol/L.h
Mw N <sub>2</sub> O	4.40E+01	g/mol	Mw N <sub>2</sub> O	4.40E+01	g/mol
N <sub>2</sub> O rate	1.77E-05	g/L.h	N <sub>2</sub> O rate	4.93E-07	g/L.h
N <sub>2</sub> O rate	1.77E-02	g/m <sup>3</sup> .h	N <sub>2</sub> O rate	4.93E-04	g/m <sup>3</sup> .h
N <sub>2</sub> O rate	1.55E+02	g/m <sup>3</sup> .year	N <sub>2</sub> O rate	4.32	g/m <sup>3</sup> .year
N <sub>2</sub> O rate	1.55E-01	kg N <sub>2</sub> O/m <sup>3</sup> .year	N <sub>2</sub> O rate	4.32E-03	kg N <sub>2</sub> O/m <sup>3</sup> .year
N <sub>2</sub> O (HRT-5d)	2.12E-03	kg N <sub>2</sub> O/m <sup>3</sup> treated water	N <sub>2</sub> O (HRT-5d)	5.92E-05	kg N <sub>2</sub> O/m <sup>3</sup> treated water
N <sub>2</sub> O (HRT-1d)	4.25E-04	kg N <sub>2</sub> O/m <sup>3</sup> treated water	N <sub>2</sub> O (HRT-1d)	1.18E-05	kg N <sub>2</sub> O/m <sup>3</sup> treated water
N <sub>2</sub> O (HRT-12h)	2.12E-04	kg N <sub>2</sub> O/m <sup>3</sup> treated water	N <sub>2</sub> O (HRT-12h)	5.92E-06	kg N <sub>2</sub> O/m <sup>3</sup> treated water

**Table 8.3** Estimation of N<sub>2</sub>O impact in electricity equivalent assuming a TKN effluent of 2 mg/L.

TKN Inf (mgN/ L)	TKN Eff (mgN/ L)	TKN oxidized (mgN/ L)	TKN oxidized (g/m <sup>3</sup> )	TKN (molN/ m <sup>3</sup> )	1.5% of molN/m <sup>3</sup>	N <sub>2</sub> O (mol/ m <sup>3</sup> )	N <sub>2</sub> O (kg/ m <sup>3</sup> )	CO <sub>2e</sub> (kg/ m <sup>3</sup> )	kWh/ m <sup>3</sup>
10	2	8	8	0.57	0.01	0.004	0.0002	0.06	0.14
20	2	18	18	1.29	0.02	0.010	0.0004	0.13	0.33
30	2	28	28	2.00	0.03	0.015	0.0007	0.21	0.51
40	2	38	38	2.71	0.04	0.021	0.0009	0.28	0.69
50	2	48	48	3.43	0.05	0.026	0.0011	0.36	0.87
60	2	58	58	4.14	0.06	0.032	0.0014	0.43	1.05
70	2	68	68	4.86	0.07	0.037	0.0016	0.50	1.23
80	2	78	78	5.57	0.08	0.042	0.0019	0.58	1.41
90	2	88	88	6.29	0.10	0.048	0.0021	0.65	1.59
100	2	98	98	7.00	0.11	0.053	0.0023	0.73	1.77
110	2	108	108	7.71	0.12	0.059	0.0026	0.80	1.95
120	2	118	118	8.43	0.13	0.064	0.0028	0.87	2.13
130	2	128	128	9.14	0.14	0.069	0.0031	0.95	2.31
140	2	138	138	9.86	0.15	0.075	0.0033	1.02	2.49
150	2	148	148	10.57	0.16	0.080	0.0035	1.10	2.67

## 8.5 Flow cytometry dot plots for activated sludge samples

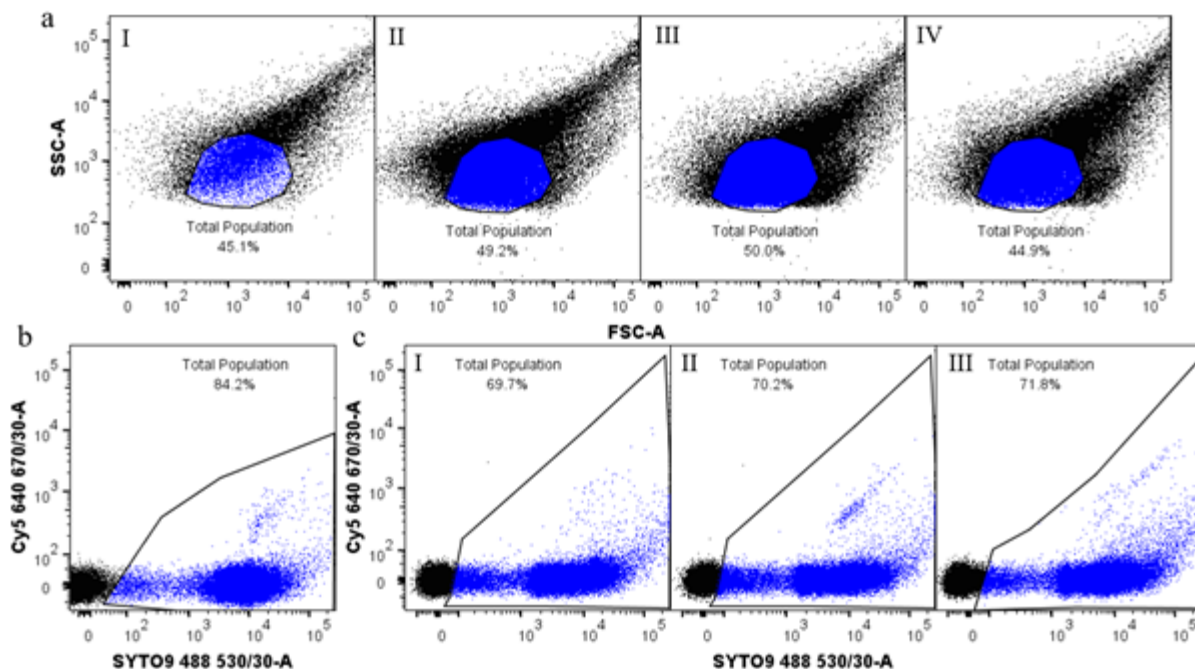


**Figure 8.1** Flow cytometry outputs of bacteria cells from activated sludge samples fixed with glycerol (a), paraformaldehyde (b) and ethanol (c). Cells fixed in glycerol were hybridized with: Cy3 and SYTO 9 (I), Cy3 and FITC (II), Cy5 and SYTO 9 (III) and Cy5 and FITC (IV); AOB cell clusters were initially selected using scattergrams of SSC/FSC or Cy5/SYTO 9. Cells fixed in ethanol were tested at different times: 24 months (I), 6 months (II), 2 months (III). The different colours indicate the different populations: regions with a blue outline indicate the total population with the respective percentage relative to the total number of events with black.

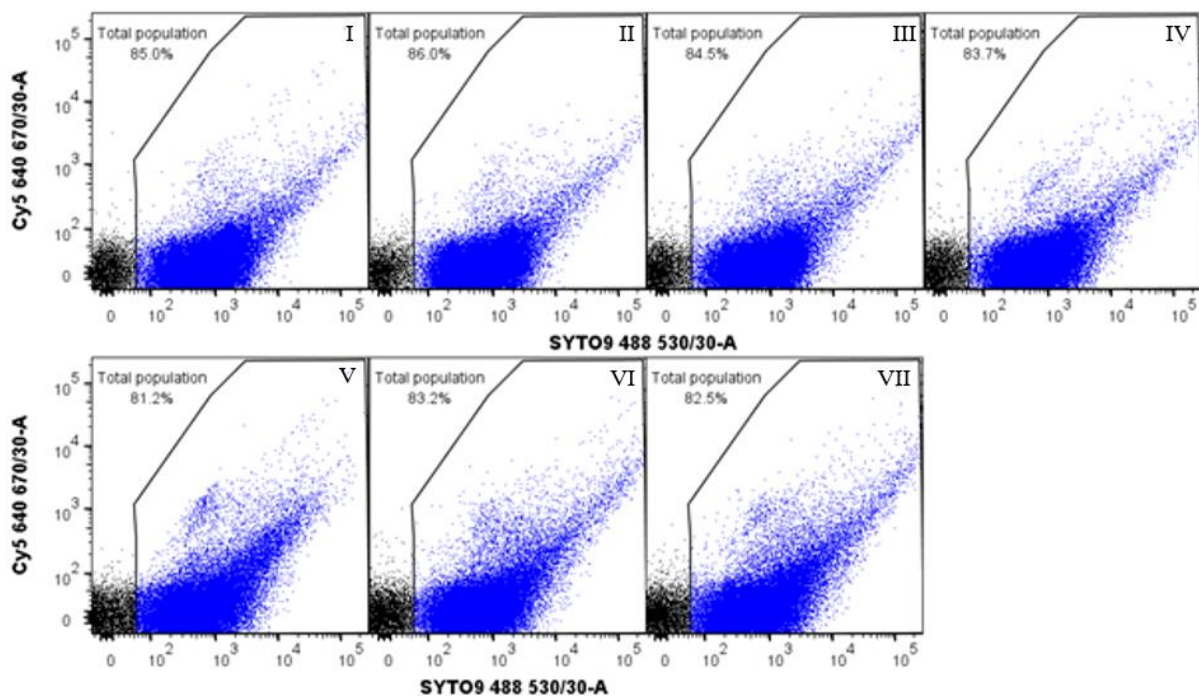


**Figure 8.2** Flow cytometry outputs of the sonication test applied to samples from activated sludge. Scattergrams of the different pre-treatments showing SYTO 9 versus Cy5: bath sonication for 2 (I), 4 (II), 6 (III), and 8 (IV) min and ultrasonication for 2x30 s at 25 W (V), 2x15 s at 74 W (VI) and 2x30 s at 74 W (VII). The different colours indicate the different populations: regions with a blue outline indicate the total population with the respective percentage relative to the total number of events with black.

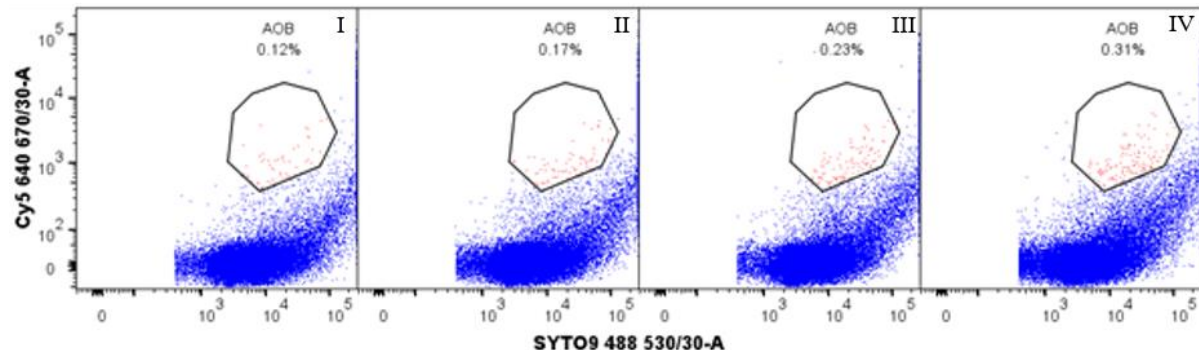


**Figure 8.3** Flow cytometry outputs of the concentration test applied to samples from activated sludge. Scattergrams of the different concentrations of Cy5 showing SYTO 9 versus Cy5: 2.5 (I), 5 (II), 10 (III), and 20 (IV) µg/µL. The different colours indicate the different populations: regions with a red outline indicate the target population with the respective percentage relative to total DNA with blue colour.

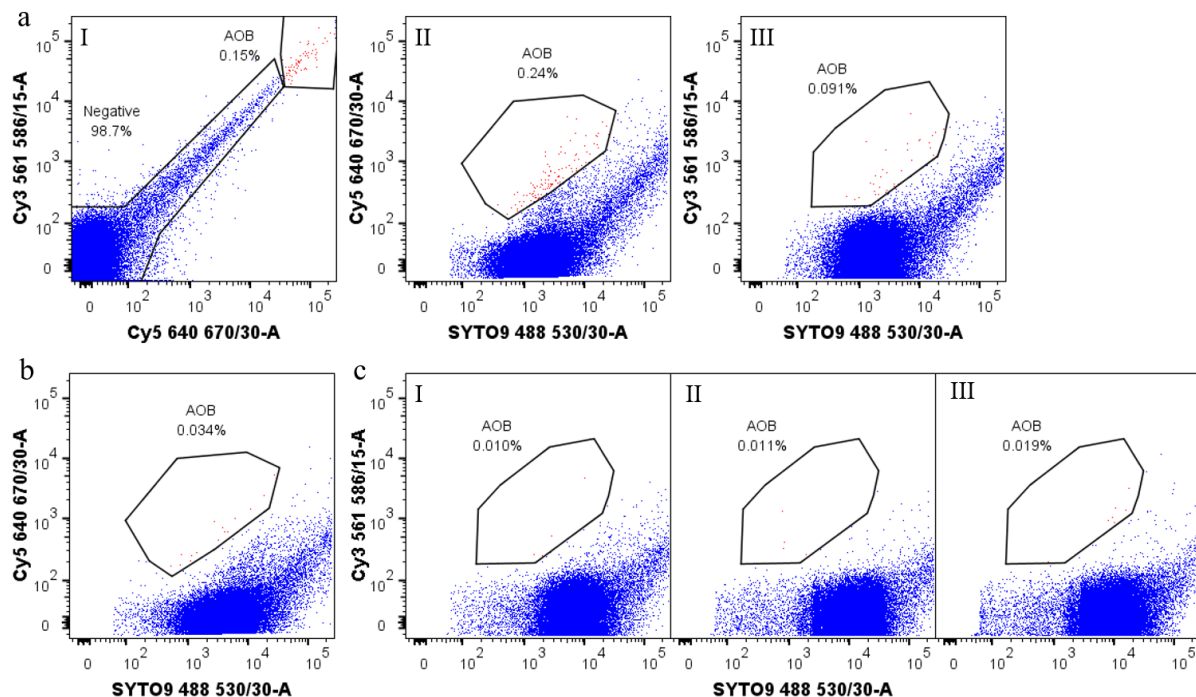


**Figure 8.4** Flow cytometry outputs of the multi probe test applied to samples from activated sludge. Cells were hybridized with all probes (a): Cy3/Cy5 (I), Cy5/SYTO 9 (II) and Cy3/SYTO 9 (III); hybridized with only Cy5 (b); hybridized with only Cy3 (c): all Cy3 (I), Nsm156 (II) and Nsv443 (III). The different colours indicate the different populations: regions with a red outline indicate the target population with the respective percentage relative to total DNA with blue colour.

## 8.6 Enrichment of AOB from activated sludge full-scale treatment plant

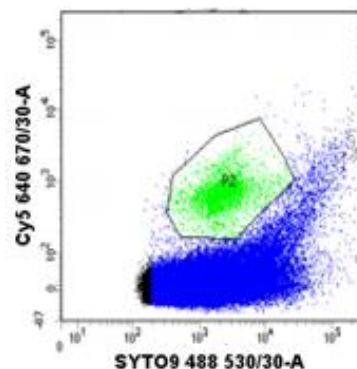


**Figure 8.5** Flow cytometry scattergrams based on SYTO 9 versus Cy5 parameters of the AOB sorted in samples collected from full-scale activated sludge plant. Each plot contains  $2 \times 10^6$  events and the AOB region of the plot indicates the events gated for sorting. The different colours indicate the different populations: region with a green outline indicate the sorted target population with the respective percentage relative to total DNA with blue colour.

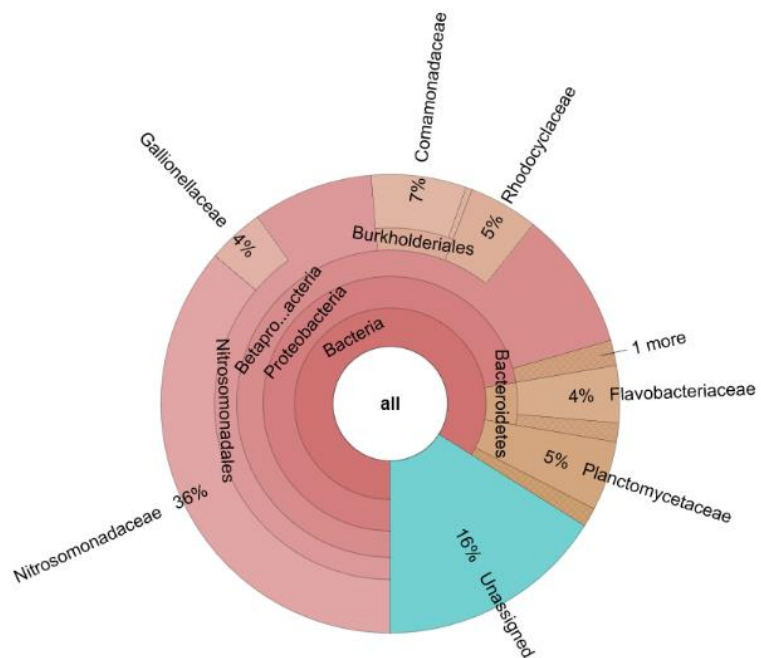


**Figure 8.6** Taxonomic distribution based on 16S gene sequences of the sorted samples collected from activated sludge treatment plant. The data were visualized using Krona (Ondov *et al.*, 2011). The percentages correlate each phylogeny within the total assigned sequences.

## 8.7 Extraction of AOB genomes

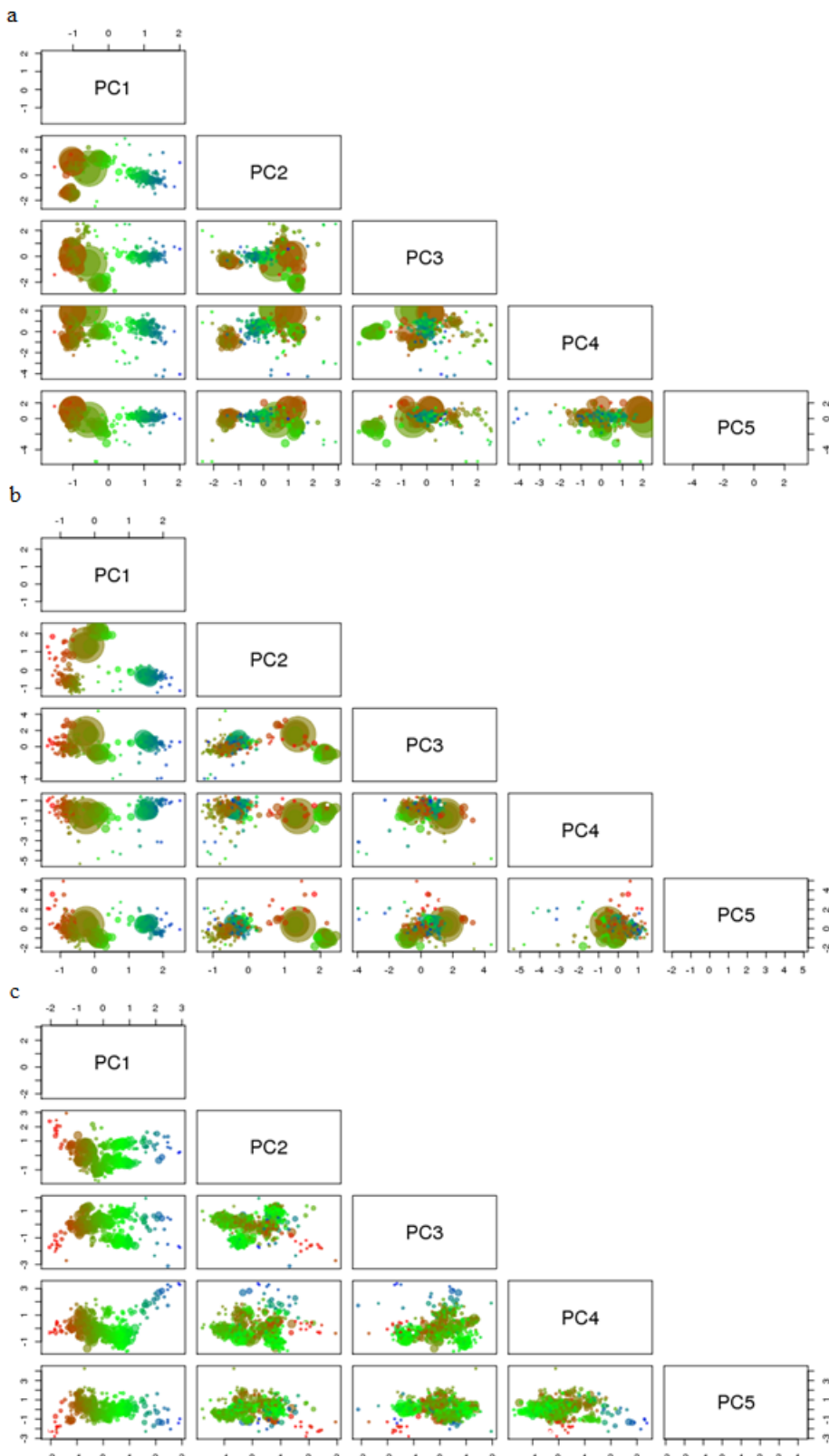


**Figure 8.7** PCA of the subset genome bins 1 (a), 2 (b) and 3 (c) in the low DO samples. The scaffolds are scaled by length and coloured by GC content.

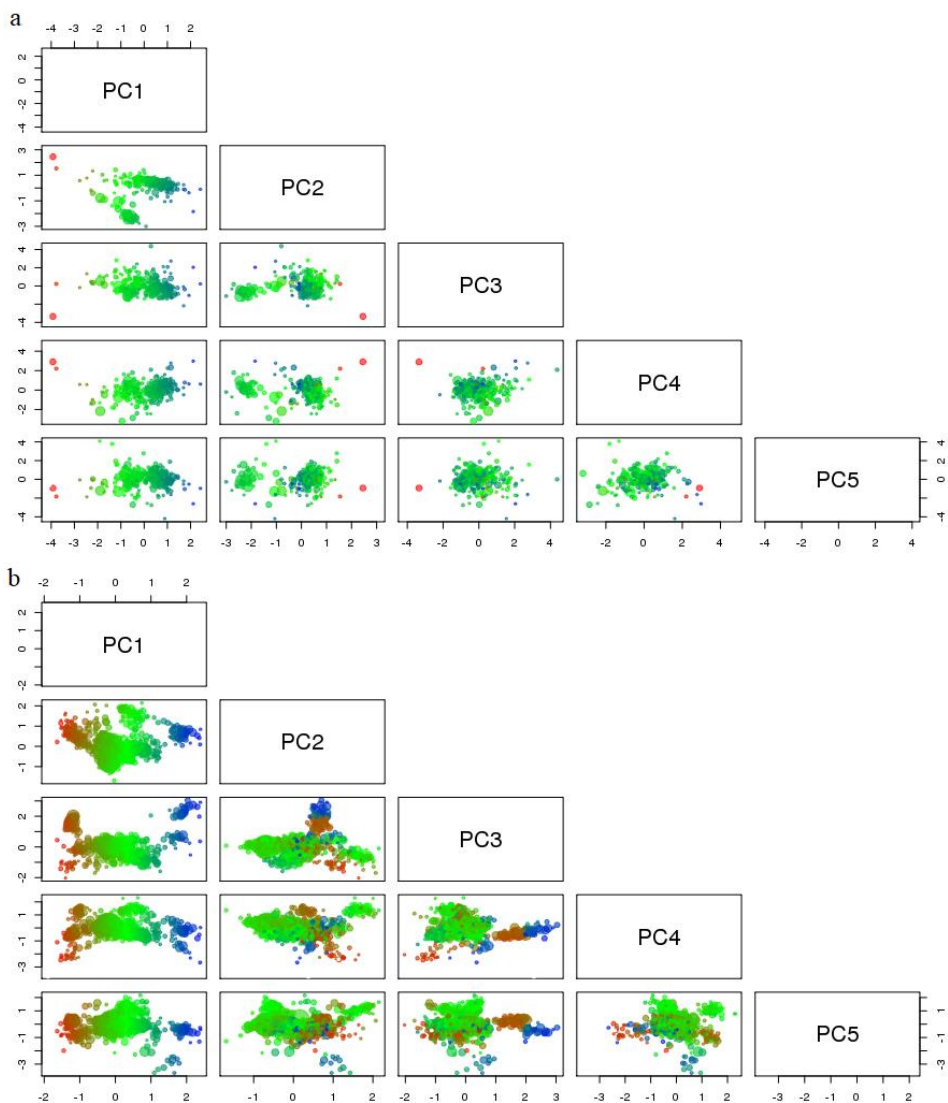


**Figure 8.8** PCA of the subset genome bins 1 (a) and 2 (b) in the high DO samples. The scaffolds are scaled by length and coloured by GC content.

## References

- Abeliovich, A. (2006) 'The Nitrite-Oxidizing Bacteria', in Dworkin, M., Falkow, S., Rosenberg, E., Schleifer, K.-H., and Stackebrandt, E. (eds) *The Prokaryotes*. 3rd edn. New York, USA: Springer, pp. 861–872.
- Abeliovich, A. and Vonshak, A. (1992) 'Anaerobic metabolism of *Nitrosomonas europaea*', *Archives Of Microbiology*, 158(4), pp. 267–270.
- Ahn, J. H., Kim, S., Park, H., Rahm, B., Pagilla, K. and Chandran, K. (2010) 'N<sub>2</sub>O Emissions from Activated Sludge Processes, 2008–2009: Results of a National Monitoring Survey in the United States', *Environmental Science and Technology*, 44(12), pp. 4505–4511.
- Ahn, J. H., Kwan, T. and Chandran, K. (2011) 'Comparison of partial and full nitrification processes applied for treating high-strength nitrogen wastewaters: Microbial ecology through nitrous oxide production', *Environmental Science and Technology*, 45(7), pp. 2734–2740.
- Alawi, M., Lipski, A., Sanders, T., Eva-Maria-Pfeiffer and Speck, E. (2007) 'Cultivation of a novel cold-adapted nitrite oxidizing betaproteobacterium from the Siberian Arctic', *The ISME Journal*. Nature Publishing Group, 1(3), pp. 256–264.
- Albertsen, M., Hugenholtz, P., Skarszewski, A., Nielsen, K. L., Tyson, G. W. and Nielsen, P. H. (2013) 'Genome sequences of rare, uncultured bacteria obtained by differential coverage binning of multiple metagenomes', *Nature Biotechnology*, 31(6), pp. 533–538.
- Amann, R. I., Binder, B. J., Olson, R. J., Chisholm, S. W., Devereux, R. and Stahl, D. A. (1990) 'Combination of 16S rRNA-Targeted Oligonucleotide Probes with Flow Cytometry for Analyzing Mixed Microbial Populations', *Applied and Environmental Microbiology*, 56(6), pp. 1919–1925.
- Amann, R. I., Krumholz, L. and Stahl, D. A. (1990) 'Fluorescent-oligonucleotide probing of whole cells for determinative, phylogenetic, and environmental studies in microbiology', *Journal of Bacteriology*, 172(2), pp. 762–770.
- Amann, R., Lemmer, H. and Wagner, M. (1998) 'Monitoring the community structure of wastewater treatment plants: a comparison of old and new techniques', *FEMS Microbiology Ecology*, 25, pp. 205–215.
- Anthonisen, A., Loehr, R., Prakasam, T. and Srinath, E. (1976) 'Inhibition of Nitrification by Ammonia and Nitrous Acid', *Journal of the Water Pollution Control Federation*, 48(5), pp. 835–852.
- APHA (1998) *Standard methods for the examination of water and wastewater*. 20th ed.

## References

- Edited by L. S. Clesceri, A. E. Greenberg, and A. D. Eaton. Washington, USA: American Public Health Association.
- Arnaldos, M., Kunkel, S. A., Stark, B. C. and Pagilla, K. R. (2013) ‘Enhanced heme protein expression by ammonia-oxidizing communities acclimated to low dissolved oxygen conditions’, *Applied Microbiology and Biotechnology*, 97(23), pp. 10211–10221.
- Arnaldos, M., Kunkel, S. A., Stark, B. C. and Pagilla, K. R. (2014) ‘Characterization of heme protein expressed by ammonia-oxidizing bacteria under low dissolved oxygen conditions’, *Applied Microbiology and Biotechnology*, 98(7), pp. 3231–3239.
- Arnaldos, M. and Pagilla, K. R. (2015) ‘Occurrence and enrichment of “bacterial sherpas”: climb to sustainability in wastewater treatment’, *Water Science and Technology*, 72(9), pp. 1481–1487.
- Arp, D. J., Chain, P. S. G. and Klotz, M. G. (2007) ‘The impact of genome analyses on our understanding of ammonia-oxidizing bacteria’, *Annual Review of Microbiology*, 61, pp. 503–528.
- Arp, D. J., Sayavedra-Soto, L. A. and Hommes, N. G. (2002) ‘Molecular biology and biochemistry of ammonia oxidation by *Nitrosomonas europaea*’, *Archives of Microbiology*, 178(4), pp. 250–255.
- Bankevich, A. *et al.* (2012) ‘SPAdes: A New Genome Assembly Algorithm and Its Applications to Single-Cell Sequencing’, *Journal of Computational Biology*, 19(5), pp. 455–477.
- Baptista, J. D. C., Lunn, M., Davenport, R. J., Swan, D. L., Read, L. F., Brown, M. R., Morais, C. and Curtis, T. P. (2014) ‘Agreement between *amoA* gene-specific quantitative PCR and fluorescence in situ hybridization in the measurement of ammonia-oxidizing bacteria in activated sludge’, *Applied and Environmental Microbiology*, 80(19), pp. 5901–5910.
- Barnes, D. and Bliss, P. J. (1983) *Biological Control of Nitrogen in Wastewater Treatment*. New York, USA: Spon Press.
- Beaumont, H. J. E., Lens, S. I., Reijnders, W. N. M., Westerhoff, H. V. and Van Spanning, R. J. M. (2004) ‘Expression of nitrite reductase in *Nitrosomonas europaea* involves NsrR, a novel nitrite-sensitive transcription repressor’, *Molecular Microbiology*, 54(1), pp. 148–158.
- Beaumont, H. J. E., Lens, S. I., Westerhoff, H. V. and Van Spanning, R. J. M. (2005) ‘Novel *nirK* cluster genes in *Nitrosomonas europaea* are required for NirK-dependent tolerance to nitrite’, *Journal of Bacteriology*, 187(19), pp. 6849–6851.
- Bellucci, M., Ofișeru, I. D., Graham, D. W., Head, I. M. and Curtis, T. P. (2011) ‘Low-

## References

- dissolved-oxygen nitrifying systems exploit ammonia-oxidizing bacteria with unusually high yields', *Applied and Environmental Microbiology*, 77(21), pp. 7787–7796.
- Bergmann, D. and Hooper, A. (1994) 'Sequence of the gene, *amoB*, for the 43-kDa polypeptide of ammonia monooxygenase of *Nitrosomonas europaea*', 204(2), pp. 759–762.
- Bergmann, D. J., Arciero, D. M. and Hooper, A. B. (1994) 'Organization of the *hao* gene cluster of *Nitrosomonas europaea*: genes for two tetraheme c cytochromes', *Journal of Bacteriology*, 176(11), pp. 3148–3153.
- Bergmann, D. J., Hooper, A. B. and Klotz, M. G. (2005) 'Structure and Sequence Conservation of *hao* Cluster Genes of Autotrophic Ammonia-Oxidizing Bacteria : Evidence for Their Evolutionary History Structure and Sequence', *Applied Environmental Microbiology*, 71(9), pp. 5371–5382.
- Beyer, S., Gilch, S., Meyer, O. and Schmidt, I. (2009) 'Transcription of genes coding for metabolic key functions in *Nitrosomonas europaea* during aerobic and anaerobic growth', *Journal of Molecular Microbiology and Biotechnology*, 16(3–4), pp. 187–197.
- de Bie, M. J. M., Speksnijder, A. G. C. L., Kowalchuk, G. A., Schuurman, T., Zwart, G., Stephen, J. R., Diekmann, O. E. and Laanbroek, H. J. (2001) 'Shifts in the dominant populations of ammonia-oxidizing β-subclass Proteobacteria along the eutrophic Schelde estuary', *Aquatic Microbial Ecology*, 23(3), pp. 225–236.
- Blackburne, R., Vadivelu, V. M., Yuan, Z. and Keller, J. (2007) 'Kinetic characterisation of an enriched *Nitrospira* culture with comparison to *Nitrobacter*', *Water Research*, 41(14), pp. 3033–3042.
- Blackburne, R., Yuan, Z. and Keller, J. (2008) 'Partial nitrification to nitrite using low dissolved oxygen concentration as the main selection factor', *Biodegradation*, 19(2), pp. 303–312.
- Blainey, P. C., Mosier, A. C., Potanina, A., Francis, C. A. and Quake, S. R. (2011) 'Genome of a low-salinity ammonia-oxidizing archaeon determined by single-cell and metagenomic analysis', *PLoS ONE*, 6(2), pp. 1–12.
- Bock, E. (1976) 'Growth of nitrobacter in the presence of organic matter. II. Chemoorganotrophic growth of *Nitrobacter agilis*.', *Archives of Microbiology*, 108(3), pp. 305–312.
- Bock, E., Schmidt, I., Stüven, R. and Zart, D. (1995) 'Nitrogen loss caused by denitrifying *Nitrosomonas* cells using ammonium or hydrogen as electron donors and nitrite as electron acceptor', *Archives of Microbiology*, 163(1), pp. 16–20.
- Bollmann, A., Bär-Gilissen, M.-J. and Laanbroek, H. J. (2002) 'Growth at Low Ammonium Concentrations and Starvation Response as Potential Factors Involved in Niche

## References

- Differentiation among Ammonia-Oxidizing Bacteria', *Applied and Environmental Microbiology*, 68(10), pp. 4751–4757.
- Bonin, P., Tamburini, C. and Michotey, V. (2002) 'Determination of the bacterial processes which are sources of nitrous oxide production in marine samples', *Water Research*, 36(3), pp. 722–732.
- Brown, C. T., Hug, L. A., Thomas, B. C., Sharon, I., Castelle, C. J., Singh, A., Wilkins, M. J., Wrighton, K. C., Williams, K. H. and Banfield, J. F. (2015) 'Unusual biology across a group comprising more than 15% of domain Bacteria', *Nature*, 523, pp. 208–211.
- Buesing, N. and Gessner, M. O. (2002) 'Comparison of detachment procedures for direct counts of bacteria associated with sediment particles plant litter and epiphytic biofilms', *Aquatic Microbial Ecology*, 27(1), pp. 29–36.
- Byrns, G., Wheatley, a and Smedley, V. (2012) 'Carbon dioxide releases from wastewater treatment: potential use in the UK', *Engineering Sustainability*, 166(ES3), pp. 111–121.
- Caporaso, J. G. *et al.* (2010) 'QIIME allows analysis of high-throughput community sequencing data', *Nature methods*, 7(5), pp. 335–336.
- Caporaso, J. G., Lauber, C. L., Walters, W. A., Berg-Lyons, D., Lozupone, C. A., Turnbaugh, P. J., Fierer, N. and Knight, R. (2011) 'Global patterns of 16S rRNA diversity at a depth of millions of sequences per sample.', *Proceedings of the National Academy of Sciences of the United States of America*, 108 Suppl(Supplement\_1), pp. 4516–22.
- Casciotti, K. L. and Ward, B. B. (2001) 'Dissimilatory Nitrite Reductase Genes from Autotrophic Ammonia-Oxidizing Bacteria', *Applied and Environmental Microbiology*, 67(5), pp. 2213–2221.
- Chain, P. *et al.* (2003) 'Complete Genome Sequence of the Ammonia-Oxidizing Bacterium and Obligate Chemolithoautotroph *Nitrosomonas europaea*', *Journal of Bacteriology*, 185(9), pp. 2759–2773.
- Chandran, K., Stein, L. Y., Klotz, M. G. and van Loosdrecht, M. C. M. (2011) 'Nitrous oxide production by lithotrophic ammonia-oxidizing bacteria and implications for engineered nitrogen-removal systems', *Biochemical Society Transactions*, 39(6), pp. 1832–1837.
- Ciais, P. *et al.* (2013) 'Carbon and Other Biogeochemical Cycles', in Stocker, T. F., Qin, D., Plattner, G.-K., Tignor, M., Allen, S. K., Boschung, J., Nauels, A., Xia, Y., Bex, V., and Midgley, P. M. (eds) *Climate Change 2013: The Physical Science Basis. Contribution of Working Group I to the Fifth Assessment Report of the Intergovernmental Panel on Climate Change*. Cambridge, UK: Cambridge University Press, pp. 465–570.
- Clarke, K. R. and Gorley, R. N. (2015) 'PRIMER v7: User Manual/Tutorial'. Plymouth, UK: PRIMER-E.

## References

- Colliver, B. B. and Stephenson, T. (2000) 'Production of nitrogen oxide and dinitrogen oxide by autotrophic nitrifiers', *Biotechnology Advances*, 18(3), pp. 219–232.
- Cordero, O. X. and Polz, M. F. (2014) 'Explaining microbial genomic diversity in light of evolutionary ecology', *Nature Review Microbiology*. Nature Publishing Group, 12(4), pp. 263–273.
- Coskuner, G., Ballinger, S. J., Davenport, R. J., Pickering, R. L., Solera, R., Head, I. M. and Curtis, T. P. (2005) 'Agreement between Theory and Measurement in Quantification of Ammonia-Oxidizing Bacteria', *Applied and Environmental Microbiology*, 71(10), pp. 6325–6334.
- Curtis, T. P. (2010) 'Low-Energy Wastewater Treatment: Strategies and Technologies', in *Environmental Microbiology*. 2nd edn. New Jersey, USA: Wiley-Blackwell, pp. 301–318.
- Daims, H. *et al.* (2015) 'Complete nitrification by *Nitrospira* bacteria', *Nature*. Nature Publishing Group, 528(7583), pp. 504–509.
- Daims, H., Brühl, A., Amann, R., Schleifer, K.-H. and Wagner, M. (1999) 'The Domain-specific Probe EUB338 is Insufficient for the Detection of all Bacteria: Development and Evaluation of a more Comprehensive Probe Set', *Systematic and Applied Microbiology*, 22(3), pp. 434–444.
- Daims, H., Lücker, S. and Wagner, M. (2016) 'A New Perspective on Microbes Formerly Known as Nitrite-Oxidizing Bacteria', *Trends in Microbiology*, 24(9), pp. 699–712.
- Daims, H., Nielsen, J. L., Nielsen, P. H., Schleifer, K. H. and Wagner, M. (2001) 'In Situ Characterization of *Nitrospira*-Like Nitrite-Oxidizing Bacteria Active in Wastewater Treatment Plants', *Applied and Environmental Microbiology*, 67(11), pp. 5273–5284.
- Daims, H., Ramsing, N. B., Schleifer, K. and Wagner, M. (2001) 'Cultivation-Independent , Semiautomatic Determination of Absolute Bacterial Cell Numbers in Environmental Samples by Fluorescence In Situ Hybridization', *Society*, 67(12), pp. 5810–5818.
- DBEIS (2017) *2016 UK Provisional Greenhouse Gas Emissions*. Available at: [https://www.gov.uk/government/uploads/system/uploads/attachment\\_data/file/604327/2016\\_Provisional\\_emissions\\_statistics\\_one\\_page\\_summary.pdf](https://www.gov.uk/government/uploads/system/uploads/attachment_data/file/604327/2016_Provisional_emissions_statistics_one_page_summary.pdf) (Accessed: 5 May 2017).
- Dechesne, A., Musovic, S., Palomo, A., Diwan, V. and Smets, B. F. (2016) 'Underestimation of ammonia-oxidizing bacteria abundance by amplification bias in *amoA*-targeted qPCR', *Microbial Biotechnology*, 9(4), pp. 519–524.
- DeLong, E. F. (2005) 'Microbial community genomics in the ocean.', *Nature reviews. Microbiology*, 3(6), pp. 459–69.
- DeLong, E. F. and Karl, D. M. (2005) 'Genomic perspectives in microbial oceanography', *Nature*, 437(7057), pp. 336–42.

## References

- Delwiche, C. C. and Finstein, M. S. (1965) 'Carbon and Energy Sources for the Nitrifying Autotroph *Nitrobacter*', *Journal of Bacteriology*, 90(1), pp. 102–107.
- Dispirito, A. A., Lipscomb, J. D. and Hooper, A. B. (1986) 'Cytochrome aa<sub>3</sub> from *Nitrosomonas europaea*', *The Journal of Biological Chemistry*, 261(36), pp. 17048–17056.
- Dröge, J. and McHardy, A. C. (2012) 'Taxonomic binning of metagenome samples generated by next-generation sequencing technologies', *Briefings in Bioinformatics*, 13(6), pp. 646–655.
- Dupont, C. L. *et al.* (2012) 'Genomic insights to SAR86, an abundant and uncultivated marine bacterial lineage', *The ISME Journal*. Nature Publishing Group, 6(6), pp. 1186–1199.
- Dyczak, M. A., Londry, K. L. and Oleszkiewicz, J. A. (2008) 'Activated sludge operational regime has significant impact on the type of nitrifying community and its nitrification rates', *Water Research*, 42(8–9), pp. 2320–2328.
- Edgar, R. C. (2010) 'Search and clustering orders of magnitude faster than BLAST', *Bioinformatics*, 26(19), pp. 2460–2461.
- Ehrich, S., Behrens, D., Lebedeva, E. V., Ludwig, W. and Bock, E. (1995) 'A new obligately chemolithoautotrophic, nitrite-oxidizing nacterium, *Nitrospira moscoviensis* sp. nov. and its phylogenetic relationship', *Archives of Microbiology*, 164(1), pp. 16–23.
- Epstein, S. S. and Rossel, J. (1995) 'Enumeration of sandy sediment bacteria: Search for optimal protocol', *Marine Ecology Progress Series*, 117(1–3), pp. 289–298.
- Evans, G. M. and Furlong, J. C. (2003) *Environmental Biotechnology. Theory and Application*. West Sussex, UK: John Wiley and Sons, pp. 124.
- Falcioni, T., Manti, A., Boi, P., Canonico, B., Balsamo, M. and Papa, S. (2006) 'Comparison of disruption procedures for enumeration of activated sludge floc bacteria by flow cytometry', *Cytometry Part B - Clinical Cytometry*, 70(3), pp. 149–153.
- Fitzgerald, C. M., Camejo, P., Oshlag, J. Z. and Noguera, D. R. (2015) 'Ammonia-oxidizing microbial communities in reactors with efficient nitrification at low-dissolved oxygen', *Water Research*, 70, pp. 38–51.
- Foladori, P., Bruni, L., Tamburini, S. and Ziglio, G. (2010) 'Direct quantification of bacterial biomass in influent, effluent and activated sludge of wastewater treatment plants by using flow cytometry', *Water Research*, 44(13), pp. 3807–3818.
- Foladori, P., Tamburini, S. and Bruni, L. (2010) 'Bacteria permeabilisation and disruption caused by sludge reduction technologies evaluated by flow cytometry', *Water Research*, 44(17), pp. 4888–4899.
- Francis, C. A., Roberts, K. J., Beman, J. M., Santoro, A. E. and Oakley, B. B. (2005)

## References

- ‘Ubiquity and diversity of ammonia-oxidizing archaea in water columns and sediments of the ocean’, *Proceedings of the National Academy of Sciences*, 102(41), pp. 14683–14688.
- Fuchs, B. M., Zubkov, M. V., Sahm, K., Burkhill, P. H. and Amann, R. (2000) ‘Changes in community composition during dilution cultures of marine bacterioplankton as assessed by flow cytometric and molecular biological techniques’, *Environmental Microbiology*, 2(2), pp. 191–201.
- Fujitani, H., Kumagai, A., Ushiki, N., Momiuchi, K. and Tsuneda, S. (2015) ‘Selective isolation of ammonia-oxidizing bacteria from autotrophic nitrifying granules by applying cell-sorting and sub-culturing of microcolonies’, *Frontiers in Microbiology*, 6, pp. 1–10.
- Fujitani, H., Ushiki, N., Tsuneda, S. and Aoi, Y. (2014) ‘Isolation of sublineage I *Nitrospira* by a novel cultivation strategy’, *Environmental Microbiology*, 16(10), pp. 3030–3040.
- Galhardo, R. S., Hastings, P. J. and Rosenberg, S. M. (2012) ‘Mutation as a Stress Response and the Regulation of Evolvability’, *Critical Reviews in Biochemistry and Molecular Biology*, 42(5), pp. 399–435.
- Garbeva, P., Baggs, E. M. and Prosser, J. I. (2007) ‘Phylogeny of nitrite reductase (*nirK*) and nitric oxide reductase (*norB*) genes from *Nitrosospira* species isolated from soil’, *FEMS Microbiology Letters*, 266(1), pp. 83–89.
- Geets, J., Boon, N. and Verstraete, W. (2006) ‘Strategies of aerobic ammonia-oxidizing bacteria for coping with nutrient and oxygen fluctuations’, *FEMS Microbiology Ecology*, 58(1), pp. 1–13.
- Gieseke, A., Purkhold, U., Wagner, M., Amann, R. and Schramm, A. (2001) ‘Community Structure and Activity Dynamics of Nitrifying Bacteria in a Phosphate-Removing Biofilm’, *Applied and Environmental Microbiology*, 67(3), pp. 1351–1362.
- Gilbert, E. M., Agrawal, S., Brunner, F., Schwartz, T., Horn, H. and Lackner, S. (2014) ‘Response of different *Nitrospira* Species to anoxic periods depends on operational DO’, *Environmental Science and Technology*, 48(5), pp. 2934–2941.
- Gomez-Alvarez, V., Teal, T. K. and Schmidt, T. M. (2009) ‘Systematic artifacts in metagenomes from complex microbial communities’, *The ISME Journal*. Nature Publishing Group, 3(11), pp. 1314–1317.
- GOV UK (2016) *Greenhouse gas reporting - Conversion factors 2016*, GOV UK. Available at: <https://www.gov.uk/government/publications/greenhouse-gas-reporting-conversion-factors-2016> (Accessed: 5 May 2017).
- Grady, C. P. L. J., Daigger, G. T. and Lim, H. C. (1999) *Biological Wastewater Treatment*. 2nd edn. New York, USA: Marcel Dekker Inc.
- Guo, J., Peng, Y., Wang, S., Zheng, Y., Huang, H. and Wang, Z. (2009) ‘Long-term effect of

## References

- dissolved oxygen on partial nitrification performance and microbial community structure', *Bioresource Technology*, 100(11), pp. 2796–2802.
- Hanaki, K., Hong, Z. and Matsuo, T. (1992) 'Production of Nitrous Oxide Gas During Denitrification of Wastewater', *Water Science and Technology*, 26(5–6), pp. 1027–1036.
- Hanaki, K., Wantawin, C. and Ohgaki, S. (1990) 'Nitrification at low levels of dissolved oxygen with and without organic loading in a suspended-growth reactor', *Water Research*, 24(3), pp. 297–302.
- Haroon, M. F., Skennerton, C. T., Steen, J. A., Lachner, N., Hugenholtz, P. and Tyson, G. W. (2013) 'In-solution fluorescence in situ hybridization and Fluorescence-activated cell sorting for single cell and population genome recovery', *Methods in Enzymology*, 531, pp. 3–19.
- Head, I. M., Hiorns, W. D., Embley, T. M., McCarthy, A. J. and Saunders, J. R. (1993) 'The phylogeny of autotrophic ammonia-oxidizing bacteria as determined by analysis of 16S ribosomal RNA gene sequences', *Journal of General Microbiology*, 139(6), pp. 1147–1153.
- Hollocher, T. C., Tate, M. E. and Nicholas, D. J. D. (1981) 'Nitrosomonas europaea', *The Journal of Biological Chemistry*, 256(21), pp. 10834–10836.
- Hommes, N. G., Sayavedra-Soto, L. A. and Arp, D. J. (2002) 'The roles of the three gene copies encoding hydroxylamine oxidoreductase in *Nitrosomonas europaea*', *Archives of Microbiology*, 178(6), pp. 471–476.
- Hommes, N. G., Sayavedra-Soto, L. A. and Arp, D. J. (2003) 'Chemolithoorganotrophic Growth of *Nitrosomonas europaea* on Fructose', *Journal of Bacteriology*, 185(23), pp. 6809–6814.
- Hooper, A. B. and Terry, K. R. (1979) 'Hydroxylamine oxidoreductase of *Nitrosomonas* production of nitric oxide from hydroxylamine', *Biochimica et Biophysica Acta*, 571(1), pp. 12–20.
- Hooper, A. B., Vannelli, T., Bergmann, D. J. and Arciero, D. M. (1997) 'Enzymology of the oxidation of ammonia to nitrite by bacteria', *International Journal of General and Molecular Microbiology*, 71(1–2), pp. 59–67.
- Huson, D., Mitra, S. and Ruscheweyh, H. (2011) 'Integrative analysis of environmental sequences using MEGAN4', *Genome Research*, 21(9), pp. 1552–1560.
- Hyatt, D., Chen, G.-L., LoCascio, P. F., Land, M. L., Larimer, F. W. and Hauser, L. J. (2010) 'Prodigal: prokaryotic gene recognition and translation initiation site identification', *BMC Bioinformatics*, 11(1), p. 119.
- IPCC (2007) *Climate Change 2007 The Physical Science Basis*. Edited by S. Solomon, D.

## References

- Quin, M. Manning, M. Marquis, K. Averyt, M. Tignor, H. Jr., and Z. Chen. Cambridge, UK: Cambridge University Press.
- Itokawa, H., Hanaki, K. and Matsuo, T. (2001) ‘Nitrous oxide production in high-loading biological nitrogen removal process under low COD/N ratio condition’, *Water Research*, 35(3), pp. 657–664.
- Jetten, M. S. M., Wagner, M., Fuerst, J., Van Loosdrecht, M., Kuenen, G. and Strous, M. (2001) ‘Microbiology and application of the anaerobic ammonium oxidation (‘anammox’) process’, *Current Opinion in Biotechnology*, 12(3), pp. 283–288.
- Jia, W., Liang, S., Zhang, J., Ngo, H. H., Guo, W., Yan, Y. and Zou, Y. (2013) ‘Nitrous oxide emission in low-oxygen simultaneous nitrification and denitrification process: Sources and mechanisms’, *Bioresource Technology*, 136, pp. 444–451.
- Jin, R. C., Yang, G.-F., Yu, J.-J. and Zheng, P. (2012) ‘The inhibition of the Anammox process: A review’, *Chemical Engineering Journal*, 197, pp. 67–79.
- Joshi, N. and Fass, J. (2011) *Sickle: A sliding-window, adaptive, quality-based trimming tool for FastQ files (Version 1.33)*[Software]. Available at: <https://github.com/najoshi/sickle>.
- Kampschreur, M. J., Tan, N. C. G., Kleerebezem, R., Picioreanu, C., Jetten, M. S. M. and Van Loosdrecht, M. C. M. (2008) ‘Effect of dynamic process conditions on nitrogen oxides emission from a nitrifying culture’, *Environmental Science and Technology*, 42(2), pp. 429–435.
- Kampschreur, M. J., Temmink, H., Kleerebezem, R., Jetten, M. S. M. and van Loosdrecht, M. C. M. (2009) ‘Nitrous oxide emission during wastewater treatment’, *Water Research*, 43(17), pp. 4093–4103.
- Katsogiannis, A. N., Kornaros, M. and Lyberatos, G. (2003) ‘Enhanced nitrogen removal in SBRs bypassing nitrate generate accomplished by multiple aerobic/anoxic phase pairs’, *Water Science and Technology*, 47(11), pp. 53–59.
- Keluskar, R., Nerurkar, A. and Desai, A. (2013) ‘Mutualism between autotrophic ammonia-oxidizing bacteria (AOB) and heterotrophs present in an ammonia-oxidizing colony’, *Archives of Microbiology*, 195(10–11), pp. 737–747.
- van Kessel, M. A. H. J., Speth, D. R., Albertsen, M., Nielsen, P. H., Op den Camp, H. J. M., Kartal, B., Jetten, M. S. M. and Lücker, S. (2015) ‘Complete nitrification by a single microorganism’, *Nature*, 528(7583), pp. 555–559.
- Kim, D. J. and Kim, S. H. (2006) ‘Effect of nitrite concentration on the distribution and competition of nitrite-oxidizing bacteria in nitrification reactor systems and their kinetic characteristics’, *Water Research*, 40(5), pp. 887–894.
- Kindaichi, T., Ito, T. and Okabe, S. (2004) ‘Ecophysiological Interaction between Nitrifying

## References

- Bacteria and Heterotrophic Bacteria in Autotrophic Nitrifying Biofilms as Determined by Microautoradiography-Fluorescence In Situ Hybridization', *Applied and Environmental Microbiology*, 70(3), pp. 1641–1650.
- Kindaichi, T., Kawano, Y., Ito, T., Satoh, H. and Okabe, S. (2006) 'Population Dynamics and In Situ Kinetics of Nitrifying Bacteria in Autotrophic Nitrifying Biofilms as Determined by Real-Time Quantitative PCR', *Biotechnology and Bioengineering*, 94(6), pp. 1111–1121.
- Klein, D. (2002) 'Quantification using real-time PCR technology: applications and limitations', *Trends in Molecular Medicine*, 8(6), pp. 257–260.
- Klotz, M. G., Arp, D. J., Chain, P. S. G., El-Sheikh, A. F., Hauser, L. J., Hommes, N. G., Larimer, F. W., Malfatti, S. A., Norton, J. M., Poret-Peterson, A. T., Vergez, L. M. and Ward, B. B. (2006) 'Complete genome sequence of the marine, chemolithoautotrophic, ammonia-oxidizing bacterium *Nitrosococcus oceani* ATCC 19707', *Applied and Environmental Microbiology*, 72(9), pp. 6299–6315.
- Klotz, M. G. and Stein, L. Y. (2011) 'Genomics of ammonia-oxidizing bacteria and insights into their evolution', in Ward, B. B., Arp, D. J., and Klotz, M. G. (eds) *Nitrification*. Washington, USA: ASM Press, pp. 57–94.
- Knapp, C. W. and Graham, D. W. (2007) 'Nitrite-oxidizing bacteria guild ecology associated with nitrification failure in a continuous-flow reactor', *FEMS Microbiology Ecology*, 62(2), pp. 195–201.
- Koch, H., Lücker, S., Albertsen, M., Kitzinger, K., Herbold, C., Speck, E., Nielsen, P. H., Wagner, M. and Daims, H. (2015) 'Expanded metabolic versatility of ubiquitous nitrite-oxidizing bacteria from the genus *Nitrospira*', *Proceedings of the National Academy of Sciences*, 112(36), pp. 11371–11376.
- Könneke, M., Bernhard, A. E., de la Torre, J. R., Walker, C. B., Waterbury, J. B. and Stahl, D. A. (2005) 'Isolation of an autotrophic ammonia-oxidizing marine archaeon', *Nature*, 437(7058), pp. 543–546.
- Koops, H., Purkhold, U., Pommerening-Röser, A., Timmermann, G. and Wagner, M. (2006) 'The Lithoautotrophic Ammonia-Oxidizing Bacteria', in Dworkin, M., Falkow, S., Rosenberg, E., Schleifer, K.-H., and Stackebrandt, E. (eds) *Prokaryotes*. 3rd edn. New York, USA: Springer New York, pp. 778–811.
- Koper, T. E., El-sheikh, A. F., Norton, J. M. and Klotz, M. G. (2004) 'Urease-Encoding Genes in Ammonia-Oxidizing Bacteria', *Applied and Environmental Microbiology*, 70(4), pp. 2342–2348.
- Kosonen, H., Heinonen, M., Mikola, A., Haimi, H., Mulas, M., Corona, F. and Vahala, R. (2016) 'Nitrous Oxide Production at a Fully Covered Wastewater Treatment Plant: Results

## References

- of a Long-Term Online Monitoring Campaign’, *Environmental Science and Technology*, 50(11), pp. 5547–5554.
- Kowalchuk, G. A. and Stephen, J. R. (2001) ‘Ammonia-Oxidizing Bacteria: A Model for Molecular Microbial Ecology’, *Annual Review of Microbiology*, 55(1), pp. 485–529.
- Kozlowski, J. A., Kits, K. D. and Stein, L. Y. (2016) ‘Complete Genome Sequence of *Nitrosomonas ureae* Strain Nm10, an Oligotrophic Group 6a Nitrosomonad’, *American Society for Microbiology*, 4(2), pp. 4–5.
- Kuai, L. and Verstraete, W. (1998) ‘Ammonium Removal by the Oxygen-Limited Autotrophic Nitrification-Denitrification System’, *Applied and Environmental Microbiology*, 64(11), pp. 4500–4506.
- Kunin, V., Copeland, A., Lapidus, A., Mavromatis, K. and Hugenholtz, P. (2008) ‘A Bioinformatician’s Guide to Metagenomics’, *Microbiology and Molecular Biology Reviews*, 72(4), pp. 557–578.
- Laanbroek, H. J. and Gerards, S. (1993) ‘Competition for limiting amounts of oxygen between *Nitrosomonas europaea* and *Nitrobacter winogradskyi* grown in mixed continuous cultures’, *Archives of Microbiology*, 159, pp. 453–459.
- Law, Y., Ye, L., Pan, Y. and Yuan, Z. (2012) ‘Nitrous oxide emissions from wastewater treatment processes’, *Philosophical Transactions of the Royal Society B: Biological Sciences*, 367(1593), pp. 1265–1277.
- Lee, S. H., Malone, C. and Kemp, P. F. (1993) ‘Use of multiple 16S rRNA-targeted fluorescent probes to increase signal strength and measure cellular RNA from natural planktonic bacteria’, *Marine Ecology Progress Series*, 101(1–2), pp. 193–202.
- Li, H. and Durbin, R. (2010) ‘Fast and accurate long-read alignment with Burrows-Wheeler transform’, *Bioinformatics*, 26(5), pp. 589–595.
- Liu, G. and Wang, J. (2013) ‘Long-term low DO enriches and shifts nitrifier community in activated sludge’, *Environmental Science and Technology*, 47(10), pp. 5109–5117.
- Lücker, S., Nowka, B., Rattei, T., Speck, E. and Daims, H. (2013) ‘The genome of *Nitrospina gracilis* illuminates the metabolism and evolution of the major marine nitrite oxidizer’, *Frontiers in Microbiology*, 4(1), pp. 1–19.
- Ma, L., Mao, G., Liu, J., Yu, H., Gao, G. and Wang, Y. (2013) ‘Rapid quantification of bacteria and viruses in influent, settled water, activated sludge and effluent from a wastewater treatment plant using flow cytometry’, *Water Science and Technology*, 68(8), pp. 1763–1769.
- Martens-Habbena, W., Berube, P. M., Urakawa, H., de la Torre, J. R. and Stahl, D. A. (2009) ‘Ammonia oxidation kinetics determine niche separation of nitrifying Archaea and

## References

- Bacteria', *Nature*, 461(7266), pp. 976–979.
- Martin, M. (2011) 'Cutadapt removes adapter sequences from high-throughput sequencing reads', *EMBnet.journal*, 17(1), pp. 10–12.
- McCarty, P. L., Bae, J. and Kim, J. (2011) 'Domestic Wastewater Treatment as a Net Energy Producer - Can This be Achieved?', *Environmental Science and Technology*, 45(17), pp. 7100–6.
- McMurdie, P. J. and Holmes, S. (2013) 'Phyloseq: An R Package for Reproducible Interactive Analysis and Graphics of Microbiome Census Data', *PLoS ONE*, 8(4), pp. 1–11.
- McTavish, H., Fuchs, J. A. and Hooper, A. B. (1993) 'Sequence of the Gene Coding for Ammonia Monooxygenase in *Nitrosomonas europaea*', *Journal of Bacteriology*, 175(8), pp. 2436–2444.
- Milner, M. G., Curtis, T. P. and Davenport, R. J. (2008) 'Presence and activity of ammonia-oxidising bacteria detected amongst the overall bacterial diversity along a physico-chemical gradient of a nitrifying wastewater treatment plant', *Water Research*, 42(12), pp. 2863–2872.
- Mobarry, B. K., Wagner, M., Urbain, V., Rittmann, B. E. and Stahl, D. (1996) 'Phylogenetic probes for analyzing abundance and spatial organization of nitrifying bacteria', *Applied and Environmental Microbiology*, 62(6), pp. 2156–2162.
- Montzka, S. A. *et al.* (2002) 'Controlled substances and other source gases', in *Scientific Assessment of Ozone Depletion*. Geneva, Switzerland: Global Ozone Research and Monitoring Project—Report No. 47.
- Mota, C., Head, M. A., Ridenoure, J. A., Cheng, J. J. and de Los Reyes III, F. L. (2005) 'Effects of Aeration Cycles on Nitrifying Bacterial Populations and Nitrogen Removal in Intermittently Aerated Reactors', *Applied and Environmental Microbiology*, 71(12), pp. 8565–8572.
- Moussa, M. S., Sumanasekera, D. U., Ibrahim, S. H., Lubberding, H. J., Hooijmans, C. M., Gijzen, H. J. and Van Loosdrecht, M. C. M. (2006) 'Long term effects of salt on activity, population structure and floc characteristics in enriched bacterial cultures of nitrifiers', *Water Research*, 40(7), pp. 1377–1388.
- Mulder, A., van de Graaf, A. A., Robertson, L. A. and Kuenen, J. G. (1995) 'Anaerobic ammonium oxidation discovered in a denitrifying fluidized bed reactor', *FEMS Microbiology Ecology*, 16(3), pp. 177–184.
- Müller, S. and Nebe-von-Caron, G. (2010) 'Functional single-cell analyses: Flow cytometry and cell sorting of microbial populations and communities', *FEMS Microbiology Reviews*,

## References

- 34(4), pp. 554–587.
- Myhre, G. et al. (2013) ‘Anthropogenic and Natural Radiative Forcing’, in Stocker, T. F., Qin, D., Plattner, G.-K., Tignor, M., Allen, S. K., Boschung, J., Nauels, A., Xia, Y., Bex, V., and Midgley, P. M. (eds) *Climate Change 2013: The Physical Science Basis. Contribution of Working Group I to the Fifth Assessment Report of the Intergovernmental Panel on Climate Change*. Cambridge, UK: Cambridge University Press, pp. 659–740.
- Nettmann, E., Fröhling, A., Heeg, K., Klocke, M., Schlüter, O. and Mumme, J. (2013) ‘Development of a flow-fluorescence in situ hybridization protocol for the analysis of microbial communities in anaerobic fermentation liquor.’, *BMC Microbiology*, 13(1), p. 1–15.
- Ngugi, D. K., Blom, J., Stepanauskas, R. and Stingl, U. (2016) ‘Diversification and niche adaptations of *Nitrospina*-like bacteria in the polyextreme interfaces of Red Sea brines’, *The ISME Journal*. Nature Publishing Group, 10(6), pp. 1383–1399.
- van Niftrik, L. and Jetten, M. S. M. (2012) ‘Anaerobic Ammonium-Oxidizing Bacteria: Unique Microorganisms with Exceptional Properties’, *Microbiology and Molecular Biology Reviews*, 76(3), pp. 585–596.
- Nogueira, R., Elenter, D., Brito, A., Melo, L. F., M.Wagner and Morgenroth, E. (2005) ‘Evaluating heterotrophic growth in a nitrifying biofilm reactor using fluorescence in situ hybridization and mathematical modeling’, *Water Science and Technology*, 52(7), pp. 135–141.
- Norton, J. M., Klotz, M. G., Stein, L. Y., Arp, D. J., Bottomley, P. J., Chain, P. S. G., Hauser, L. J., Land, M. L., Larimer, F. W., Shin, M. W. and Starkenburg, S. R. (2008) ‘Complete genome sequence of *Nitrosospira multiformis*, an ammonia-oxidizing bacterium from the soil environment’, *Applied and Environmental Microbiology*, 74(11), pp. 3559–3572.
- Ofițeru, I. D. and Curtis, T. P. (2009) ‘Modeling Risk of Failure in Nitrification: Simple Model Incorporating Abundance and Diversity’, *Journal of Environmental Engineering*, 135(8), pp. 660–665.
- Ofwat (2010) *Playing our part – reducing greenhouse gas emissions in the water and sewerage sectors*. Available at: [http://webarchive.nationalarchives.gov.uk/20150604043546/http://www.ofwat.gov.uk/sustainability/climatechange/prs\\_web\\_1007emissions](http://webarchive.nationalarchives.gov.uk/20150604043546/http://www.ofwat.gov.uk/sustainability/climatechange/prs_web_1007emissions).
- Ondov, B. D., Bergman, N. H. and Phillippy, A. M. (2011) ‘Interactive metagenomic visualization in a Web browser’, *BMC Bioinformatics*, 12(1), p. 385.
- Painter, H. A. (1986) ‘Nitrification in the treatment of sewage and waste waters’, in Prosser, J. I. (ed.) *Nitrification*. Oxford, UK: IRL Press, pp. 185–211.

## References

- Park, H.-D. and Noguera, D. R. (2004) 'Evaluating the effect of dissolved oxygen on ammonia-oxidizing bacterial communities in activated sludge', *Water Research*, 38(14–15), pp. 3275–3286.
- Park, H. D. and Noguera, D. R. (2007) 'Characterization of two ammonia-oxidizing bacteria isolated from reactors operated with low dissolved oxygen concentrations', *Journal of Applied Microbiology*, 102(5), pp. 1401–1417.
- Park, H. D., Wells, G. F., Bae, H., Griddle, C. S. and Francis, C. A. (2006) 'Occurrence of ammonia-oxidizing archaea in wastewater treatment plant bioreactors', *Applied and Environmental Microbiology*, 72(8), pp. 5643–5647.
- Peng, Y. and Zhu, G. (2006) 'Biological nitrogen removal with nitrification and denitrification via nitrite pathway', *Applied Microbiology and Biotechnology*, 73(1), pp. 15–26.
- Pernthaler, A. and Amann, R. (2004) 'Simultaneous Fluorescence In Situ Hybridization of mRNA and rRNA in Environmental Bacteria', *Applied and Environmental Microbiology*, 70(9), pp. 5426–5433.
- Pernthaler, A., Pernthaler, J. and Amann, R. (2002) 'Fluorescence In Situ Hybridization and Catalyzed Reporter Deposition for the Identification of Marine Bacteria', *Applied and Environmental Microbiology*, 68(6), pp. 3094–3101.
- Pester, M., Maixner, F., Berry, D., Rattei, T., Koch, H., Lücker, S., Nowka, B., Richter, A., Spieck, E., Lebedeva, E., Loy, A., Wagner, M. and Daims, H. (2014) 'NxrB encoding the beta subunit of nitrite oxidoreductase as functional and phylogenetic marker for nitrite-oxidizing *Nitrospira*', *Environmental Microbiology*, 16(10), pp. 3055–3071.
- Phillips, D. L. and Fan, M. M. (2005) *Aeration control using continuous dissolved oxygen monitoring in an activated sludge wastewater treatment process*. Proceedings of the Water Environment Federation.
- Picioreanu, C., van Loosdrecht, M. C. M. and Heijnen, J. J. (1997) 'Modelling the effect of oxygen concentration on nitrite accumulation in a biofilm airlift suspension reactor', *Water Science and Technology*, 36(1), pp. 147–156.
- Podar, M., Abulencia, C. B., Walcher, M., Hutchison, D., Zengler, K., Garcia, J. A., Holland, T., Cotton, D., Hauser, L. and Keller, M. (2007) 'Targeted access to the genomes of low-abundance organisms in complex microbial communities', *Applied and Environmental Microbiology*, 73(10), pp. 3205–3214.
- Poth, M. and Focht, D. D. (1985) '15N Kinetic Analysis of N<sub>2</sub>O Production by *Nitrosomonas europaea*: an Examination of Nitrifier Denitrification', *Applied and Environmental Microbiology*, 49(5), pp. 1134–1141.

## References

- Prosser, J. I. (1986) *Nitrification*. Edited by J. I. Prosser. Oxford, UK: IRL Press.
- Prosser, J. I. (1989) 'Autotrophic nitrification in bacteria', *Advances in Microbial Physiology*, 30, pp. 125–181.
- Prosser, J. I. (2005) 'Nitrification', in Hillel, D. and Hatfield, J. L. (eds) *Nitrogen in Soils*. Oxford, UK: Elsevier, pp. 31–39.
- Purkhold, U., Pommerening-röser, A., Schmid, M. C., Koops, H.-P., Juretschko, S. and Wagner, M. (2000) 'Phylogeny of All Recognized Species of Ammonia Oxidizers Based on Comparative 16S rRNA and amoA Sequence Analysis : Implications for Molecular Diversity Surveys', *Applied and Environmental Microbiology*, 66(12), pp. 5368–5382.
- Ravishankara, A. R., Daniel, J. S. and Portmann, R. W. (2009) 'Nitrous Oxide ( $\text{N}_2\text{O}$ ): The Dominant Ozone-Depleting Substance Emitted in the 21st Century', *Science*, 326(5949), pp. 123–125.
- Rittmann, B. E., Laspidou, C. S., Flax, J., van der Waarde, J. J., Geurkink, B., Henssen, M. J. C., Brouwer, H., Klapwijk, A. and Wetterauw, M. (1999) 'Molecular and modeling analyses of the structure and function of nitrifying activated sludge', *Water Science and Technology*, 39(1), pp. 51–59.
- Rittmann, B. E. and McCarty, P. L. (2001) *Environmental Biotechnology: Principles and Applications, Environmental Biotechnology*. New York, USA: McGraw-Hill.
- Roller, M., Lucić, V., Nagy, I., Perica, T. and Vlahoviček, K. (2013) 'Environmental shaping of codon usage and functional adaptation across microbial communities', *Nucleic Acids Research*, 41(19), pp. 8842–8852.
- Ross, M. G., Russ, C., Costello, M., Hollinger, A., Lennon, N. J., Hegarty, R., Nusbaum, C. and Jaffe, D. B. (2013) 'Characterizing and measuring bias in sequence data', *Genome biology*, 14(5), pp. 1–20.
- Rotthauwe, J. H., Witzel, K. P. and W, L. (1997) 'The Ammonia Monooxygenase Structural Gene *amoA* as a Functional Marker: Molecular Fine-Scale Analysis of Natural Ammonia-Oxidizing Populations', *Applied and Environmental Microbiology*, 63(12), pp. 4704–4712.
- Sayavedra-Soto, L. A. and Arp, D. (2011) 'Ammonia-Oxidizing Bacteria: Their Biochemistry and Molecular Biology', in Ward, B. B., Arp, D. J., and Klotz, M. G. (eds) *Nitrification*. Washington, USA: ASM Press, pp. 11–37.
- Sayavedra-Soto, L. A., Hommes, N. G., Alzerreca, J. J., Arp, D. J., Norton, J. M. and Klotz, M. G. (1998) 'Transcription of the *amoC*, *amoA* and *amoB* genes in *Nitrosomonas europaea* and *Nitrosospira* sp. NpAV', *FEMS Microbiology Letters*, 167(1), pp. 81–88.
- Sayavedra-Soto, L., Hommes, N. and Arp, D. (1994) 'Characterization of the Gene Encoding Hydroxylamine Oxidoreductase in *Nitrosomonas europaea*', *Journal of Bacteriology*,

## References

- 176(2), pp. 504–510.
- Schmidt, I. (2009) ‘Chemoorganoheterotrophic growth of *Nitrosomonas europaea* and *Nitrosomonas eutropha*’, *Current Microbiology*, 59(2), pp. 130–138.
- Schmidt, I. and Bock, E. (1997) ‘Anaerobic ammonia oxidation with nitrogen dioxide by *Nitrosomonas eutropha*’, *Archives of Microbiology*, 167(2–3), pp. 106–111.
- Schmidt, I. and Bock, E. (1998) ‘Anaerobic ammonia oxidation by cell-free extracts of *Nitrosomonas eutropha*’, *International Journal of General and Molecular Microbiology*, 73(3), pp. 271–278.
- Schmidt, I., Sliekers, O., Schmid, M., Bock, E., Fuerst, J., Kuenen, J. G., Jetten, M. S. M. and Strous, M. (2003) ‘New concepts of microbial treatment processes for the nitrogen removal in wastewater’, *FEMS Microbiology Reviews*, 27(4), pp. 481–492.
- Schmidt, I., van Spanning, R. J. M. and Jetten, M. S. M. (2004) ‘Denitrification and ammonia oxidation by *Nitrosomonas europaea* wild-type, and NirK- and NorB-deficient mutants’, *Microbiology*, 150(12), pp. 4107–4114.
- Schramm, A., de Beer, D., van den Heuvel, J. C., Ottengraf, S. and Rudolf, A. (1999) ‘Microscale Distribution of Populations and Activities of *Nitrosospira* and *Nitrospira* spp. along a Macroscale Gradient in a Nitrifying Bioreactor : Quantification by In Situ Hybridization and the Use of Microsensors’, *Applied and Environmental Microbiology*, 65(8), pp. 3690–3696.
- Schluthess, R. v., Kühni, M. and Gujer, W. (1995) ‘Release of nitric and nitrous oxides from denitrifying activated sludge’, *Water Research*, 29(1), pp. 215–226.
- Seemann, T. (2014) ‘Prokka: Rapid prokaryotic genome annotation’, *Bioinformatics*, 30(14), pp. 2068–2069.
- Shi, C. Y. (2011) *Mass Flow and Energy Efficiency of Municipal Wastewater Treatment Plants*. London, UK: IWA Publishing.
- Shoun, H. and Tanimoto, T. (1991) ‘Denitrification by the fungus *Fusarium oxysporum* and involvement of cytochrome P-450 in the respiratory nitrite reduction.’, *The Journal of Biological Chemistry*, 266(17), pp. 11078–11082.
- Sims, D., Sudbery, I., Ilott, N. E., Heger, A. and Ponting, C. P. (2014) ‘Sequencing depth and coverage: key considerations in genomic analyses.’, *Nature reviews. Genetics*. Nature Publishing Group, 15(2), pp. 121–32.
- Sonthiphand, P. and Limpiyakorn, T. (2011) ‘Change in ammonia-oxidizing microorganisms in enriched nitrifying activated sludge’, *Applied Microbiology and Biotechnology*, 89(3), pp. 843–853.
- Sorokin, D. Y., Lücker, S., Vejmelkova, D., Kostrikina, N. A., Kleerebezem, R., Rijpstra, W.

## References

- I. C., Damsté, J. S. S., Le Paslier, D., Muyzer, G., Wagner, M., van Loosdrecht, M. C. M. and Daims, H. (2012) ‘Nitrification expanded: discovery, physiology and genomics of a nitrite-oxidizing bacterium from the phylum Chloroflexi’, *The ISME Journal*. Nature Publishing Group, 6(12), pp. 2245–2256.
- Speck, E., Keuter, S., Wenzel, T., Bock, E. and Ludwig, W. (2014) ‘Characterization of a new marine nitrite oxidizing bacterium, *Nitrospina watsonii* sp. nov., a member of the newly proposed phylum “Nitrospinae”’, *Systematic and Applied Microbiology*, 37(3), pp. 170–176.
- Starkenburg, S. R., Arp, D. J. and Bottomley, P. J. (2008) ‘D-Lactate metabolism and the obligate requirement for CO<sub>2</sub> during growth on nitrite by the facultative lithoautotroph *Nitrobacter hamburgensis*’, *Microbiology*, 154(8), pp. 2473–2481.
- Starkenburg, S. R., Speck, E. and Bottomley, P. (2011) ‘Metabolism and Genomics of Nitrite-Oxidizing Bacteria: Emphasis on Studies of Pure Cultures and of *Nitrobacter* Species’, in Ward, B. B., Arp, D. J., and Klotz, M. G. (eds) *Nitrification*. Washington, USA: ASM Press, pp. 267–693.
- Stein, L. Y. and Arp, D. J. (1998) ‘Loss of ammonia monooxygenase activity in *Nitrosomonas europaea* upon exposure to nitrite’, *Applied and Environmental Microbiology*, 64(10), pp. 4098–4102.
- Stein, L. Y., Arp, D. J., Berube, P. M., Chain, P. S. G., Hauser, L., Jetten, M. S. M., Klotz, M. G., Larimer, F. W., Norton, J. M., Op Den Camp, H. J. M., Shin, M. and Wei, X. (2007) ‘Whole-genome analysis of the ammonia-oxidizing bacterium, *Nitrosomonas eutropha* C91: implications for niche adaptation’, *Environmental Microbiology*, 9(12), pp. 2993–3007.
- Stenström, F., Tjus, K. and La Cour Jansen, J. (2014) ‘Oxygen-induced dynamics of nitrous oxide in water and off-gas during the treatment of digester supernatant’, *Water Science and Technology*, 69(1), pp. 84–91.
- Stenstrom, M. K. and Poduska, R. A. (1980) ‘The effect of dissolved oxygen concentration on nitrification’, *Water Research*, 14(6), pp. 643–649.
- Stenstrom, M. K. and Song, S. S. (1991) ‘Effects of oxygen transport limitation on nitrification in the activated sludge process’, *Research Journal Water Pollution Control Federation*, 63(3), pp. 208–219.
- Strous, M., Heijnen, J. J., Kuenen, J. G. and Jetten, M. S. M. (1998) ‘The sequencing batch reactor as a powerful tool for the study of slowly growing anaerobic ammonium-oxidizing microorganisms’, *Applied Microbiology and Biotechnology*, 50(5), pp. 589–596.
- Strous, M., Kuenen, J. G. and Jetten, M. S. M. (1999) ‘Key Physiology of Anaerobic

## References

- Ammonium Oxidation', *Applied and Environmental Microbiology*, 65(7), pp. 3248–3250.
- Tallec, G., Garnier, J., Billen, G. and Gousailles, M. (2006) 'Nitrous oxide emissions from secondary activated sludge in nitrifying conditions of urban wastewater treatment plants: Effect of oxygenation level', *Water Research*, 40(15), pp. 2972–2980.
- Tarre, S. and Green, M. (2004) 'High-rate nitrification at low pH in suspended- and attached-biomass reactors', *Applied and Environmental Microbiology*, 70(11), pp. 6481–6487.
- Tchobanoglous, G., Burton, F. L. and Stensel, H. D. (2003) *Wastewater engineering: treatment and reuse*. 4th edn. New York, USA: Metcalf and Eddy Inc. McGraw-Hill.
- Teske, A., Alm, E., Regan, J. M., Toze, S., Rittmann, B. E. and Stahl, D. A. (1994) 'Evolutionary Relationships among Ammonia- and Nitrite-Oxidizing Bacteria', *Journal of Bacteriology*, 176(21), pp. 6623–6630.
- Thörn, M. and Sörensson, F. (1996) 'Variation of nitrous oxide formation in the denitrification basin in a wastewater treatment plant with nitrogen removal', *Water Research*, 30(6), pp. 1543–1547.
- Tracy, B. P., Gaida, S. M. and Papoutsakis, E. T. (2010) 'Flow cytometry for bacteria: Enabling metabolic engineering, synthetic biology and the elucidation of complex phenotypes', *Current Opinion in Biotechnology*, 21(1), pp. 85–99.
- Treusch, A. H., Leininger, S., Kietzin, A., Schuster, S. C., Klenk, H. P. and Schleper, C. (2005) 'Novel genes for nitrite reductase and Amo-related proteins indicate a role of uncultivated mesophilic crenarchaeota in nitrogen cycling', *Environmental Microbiology*, 7(12), pp. 1985–1995.
- Tringe, S. G., von Mering, C., Kobayashi, A., Salamov, A. A., Chen, K., Chang, H. W., Podar, M., Short, J. M., Mathur, E. J., Detter, J. C., Bork, P., Hugenholtz, P. and Rubin, E. (2005) 'Comparative metagenomics of microbial communities', *Science*, 308(5721), pp. 554–557.
- U.S. Environmental Protection Agency (2006) *Global Anthropogenic Non-CO<sub>2</sub> Greenhouse Gas Emissions: 1990-2020*. Available at: <https://www.epa.gov/sites/production/files/2016-05/documents/globalanthroemissionsreport.pdf>.
- Upadhyay, A. K., Hooper, A. B. and Hendrich, M. P. (2006) 'NO Reductase Activity of the Tetraheme Cytochrome c554 of *Nitrosomonas europaea*', *Journal of the American Chemical Society*, 128(15), pp. 4330–4337.
- Upstill-Goddard, R. C., Rees, A. P. and Owens, N. J. P. (1996) 'Simultaneous high-precision measurements of methane and nitrous oxide in water and seawater by single phase equilibration gas chromatography', *Deep Sea Research*, 43(10), pp. 1669–1682.
- US Environmental Protection Agency (1993) *Manual: Nitrogen Control*. Edited by U.S.

## References

- Environmental Protection Agency. Ohio, USA, pp. 2–19.
- US Environmental Protection Agency (2013) *Energy Efficiency in Water and Wastewater Facilities. A Guide to Developing and Implementing Greenhouse Gas Reduction Programs*. Energy. Available at: <https://www.epa.gov/sites/production/files/2015-08/documents/wastewater-guide.pdf>.
- Utåker, J. B., Bakken, L., Jiang, Q. Q. and Nes, I. F. (1995) ‘Phylogenetic Analysis of Seven New Isolates of Ammonia-Oxidizing Bacteria Based on 16S rRNA Gene Sequences’, *Systematic and Applied Microbiology*, 18(4), pp. 549–559.
- Vanparys, B., Speck, E., Heylen, K., Wittebolle, L., Geets, J., Boon, N. and De Vos, P. (2007) ‘The phylogeny of the genus *Nitrobacter* based on comparative rep-PCR, 16S rRNA and nitrite oxidoreductase gene sequence analysis’, *Systematic and Applied Microbiology*, 30(4), pp. 297–308.
- Venter, J. C. et al. (2004) ‘Environmental Genome Shotgun Sequencing of the Sargasso Sea’, *Science*, 304(5667), pp. 66–74.
- Wagner, M., Rath, G., Amann, R., Koops, H.-P. and Schleifer, K.-H. (1995) ‘In situ Identification of Ammonia-oxidizing Bacteria’, *Systematic and Applied Microbiology*, 18(2), pp. 251–264.
- Walker, C. B. et al. (2010) ‘*Nitrosopumilus maritimus* genome reveals unique mechanisms for nitrification and autotrophy in globally distributed marine crenarchaeota’, *Proceedings of the National Academy of Sciences*, 107(19), pp. 8818–8823.
- Wallner, G., Amann, R. and Beisker, W. (1993) ‘Optimizing fluorescent in situ hybridization with rRNA-targeted oligonucleotide probes for flow cytometric identification of microorganisms’, *Cytometry*, 14(2), pp. 136–143.
- Wallner, G., Fuchs, B., Spring, S., Beisker, W. and Amann, R. (1997) ‘Flow sorting for molecular analysis.’, *Applied and Environmental Microbiology*, 63(11), pp. 4178–4184.
- Wang, Q., Garrity, G. M., Tiedje, J. M. and Cole, J. R. (2007) ‘Naive Bayesian classifier for rapid assignment of rRNA sequences into the new bacterial taxonomy’, *Applied and Environmental Microbiology*, 73(16), pp. 5261–5267.
- Watson, S. W., Bock, E., Valois, F. W., Waterbury, J. B. and Schlosser, U. (1986) ‘*Nitrospira marina* gen. nov. sp. nov.: a chemolithotrophic nitrite-oxidizing bacterium’, *Archives of Microbiology*, 144(1), pp. 1–7.
- Watson, S. W. and Waterbury, J. B. (1971) ‘Characteristics of Two Marine Nitrite Oxidizing Bacteria, *Nitrospina gracilis* nov. gen. nov. sp. and *Nitrococcus mobilis* nov. gen. nov. sp.’, *Archives of Microbiology*, 77, pp. 203–230.
- Weiss, R. F. and Price, B. A. (1980) ‘Nitrous oxide solubility in water and seawater’, *Marine*

## References

- Chemistry*, 8(4), pp. 347–359.
- Whittaker, M., Bergmann, D., Arciero, D. and Hooper, A. B. (2000) ‘Electron transfer during the oxidation of ammonia by the chemolithotrophic bacterium *Nitrosomonas europaea*’, *Biochimica et Biophysica Acta - Bioenergetics*, 1459(2–3), pp. 346–355.
- Wick, R. R., Schultz, M. B., Zobel, J. and Holt, K. E. (2015) ‘Bandage: Interactive visualization of de novo genome assemblies’, *Bioinformatics*, 31(20), pp. 3350–3352.
- Woese, C. R. (1987) ‘Bacterial Evolution’, *Microbiological Reviews*, 51(2), pp. 221–71.
- Woese, C. R., Stackebrandt, E., Weisburg, W. G., Paster, B. J., Madigan, M. T., Fowler, V. J., Hahn, C. M., Blanz, P., Gupta, R., Nealson, K. H. and Fox, G. E. (1984) ‘The phylogeny of purple bacteria: the alpha subdivision’, *Systematic and Applied Microbiology*, 5, pp. 315–26.
- Wood, P. M. (1986) ‘Nitrification as an energy source’, in Prosser (ed.) *Nitrification*. Oxford, UK: IRL Press, pp. 39–62.
- Ye, L., Zhang, T., Wang, T. and Fang, Z. (2012) ‘Microbial Structures, Functions, and Metabolic Pathways in Wastewater Treatment Bioreactors Revealed Using High-Throughput Sequencing’, *Environmental Science & Technology*, 46(24), pp. 13244–13252.
- Yilmaz, P., Parfrey, L. W., Yarza, P., Gerken, J., Pruesse, E., Quast, C., Schweer, T., Peplies, J., Ludwig, W. and Glöckner, F. O. (2014) ‘The SILVA and “All-species Living Tree Project (LTP)” taxonomic frameworks’, *Nucleic Acids Research*, 42(1), pp. 643–648.
- Yilmaz, S., Haroon, M. F., Rabkin, B. a., Tyson, G. W. and Hugenholtz, P. (2010) ‘Fixation-free fluorescence in situ hybridization for targeted enrichment of microbial populations.’, *The ISME journal*. Nature Publishing Group, 4(10), pp. 1352–1356.
- Yu, R., Kampschreur, M. J., van Loosdrecht, M. C. M. and Chandran, K. (2010) ‘Mechanisms and Specific Directionality of Autotrophic Nitrous Oxide and Nitric Oxide Generation during Transient Anoxia’, *Environmental Science and Technology*, 44(4), pp. 1313–1319.
- Zart, D. and Bock, E. (1998) ‘High rate of aerobic nitrification and denitrification by *Nitrosomonas eutropha* grown in a fermentor with complete biomass retention in the presence of gaseous NO<sub>2</sub> or NO’, *Archives of Microbiology*, 169(4), pp. 282–286.
- Zhan, A. and MacIsaac, H. J. (2015) ‘Rare biosphere exploration using high-throughput sequencing: research progress and perspectives’, *Conservation Genetics*, 16(3), pp. 513–522.
- Zhang, T., Jin, T., Yan, Q., Shao, M., Wells, G., Criddle, C. and Fang, H. H. P. (2009) ‘Occurrence of ammonia-oxidizing Archaea in activated sludges of a laboratory scale reactor and two wastewater treatment plants’, *Journal of Applied Microbiology*, 107(3), pp.

References

- 970–977.
- Zhou, J., He, Z., Yang, Y., Deng, Y., Tringe, S. G. and Alvarez-Cohen, L. (2015) ‘High-Throughput Metagenomic Technologies for Complex Microbial Community Analysis: Open and Closed Formats’, *American Society for Microbiology*, 6(1), pp. 1–17.
- Zumft, W. G. (1997) ‘Cell biology and molecular basis of denitrification’, *Microbiology and Molecular Biology Reviews*, 61(4), pp. 533–616.